Electrochemical cleavage of peptide bonds for mass spectrometry-based proteomics

Zhang, Tao

Electrochemical Cleavage of Peptide Bonds for Mass Spectrometry-based Proteomics

Tao Zhang

Printing of this thesis has been generously supported by:

rijksuniversiteit
groningen

ISBN

978-94-034-0280-2 (Electronic version)

978-94-034-0279-6 (Printed book)

Layout

Tao Zhang

Printing

Ridderprint, Ridderkerk, The Netherlands

Publisher

University of Groningen

Cover design

Wenjun Wang & Zhuojun Meng

The research reported in this thesis was carried out in the Analytical Biochemistry group at the University of Groningen, The Netherlands. This work was financially supported by the China Scholarship Council and The Dutch Technology Foundation STW(Grant 11957).

university of groningen

Electrochemical Cleavage of Peptide Bonds for Mass Spectrometry-based Proteomics

PhD Thesis

to obtain the degree of PhD at the

University of Groningen

on the authority of the

Rector Magnificus Prof. E. Sterken

and in accordance with

the decision by the College of Deans.

This thesis will be defended in public on

Friday 24 November 2017 at 11.00 hours

by

Tao Zhang

born on 14 November 1986
in Shandong, China

Supervisors

Prof. Dr. R. P. H. Bischoff

Co-Supervisor

Dr. H. P. Permentier

Assessment committee

Prof. Dr. U. Karst

Prof. Dr. F. J. Dekker

Prof. Dr. E. M. J. Verpoorte

Dedicated to my beloved
wife
and all the members of my family.

Electrochemical cleavage of peptide bonds for mass spectrometry-based proteomics

PhD Thesis

Tao Zhang

Table of Contents

Chapter 1. General introduction and thesis scope **1**

1.1 Oxidative cleavage of peptide bonds 2

1.2 EC-MS in proteomics and protein analysis 3

1.3 Specific cleavage of peptide bonds in MS-based proteomics 6

1.4 Aim of this thesis 8

1.5 Thesis outline 9

1.6 References 12

Chapter 2. Electrochemical protein cleavage in a microfluidic cell with integrated boron doped diamond electrodes **15**

2.1 Introduction 16

2.2 Experimental section 20

2.2.1 Microfluidic electrochemical cell fabrication 20

2.2.2 Chemicals 20

2.2.3 Instrumentation and Measurements 21

2.3 Results and Discussion 22

2.3.1 Microfluidic electrochemical cell design 22

2.3.2 BDD material and microfluidic electrochemical cell characterization 25

2.3.3 Electrochemical cleavage of tripeptides 27

2.3.4 Electrochemical cleavage of ACTH 1-10 29

2.3.5 Electrochemical cleavage of insulin 30

2.3.6 Electrochemical cleavage of lysozyme 31

2.4 Conclusions 34

2.5 References 36

2.6 Supporting Information 39

Chapter 3. Efficient and selective chemical labeling of electrochemically-generated peptides based on spirolactone chemistry **49**

3.1 Introduction 50

3.2 Experimental section 51
3.2.1 Materials and Chemicals.....51
3.2.2 N-terminal acetylation of peptides and Ac-peptide purification 51
3.2.3 Electrochemical cleavage 52
3.2.4 Intramolecular rearrangement of spirolactone-containing peptides 53
3.2.5 Analysis of intramolecular rearrangements product by LC-MS analysis.....53
3.2.6 Isomer preparation and NMR analysis 54
3.2.7 Chemical coupling of electrochemically cleaved peptides with amine-containing reagents 55
3.2.8 High-resolution MS/MS analysis 56
3.3 Results and Discussion 57
3.3.1 Molecular rearrangement of LW+14 and formation of isomers 57
3.3.2 Stabilization of peptide-spirolactones against intramolecular rearrangement 62
3.3.3 Chemical labelling of electrochemically-generated peptide-spirolactones ..63
3.4 Conclusions 65
3.5 References 66
3.6 Supporting Information 69
Chapter 4. Specific affinity enrichment of electrochemically cleaved peptides based on Cu (II)-mediated spirolactone tagging 81
4.1 Introduction 82
4.2 Experimental section 83
4.2.1 Materials and Methods 83
4.2.2 Peptide and protein preparation 84
4.2.3 Electrochemical cleavage 84
4.2.4 Effect of Cu (II) on stability of cleavage products and chemical tagging ...85
4.2.5 Biotinylation of EC-lysozyme with amine-PEG_2-biotin 86
4.2.6 Removal of excess biotin by SPE after biotinylation 87
4.2.7 Affinity enrichment of biotinylated peptides 87

4.2.8 Analysis by LC-MS/MS 88
4.2.9 Data analysis and database searching 88
4.3 Results and Discussion 89
4.3.1 Stabilization of peptide-spirolactones against intramolecular rearrangement in the presence of Cu (II) ions 89
4.3.2 Cu (II)-mediated spirolactone chemical tagging 91
4.3.3 Affinity enrichment of biotinylated peptides 93
4.3.4 Affinity enrichment of biotinylated spirolactone-containing peptides from EC-cleaved lysozyme 95
4.4 Conclusions 97
4.5 References 98
4.6 Supporting Information 100
Chapter 5. Products of Gly-Met-Gly after radiolytical and electrochemical oxidation in oxygenated aqueous solution 103
5.1 Introduction 104
5.2 Experimental section 106
5.2.1 Materials 106
5.2.2 Reaction of Gly-Met-Gly with H_2O_2 106
5.2.3 Steady-state gamma-radiolysis 107
5.2.4 OPA derivatization of irradiated samples and HPLC analysis 107
5.2.5 Electrochemical oxidation and EC-MS analysis 107
5.2.6 HPLC-MS/MS measurements 108
5.3 Results and Discussion 108
5.3.1 Reaction of Gly-Met-Gly with H_2O_2 108
5.3.2 Reaction of $HO^{\bullet}$ radicals with Gly-Met-Gly in oxygenated aqueous solution upon gamma-radiolysis 110
5.3.3 Product identification by LC-MS and high-resolution MS/MS 111
5.3.4 Electrochemical oxidation of Gly-Met-Gly 116
5.4 Discussion 117

5.5 Conclusions 118
5.6 References 119
Chapter 6. Cleavage of peptide bonds under oxidizing conditions: mechanisms, analytical strategies and future perspectives 121
6.1 Introduction.....122
6.2 Cleavage of protein backbone via radiolysis-induced ROS 125
6.2.1 Peptide bond cleavage via the diamide and α-amidation pathways 125
6.2.2 Peptide bond cleavage via oxidation of glutamyl and prolyl residues 126
6.2.3 Backbone cleavage following β-scission 128
6.3 Cleavage of peptide bonds via electrochemical oxidation 128
6.3.1 Peptide bond cleavage via oxidation of Tyr 129
6.3.2 Peptide bond cleavage via oxidation of Trp 131
6.4 Analytical strategies to investigate oxidative cleavage of proteins *in vitro* and *in vivo* 132
6.4.1 Analytical strategy for carbonyl derivatives 133
6.4.1.1 DNPH derivatives 134
6.4.1.2 Affinity detection and enrichment 134
6.4.1.3 MS-based analytical strategies 135
6.4.1.4 Analysis in biological samples 136
6.4.2 Current strategies for the analysis of spirolactone derivatives 137
6.5 Conclusion and perspective 140
6.6 References 142
Chapter 7. Summary and future research 149
Chapter 8. Samenvatting en toekomstig onderzoek 153
Appendix 157
List of Publications 157
Acknowledgements 159

Chapter 1

Introduction

Abstract: This chapter presents a brief introduction to the oxidative cleavage of peptide bonds and the specific digestion of proteins in MS-based proteomics. Electrochemistry combined with mass spectrometry and its application in proteomics and protein analysis are also introduced. The aim of this thesis is discussed followed by a brief outline of the thesis.

1.1 Oxidative cleavage of peptide bonds

Important biological processes, including a wide variety of diseases and aging, are related to the oxidation of proteins leading to excessive chemical modifications and ultimately loss of biological function. [1-4] Damaged proteins have no specific repair mechanism and are usually marked for degradation upon irreversible modification and peptide bond cleavage. [4-6] This oxidative modification of peptide bonds is one of the most important modifications after exposure to an oxidizing environment, resulting from attacks by different types of radical species, including reactive oxygen species (ROS), reactive nitrogen species (RNS), and species generated from halogen salts and halogenated compounds. [7-8] ROS, including hydrogen peroxide (H_2O_2), the superoxide anion (O_2^-) and the hydroxyl radical ($HO^\bullet$), are produced naturally from various metabolic pathways, physical, chemical and biological factors, and under pathological conditions and can be observed in stressed environments as hallmarks of oxidative stress. [8-10]

The study of protein cleavage due to oxidative stress has been proven to be of great importance to understand oxidation mechanisms in a broad spectrum of diseases and biological processes. [1-6] However, there is no way to date to fully understand the oxidative cleavage mechanism *in vivo*.

Mimicking *in vivo* conditions by studying *in vitro* oxidation reactions helps understanding the underlying mechanisms and can be used to produce oxidized proteins for further research. Two of the most important external sources of ROS, radiolysis and oxidizing agents, including H_2O_2 and ozone, are mostly used in mimicking oxidation of peptides and proteins *in vivo*. [11-13] More recently studies showed that oxidative cleavage of peptide bonds was generally achieved by internal free-radical transfer upon oxidation by ROS via the diamide and α-amidation pathways, or upon oxidation of glutamyl and prolyl residues. [5, 8, 14-16] Electrochemistry (EC) was found to be a useful approach to complement existing oxidation sources in characterizing direct and indirect effects of oxidation reactions on peptides and proteins. As a purely instrumental approach for direct electron transfer oxidation and to generate hydroxyl radical under special condi-

tions, interest has increased in electrochemical mimicry of biological oxidation reactions. Specific cleavage after oxidation of tryptophan (Trp) and tyrosine (Tyr) residues by electron transfer oxidation were achieved by electrochemical oxidation. [17-23] In an electrochemical cell, electrochemical reduction of molecular oxygen was used to generate hydrogen peroxide while electrochemical oxidation of water, particularly on a boron-doped diamond (BDD) electrode, was employed for hydroxyl radical production at sufficiently high potential. This ability to generate ROS in an electrochemical approach makes EC an attractive analytical tool for oxidation studies.

1.2 EC-MS in proteomics and protein analysis

Electrochemistry is sufficiently versatile with respect to electrode material, cell design, potential application and solvent conditions that many *in vivo* oxidation reactions of enzymes, like peroxidases and cytochrome P450, can be mimicked. It is also interesting to study if the same electrochemical oxidation of peptides and proteins themselves occurs *in vitro*. Mass spectrometry (MS) is a powerful tool in characterization and identification of oxidation products of peptides and proteins as well as intermediates, leading to the ability to do qualitative and quantitative analyses and mechanistic studies of oxidation reactions. These strengths make the combination of electrochemistry and mass spectrometry (EC-MS) one of the most popular ways to study the oxidation of peptides and proteins in an integrated analytical fashion. The history of the combination of EC and MS has been reviewed in detail. [24-27]

EC-MS has the advantage of being a fully automated, instrumental analytical approach. The direct coupling of an electrochemical cell with MS was developed to study the direct electrochemical oxidation and product identification in a time-resolved manner (**Figure 1 A**). Real-time identification and quantitation of reaction products may help in the selection of the optimal conditions for obtaining a particular product. For potential-dependent oxidation reactions, such as the electrochemical cleavage of peptide bonds, linear sweep voltammetry is often performed first to determine the optimal potential for the expected product. Furthermore, interest in online EC-MS has increased

due to the possibility of using miniaturized devices such as microfluidics chips, to detect unstable, reactive and short-lived intermediates of the oxidation reactions.

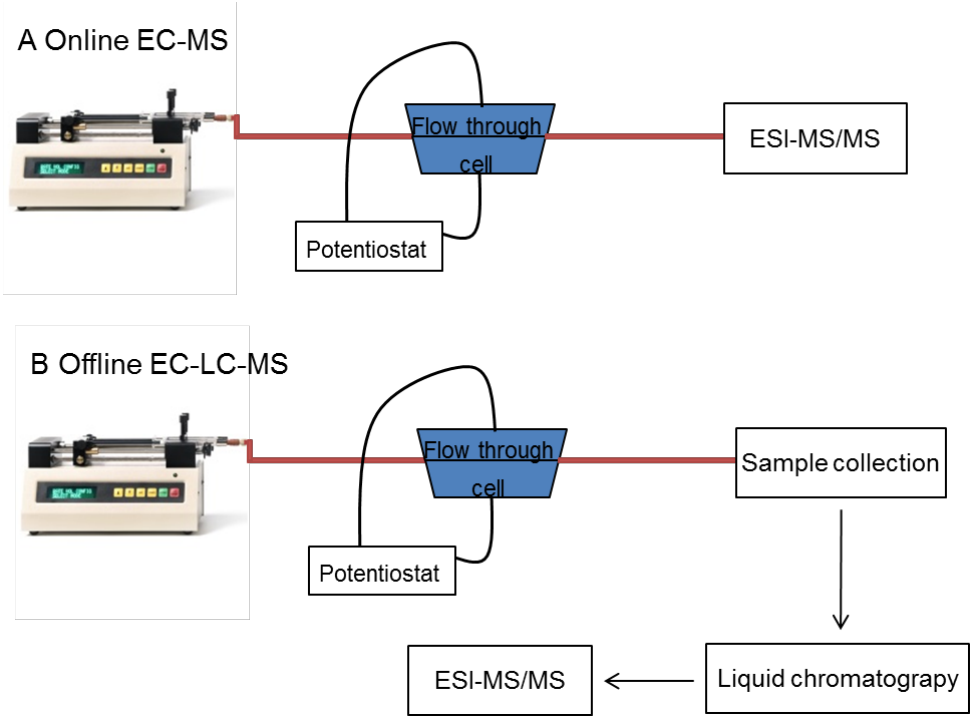

Figure 1. The EC-MS workflow: A, online EC-MS and B, offline EC-LC-MS. Online EC-MS was established by directly coupling an electrochemical cell to ESI-MS with a sample flow supplied by a syringe pump. In the offline EC-LC-MS workflow, a liquid chromatography system was used between EC and MS for sample separation. After the electrochemical reaction in the cell, the sample was collected and analyzed by LC-MS.

Since EC reactions often give rise to the formation of complex mixtures of intermediates, products, and by-products, it is difficult to identify them without separation. In order to allow for the comprehensive characterization of the electrochemical reaction mixture, an expanded set-up consisting of EC, a liquid chromatographic separation system and MS was developed as offline EC-LC-MS (**Figure 1 B**). After collection of sample from EC, different fractions of time point samples can be analyzed by LC-MS/MS. In this approach liquid chromatography was employed between EC and MS to achieve better separation and identification of complex mixtures.

The application of EC-MS in proteomics and protein analysis is attracting more attention, but remains mainly focused on studying the oxidative modification of peptides and proteins, the electrochemical reduction of disulfide bonds, selective oxidative labeling, and specific protein cleavage. [10, 12-14] Direct oxidation of peptides and proteins, related to cysteine (Cys), methionine (Met), histidine (His), tryptophan (Trp) and tyrosine (Tyr) together with the development of EC-MS techniques in protein oxidation have been studied and reviewed. [8, 10, 11, 15, 16, 27]

Electrochemical reduction of disulfide bridges in proteins and peptides is an attractive application of EC-MS. Disulfide bonds are one of the most common post-translational modifications and provide covalent cross-linkages in native proteins for maintaining their three-dimensional structure and their biological activity. Recently, electrochemical reduction has been shown to represent a fast and efficient alternative for chemical disulfide bond cleavage with immediate application in bottom-up and top-down proteomics. [28-35] In peptide mapping, electrochemistry enables the identification of disulfide-bridged peptides within enzymatic digest mixtures by inducing changes in ion abundance. [28] At the protein level, electrochemical reduction of disulfide bonds enables tandem MS sequencing with high sequence coverage. [28-29] In top-down proteomics, electrochemical reduction was integrated with a Hydrogen/Deuterium eXchange monitored by a Mass Spectrometry (HDXMS) workflow to achieve fast and efficient disulfide bond cleavage for improved of protein structure characterization. [30] Online EC reduction of disulfide bonds was also employed to overcome complexity in the top-down analysis of an antibody in combination with ESI and Fourier transform ion cyclotron resonance MS. [31-33] Very recently, EC was employed as a reduction approach in mapping disulfide bonds in proteins. In the same work, an LC-EC-MS platform combined online with EC reduction of disulfide bonds was established for the characterization of complex and highly disulfide bonded proteins. [34-35]

EC-MS can also be indirectly used in the study of oxidative protein labeling for peptide and protein characterization, which has been reviewed by Roeser *et al* and Liuni *et*

al. [36-37] Electrochemically assisted labeling was found to be useful to determine the number of Cys residues, which improves protein identification by database searching. Furthermore, based on the labeling extent of different residues within peptides and proteins, the accessibility, reactivity, or affinity of these sites can be tested.

Another achievement of EC-MS in proteomics and protein analysis is the electrochemical cleavage at the C-terminal side of tyrosine and tryptophan residues (**Figure 2**), which clearly suggests that electrochemistry could represent an instrumental alternative to chemical and enzymatic cleavage strategies in MS-based proteomics. [17-23] The major developments and achievements in this aspect will be described in the following section.

1.3 Specific cleavage of peptide bonds in MS-based proteomics

In MS-based proteomics, specific digestion of proteins plays a key role in protein identification and quantification, and peptide bond cleavage is mainly achieved by enzymatic digestion with different specificities, complemented with chemical cleavage when a certain specificity is required. [38-45] The specific electrochemical cleavage of peptides and proteins next to C-terminal of Tyr and Trp residues is very attractive since this specificity is not available by enzymatic digestion. Another interesting aspect of electrochemically cleaved peptides is that the newly generated C-terminus is converted into an unusual activated ester in the form of a spirolactone, which has been employed as a target for chemical labeling. [20] In addition, electrochemistry can be used to generate ROS, leading to specific cleavage next to phenylalanine (Phe) after its oxidation to Tyr upon exposure to ROS, particularly OH-radicals *in vitro*. [21, 23]

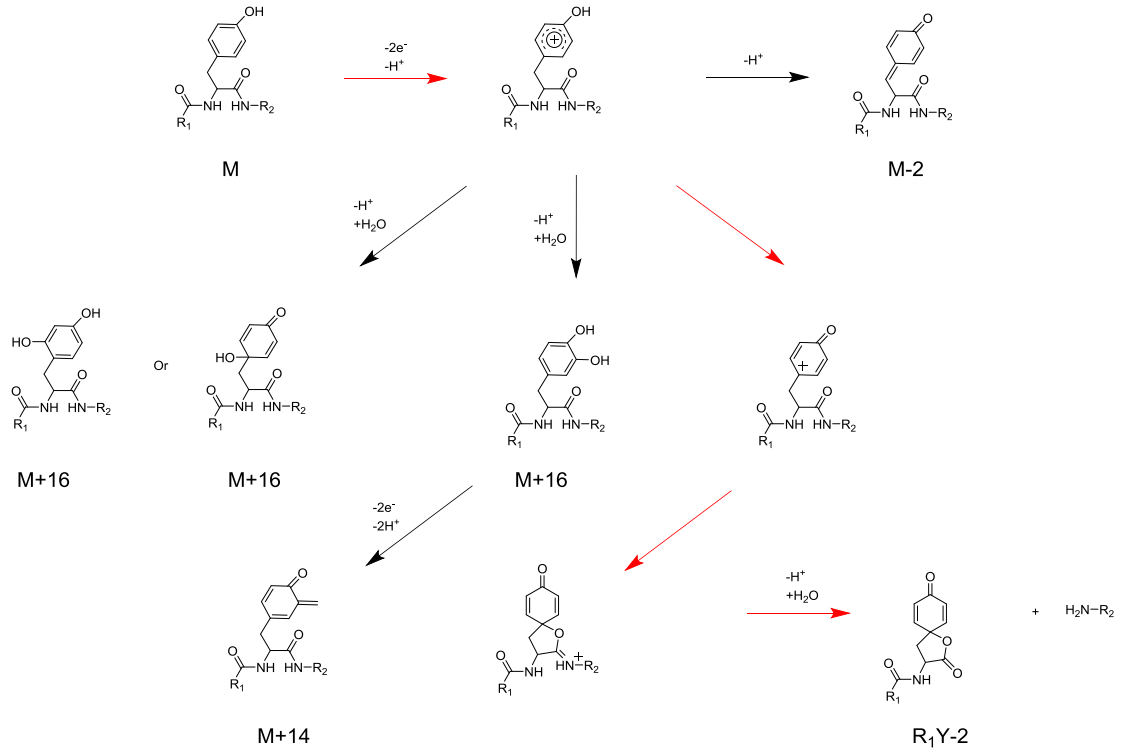

Figure 2. Proposed electrochemical oxidation and cleavage mechanism of Tyr-containing proteins. The electrochemical cleavage pathway is described in red arrows. R_1 and R_2 are the N- and C-terminal parts of the continuing peptide chain, respectively. [17-19]

Compared to widely used enzymatic protein cleavage, the electrochemical approach offers advantages of 1) being a rapid, reagent-free and purely instrumental approach, 2) supplying a specific cleavage site for which no enzyme is available, 3) cleaving proteins under conditions (e.g. strongly denaturing) that enzymes cannot tolerate, 4) providing the possibility to label reactive groups based on EC generated spirolactones and 5) generating larger peptides for identification since Trp- and Tyr-residues are less frequent in proteins than Lys or Arg.

The main drawback of electrochemical peptide cleavage compared to traditional enzymatic and chemical cleavage is the currently low cleavage yield and unavoidable generation of non-cleavage oxidation products (for example the M-2, M+14, M+16 products in **Figure 2**). Model tripeptides were used to gain more insight into the reaction mechanism, as well as

issues related to adsorption to the electrode surface which affect oxidation yield and product composition. [18-19] A variety of electrode materials have been tested, including boron doped diamond (BDD), which offers the best performance in terms of decreased adsorption, resulting in higher cleavage yields due to both a better recovery of products and a lower degree of dimer formation. [21, 23] In addition, the yield of cleavage products can be improved by proper control of the oxidation potential, the application of strongly acidic conditions, and electrode regeneration by cathodic pretreatment or electrochemical cleaning through cyclic voltammetry. [21]

Another problem that needs to be addressed is the increased complexity of reaction mixtures due to the generation of non-cleavage oxidation products in addition to cleaved peptides which poses a problem for proteomics applications. It is desirable to fish out the cleavage products by means of tagging before detection by MS. An efficient and selective labeling and capturing strategy for the cleaved peptides of interest based on specific reactions with the spirolactone moieties would decrease sample complexity and boost proteomics analysis efficiency after electrochemical protein digestion. The main challenges to tag the cleaved peptides are to prevent hydrolysis of spirolactones during the coupling reaction and to decrease the large molar excess of reagents.

1.4 Aim of this thesis

Electrochemical protein cleavage is emerging as an instrumental alternative to chemical and enzymatic approaches in MS-based proteomics and as a powerful method to study oxidation of peptides and proteins *in vitro*.

This thesis first focuses on method development of EC-MS to improve electrochemical protein cleavage and its application in MS-based proteomics combined with the

tagging of electrochemically-generated reactive intermediates. We have developed improved methods for peptide and protein cleavage, including miniaturization and improved cell configuration with BDD electrodes in collaboration with colleagues from Twente University (**Chapter 2**) and some of our industry partners, notably Antec Leyden and ESA/Dionex (now Thermo Scientific), who provided electrochemical cells and support with the specific construction, modification and treatment of cells and electrode surfaces (**Chapter 3**). To tackle the increased complexity of sample mixtures, specific enrichment based on efficient chemical labeling of electrochemically cleaved peptides was investigated (**Chapters 3 and 4**).

The second aim of this thesis is to check the feasibility of using electrochemical oxidation *in vitro* to mimic *in vivo* oxidative reactions of peptides and proteins and to study oxidation mechanisms. Product studies of Gly-Met-Gly generated by radiolytic and electrochemical oxidation were performed in collaboration with the University of Bologna (ISOF), Italy (**Chapter 5**). It is worth mentioning that the developed enrichment method targeting oxidative cleavage products with a spirolactone moiety will definitely benefit the detection and identification of oxidative intermediates *in vivo*, since a large number of different species in the human proteome makes it particularly difficult to accurately identify oxidative cleavage products in complex biological matrices.

1.5 Thesis outline

This chapter (**Chapter 1**) presents a brief introduction to the oxidative cleavage of peptide bonds and the aim of this thesis.

Chapter 2 describes the development of a microfluidic electrochemical cell that combines a cell geometry optimized for high electrochemical conversion efficiency with an integrated boron doped diamond (BDD) working electrode offering reduced adsorption of peptides and proteins. Efficient cleavage of the proteins bovine insulin and chicken egg white lysozyme was observed at 4 out of 4 and 7 out of 9 of the predicted cleavage sites, respectively. Chicken egg white lysozyme was identified based on 5

electrochemically generated peptides using a proteomics database search algorithm. These results show that electrochemical peptide bond cleavage in a microfluidic cell is a novel, fully instrumental approach towards protein analysis and eventually proteomics studies in conjunction with mass spectrometry.

Chapter 3 describes the development of a highly efficient and selective chemical labeling approach based on spirolactone chemistry. Electrochemically generated peptide-spirolactones readily undergo an intramolecular rearrangement yielding isomeric diketopiperazines precluding further chemical labeling. A strategy was established to prevent intramolecular arrangement by acetylating the N-terminal amino group prior to electrochemical oxidation and cleavage allowing the complete and selective chemical labeling of the tripeptide LWL and the decapeptide ACTH 1-10 with amine-containing reagents. As examples, we show the successful introduction of a fluorescent label and biotin for detection or affinity enrichment. Electrochemical digestion of peptides and proteins followed by efficient chemical labeling constitutes a new, powerful tool in protein chemistry.

In **Chapter 4**, we developed a specific affinity enrichment method combining electrochemical digestion, copper (II)-mediated spirolactone biotinylation and selective affinity chromatography with mass spectrometry to label and enrich electrochemically cleaved peptides after electrochemical oxidation of peptides and protein. Copper (II) was employed to achieve efficient chemical tagging of spirolactone and to prevent intramolecular rearrangement in the presence of an N-terminal amino group. Newly generated spirolactone-containing peptides were labeled with a biotin derivative containing an amino group allowing their affinity enrichment by avidin affinity chromatography and protein analysis followed by mass spectrometry. This method allows specific enrichment of electrochemically cleaved spirolactone-containing peptides from a complex mixture.

Chapter 5 focuses on hydroxyl-radical-mediated oxidation of Gly-Met-Gly by γ-ray radiolysis and electrochemical reactions and subsequent product identification. Detailed

product analysis by LC-MS and high resolution MS/MS, which were used as powerful analytical tools to elucidate the structures of the reaction products, provided detailed insight into the reactivity of the Met-containing peptides under hydroxyl-radical-mediated oxidation conditions.

Chapter 6 summarizes the results and discusses the future perspectives for oxidative peptide bond cleavage in MS-based proteomics and in the mimicking of *in vivo* oxidation reactions.

1.6 References

(1) Stadtman, E.R.; Berlett, B. S. *Drug Metab. Rev.* **1998**, 30, 225-243.

(2) Berlett, B. S.; Stadtman, E. R. *J. Bio. Chem.* **1997**, 272, 20313-20316.

(3) Finkel, T.; Holbrook, N. J. *Nature* **2000**, 408, 239-247.

(4) Davies, M. J. *Biochem. J.* **2016**, 473, 805-825.

(5) Stringfellow, H. M.; Jones, M. R.; Green, M. C.; Wilson, A. K.; Francisco, J. S. *J. Phys. Chem. A* **2014**, 118, 11399-11404.

(6) Ekkati, A. R.; Kodanko, J. J. *J. Am. Chem. Soc.* **2007**, 129, 12390-12391.

(7) Beckman, J. S.; Koppenol, W. H. *Am. J. Physiol.* **1996**, 271, C1424-C1437.

(8) Barelli, S.; Canellini, G.; Thadikkaran, L.; Crettaz, D.; Quadroni, M.; Rossier, J. S.; Tissot, J. D.; Lion. N. *Proteomics Clin. Appl.* **2008**, 2, 142-157.

(9) Nathan, C.; Ding, A. *Cell* **2010**, 03, 008.

(10) Dalle-Donne, I.; Scaloni, A.; Butterfield, D. A. *Wiley & Sons*, New York **2006**.

(11) Stadtman, E. R. *Free Radic. Res.* **2006**, 40, 1250-1258.

(12) Davies, M. J. *Biochim. Biophys. Acta* **2005**, 1703, 93-109.

(13) Headlam, H. A.; Davies, M. J. *Free Radic. Biol. Med.* **2004**, 36, 1175-1184.

(14) Faraggi, M.; Tal, Y. *Radiat. Res.* **1975**, 62, 347.

(15) Stadtman, E. R. *Ann. Rev. Biochem.* **1993**, 62, 797-821.

(16) Xu, G.; Chance, M. R. *Chem. Rev.* **2007**, 107, 3514-3543.

(17) Permentier, H. P.; Jurva, U.; Barroso, B.; Bruins, A. P. *Rapid. Commun. Mass. Spectrom.* **2003**, *17*, 1585-1592.

(18) Permentier, H. P.; Bruins, A. P. *J. Am. Soc. Mass. Spectrom.* **2004**, *15*, 1707-1716.

(19) Roeser, J.; Permentier, H. P.; Bruins, A. P.; Bischoff, R. *Anal. Chem.* **2010**, *82*, 7556-7565.

(20) Roeser, J.; Alting, N. F. A.; Permentier, H. P.; Bruins, A. P.; Bischoff, R. *Rapid. Commun. Mass. Spectrom.* **2013**, *27*, 546-552.

(21) Roeser, J.; Alting, N. F. A.; Permentier, H. P.; Bruins, A. P.; Bischoff, R. *Anal. Chem.* **2013**, *85*, 6626-6632.

(22) Zhang, T.; Niu, X.; Yuan, T.; Tessari, M.; Vries, M. P.; Permentier, H. P.; Bischoff, R. *Anal*. *Chem*. **2016**, 88, 6465-6471.

(23) van den Brink, F. T. G.; Zhang, T.; Ma, L.; Bomer, J.; Odijk, M.; Olthuis, W.; Permentier, H. P.; Bischoff, R.; Berg, A. van den. *Anal*. *Chem*. **2016**, 88, 9190-9198.

(24) Chang, H.; Johnson, D. C.; Houk, R. S. *Trands Anal*. *Chem*. **1992**, 64, 21A-33A.

(25) Liu, P.; Lu, M.; Zheng, Q.; Zhang, Y.; Dewald, H. D.; Chen, H. *Analyst* **2013**, 138, 5519-5539.

(26) Karst, U. *Angew*. *Chem*. *Int*. *Ed*. **2004**, 43, 2476-2478.

(27) Permentier, H. P.; Bruins, A. P.; Bischoff, R. *Mini*. *Rev*. *Med*. *Chem*. **2008**, 8, 46-56.

(28) Zhang, Y.; Dewald, H. D.; Chen, H. *J*. *Proteome Res*. **2011**, 10, 1293-1304.

(29) Zheng, Q.; Zhang, H.; Chen, H. *Int*. *J*. *Mass Spectrom*. **2013**, 353 84-92.

(30) Mysling, S.; Salbo, R.; Ploug, M.; Jørgensen, T. J. D. *Anal*. *Chem*. **2014**, 86, 340-345.

(31) Nicolardi, S.; Giera, M.; Kooijman, P.; Kraj, A.; Chervet, J. P.; Deelder, A. M.; Burgt, Y. E. M. van der. *J*. *Am*. *Soc*. *Mass Spectrom*. **2013**, 24, 1980-1987.

(32) Switzar, L.; Nicolardi, S.; Rutten, J. W.; Oberstein, S. A. J. L.; Aartsma-Rus, A.; Burgt, Y. E. M. van der. *J*. *Am*. *Soc*. *Mass Spectrom*. **2016**, 27, 50-58.

(33) Nicolardi, S.; Deelder, A. M.; Palmblad, M.; Burgt, Y. E. M. van der. *Anal*. *Chem*. **2014**, 86, 5376-5382

(34) Cramer, C. N.; Haselmann, K. F.; Olsen, J. V.; Nielsen, P. K. *Anal*. *Chem*. **2016**, 88, 1585-1592.

(35) Zhang, Y.; Cui, W.; Zhang, H.; Dewald, H. D.; Chen, H. *Anal*. *Chem*. **2012**, 84, 3838-3842.

(36) Roeser, J.; Bischoff, R.; Bruins, A. P.; Permentier, H. P. *Anal*. *Bioanal*. *Chem*. **2010**, 397, 3441-3455.

(37) Liuni, P.; Zhu, S.; Wilson, D. J. *Antioxid*. *Redox Signal*. **2014**, 21,497-510.

(38) Shevchenko, A.; Tomas, H.; Havlis, J.; Olsen, J. V.; Mann, M. *Nat*. *Protoc*. **2006**, *1*, 2856-2860.

(39) Vandermarliere, E.; Mueller, M.; Martens, L. *Mass Spectrom*. *Rev*. **2013**, *32*, 453-465.

(40) Olsen, J. V.; Ong, S.; Mann, M. *Mol*. *Cell*. *Proteomics* **2004**, *3*, 608-614.

(41) Crimmins, D. L.; Mische, S. M.; Denslow, N. D. *Curr*. *Protoc*. *Protein*. *Sci*. **2005**, *11*. 1-11.

(42) Li, A.; Sowder, R. C.; Henderson, L. E.; Moore, S. P.; Garfinkel, D. J.; Fisher, R. J. *Anal*. *Chem*. **2001**, *73*, 5395-5402.

(43) Tanabe, K.; Taniguchi, A.; Matsumoto, T.; Oisaki, K.; Sohma, Y.; Kanai, M. *Chem*. *Sci*. **2014**, *5*, 2747-2753.

(44) Zhang, Y.; Fonslow, B. R.; Shan, B.; Baek, M. C.; Yates, J. R., III *Chem*. *Rev*. **2013**, *113*, 2343-2394.

(45) Yates, J. R., III *J*. *Am*. *Chem*. *Soc*. **2013**, *135*, 1629-1640.

Chapter 2

Electrochemical protein cleavage in a microfluidic cell with integrated boron doped diamond electrodes

Abstract: Specific electrochemical cleavage of peptide bonds at the C-terminal side of tyrosine and tryptophan generates peptides amenable to liquid chromatography/tandem mass spectrometry (LC-MS/MS) analysis for protein identification. To this end we developed a microfluidic electrochemical cell of 160 nL volume that combines a cell geometry optimized for a high electrochemical conversion efficiency (>95 %) with an integrated boron doped diamond (BDD) working electrode offering a wide potential window in aqueous solution and reduced adsorption of peptides and proteins. Efficient cleavage of the proteins bovine insulin and chicken egg white lysozyme was observed at 4 out of 4 and 7 out of 9 of the predicted cleavage sites, respectively. Chicken egg white lysozyme was identified based on 5 electrochemically generated peptides using a proteomics database searching algorithm. These results show that electrochemical peptide bond cleavage in a microfluidic cell is a novel, fully instrumental approach towards protein analysis and eventually proteomics studies in conjunction with mass spectrometry.

Published as: Floris T.G. van den Brink, Tao Zhang, Liwei Ma, Johan Bomer, Mathieu Odijk, Wouter Olthuis, Hjalmar P. Permentier, Rainer Bischoff and Albert van den Berg. Electrochemical protein cleavage in a microfluidic cell with integrated boron doped diamond electrodes. (Equal first author). *Analytical Chemistry*, **2016**, 88, 9190-9198.

2.1 Introduction

The study of protein structures and interactions is key to the understanding of biological functions such as those related to health and the development of disease.[1] The large number of different species in the human proteome makes it particularly difficult to accurately identify and quantify proteins in complex biological matrices. Various methods based on liquid chromatography coupled to mass spectrometry (MS) have been developed to analyze complex protein mixtures from biological samples in a comprehensive manner.[2,3]

Cleaving proteins into defined peptide fragments is currently the main approach, often referred to as bottom-up proteomics. Information about the proteins, originally present in the sample, can be obtained in various ways, for example by peptide mass fingerprinting[4] or tandem MS (MS/MS) after chromatographic separation of the generated peptides. To this end experimental MS/MS spectra are compared to *in silico* generated spectra from protein sequence databases.[5] More challenging but of increasing importance is direct sequence analysis of the generated peptide fragments (*de novo* sequencing) without resorting to databases as well as the comparison of MS/MS spectra to an increasing number of spectral libraries.[6–8]

Highly specific cleavage of peptide bonds is critical for bottom-up proteomics. Enzymatic digestion using proteases is the most widespread method for cleavage of proteins at specific peptide bonds, and a number of proteases with different specificities are available. The most commonly used protease is the enzyme trypsin, which cleaves specifically at the C-terminal side of lysine and arginine (except if followed by a proline).[9] Alternatively, chemical cleavage may be used if specificity for a certain peptide bond or amino acid sequence is required for which no protease is available.[9]

Electrochemical protein cleavage is emerging as an instrumental alternative to chemical and enzymatic approaches. Over 50 years ago it was found that peptide bonds can be cleaved electrochemically at the C-terminal side of tyrosine.[10] Later, electrochemical

peptide bond cleavage at the C-terminal side of tryptophan was also described.[11] Compared to chemical and enzymatic protein cleavage, the electrochemical approach offers advantages of 1) being a rapid, purely instrumental approach that does not require additional reagents, 2) having a cleavage site specificity for which no enzymatic or chemical cleavage reagent is available, 3) opening the possibility to cleave proteins under conditions (e.g. strongly denaturing) that enzymes cannot tolerate and 4) providing the possibility to label reactive groups that are uniquely generated upon electrochemical cleavage.

It appeared early on that the choice of electrode material is crucial, as illustrated by electrochemical oxidation and cleavage of tyrosine- and tryptophan-containing dipeptides at platinum electrodes, where strong adsorption was observed.[12] Electrochemical peptide bond cleavage continued to be investigated using flow-through (coulometric) cells with porous graphite electrodes. Coupling these cells on-line to electrospray ionization mass spectrometry (ESI-MS) resulted in a system for rapid peptide analysis capable of tyrosine-specific oxidation and peptide bond cleavage, as demonstrated with a variety of peptides.[13] Following these investigations, the oxidation and cleavage mechanisms of tyrosine- and tryptophan-containing tripeptides were studied in detail.[14] Main challenges were that cleavage yields were limited due to competing oxidation reactions and recoveries were hampered due to adsorption, as exemplified for the tryptophan-containing decapeptide adrenocorticotropic hormone (ACTH) (1-10).[13] Despite these initial shortcomings, electrochemical peptide bond cleavage was successfully combined with liquid chromatography in an EC-LC-MS/MS set-up for protein analysis.[15] Problems with adsorption at the electrode surface and limited cleavage yields were aggravated in the case of proteins, requiring extensive regeneration of the porous graphite electrode surface and careful optimization of the reaction conditions to observe peptide bond cleavage.

Electrochemical peptide bond cleavage was subsequently achieved in thin-layer (amperometric) flow cells with glassy carbon (GC) and boron doped diamond (BDD) elec-

trodes.[16] Notably, BDD electrodes performed better in terms of lower adsorption, resulting in higher cleavage yields due to both a better recovery of products and a lower degree of dimer formation. Thin-layer cells are often equipped with disc electrodes over which the analyte is directed in a thin layer of liquid. The performance of thin-layer electrochemical cells in terms of conversion efficiency depends on the contact time between the analyte and the electrode surface, which in turn is determined by the time needed for the analyte to diffuse to the surface in relation to its residence time in the electrochemical cell. This ratio can be significantly shifted in favor of electrochemical conversion by reducing the cell dimensions to microfluidic length scales. Employing microfabrication technologies based on photolithography enables shorter diffusion distances, reduced cell volumes and rapid sample processing.[17] Design aspects and various applications of microfluidic electrochemical cells coupled to MS have been described previously.[18] Based on these principles, microfluidic electrochemical cells with an integrated platinum three-electrode system have been developed in our group to study drug metabolites in EC-MS experiments.[19–21] While this kind of cells may also be exploited for peptide bond cleavage, platinum electrodes are not suitable for applications involving peptides and proteins due to adsorption at the surface.[22]

While pure synthetic diamond is an insulator, it can be made conductive by appropriate doping.[23] Research on conductive diamond for electrochemical measurements started in the 1980s with ion implanted electrodes,[24] while Swain *et al*. extensively characterized the electrochemical properties of as-grown (untreated) poly-crystalline BDD.[25] BDD exhibits various striking physical, chemical and electrical properties, making it an attractive material for a variety of electrochemical applications. These include its mechanical stability, optical transparency, high chemical inertness, low double layer capacitance and background currents, and large overpotentials for hydrogen and oxygen evolution.[26] The electrochemical properties of BDD electrodes can be further tailored to specific needs through a myriad of different surface modifications. These, along with BDD synthesis and characterization techniques, have been extensively reviewed.[27–30]

In our current research, we integrated BDD electrodes into microfluidic electrochemical cells to combine the benefits of BDD with the advantages of a microfluidic electrochemical cell design for peptide bond cleavage. There have been a few reports on microstructuring BDD, such as laser micromachining,[31] lift-off,[32] or dry etching techniques.[33–36] Using inductively coupled plasma etching with O_2/Ar, Forsberg *et al*. fabricated BDD microband electrodes for electrochemical detection in poly(dimethylsiloxane) (PDMS) microchannels,[37] demonstrating the superior robustness and stability of BDD compared to gold electrodes. However, the PDMS channels could not be reused, possibly due to problems of analyte adsorption at PDMS, preventing repeated, sensitive electrochemical measurements.

Here we report for the first time on the design and fabrication of a robust and reusable glass-based microfluidic electrochemical cell with integrated BDD electrodes. This cell was used for peptide bond cleavage at the C-terminal side of tyrosine and tryptophan in the tripeptides leucine-tyrosine-leucine (LYL) and leucine-tryptophan-leucine (LWL). By coupling the device on-line to a high-resolution mass spectrometer, the relation between electrode potential and peptide bond cleavage was studied using a "mass voltammogram". We further show that hydroxyl radicals ($^{\bullet}$OH) can be generated on BDD at elevated potentials, providing an alternative oxidation mechanism. This became evident from the aromatic hydroxylation of phenylalanine in the para-position to yield tyrosine in the tripeptide leucine-phenylalanine-leucine (LFL) with subsequent peptide bond cleavage. Applicability of the microfluidic cell to larger peptides and proteins is shown by specific cleavage of peptide bonds at the C-terminal side of tyrosine and tryptophan in ACTH 1-10, bovine insulin and lysozyme from chicken egg white, demonstrating the possibility of developing this into a novel device for protein analysis and proteomics research.

2.2 Experimental section

2.2.1 Microfluidic electrochemical cell fabrication

The electrochemical cell is constructed from two wafers: the first is a BDD-on-insulator wafer containing electrodes and microchannels, the second is a borosilicate glass wafer that contains access holes for electrical and fluidic connectivity and additional microfluidic structures. In the latter, 5 µm deep structures were etched in a deep reactive ion etching process followed by powder blasting the access holes. To prepare the BDD-on-insulator wafer, 300 nm SiO_2 and 75 nm Si_3N_4 were grown on a *p*-type silicon wafer. Following this, a 300 nm thick diamond layer with a 10000 ppm boron doping was grown in a process performed by Neocoat SA (La Chaux-de-Fonds, Switzerland). Here, diamond nuclei were seeded at high density, after which the BDD layer was grown in a hot-filament chemical vapor deposition process using CH_4 and trimethylboron in H_2. The BDD working and counter electrodes were structured using an O_2 reactive ion etching (RIE) process. Next, contact pads and reference electrodes were made from sputtered platinum (120 nm) on a tantalum (10 nm) adhesion layer in a lift-off process. Channel structures were patterned over the electrodes in a 5 µm thick layer of SU-8, upon which the two wafers were immediately aligned and bonded together at elevated pressure and temperature in an anodic bond tool (EV-501, EVG, Austria). Finally, the bond strength was increased at 180 °C and 19 kg/cm² for 1 h using a hydraulic press (model 3889, Carver Inc., USA).

2.2.2 Chemicals

The tripeptides LWL and LYL were obtained from Research Plus Inc. (Barnegat, USA). LFL was purchased from Bachem (Weil am Rhein, Germany). Potassium ferricyanide, potassium ferrocyanide, potassium nitrate (KNO_3), potassium dihydrogen phosphate, dipotassium hydrogenphosphate, 1,1'-ferrocenedimethanol, human adrenocorticotropic hormone (ACTH) 1-10 (SYSMEHFRWG), chicken egg white lysozyme, insulin from bovine pancreas, iodoacetamide (IAM), dithiothreitol (DTT), ammonium

bicarbonate (99.5 %) and formic acid (98 %) were obtained from Sigma Aldrich (Steinheim, Germany). Acetonitrile (HPLC SupraGradient grade) was purchased from Biosolve (Valkenswaard, The Netherlands). Water was purified by a Millipore system (resistivity 18.2 MΩ·cm, Millipore Corp., Billerica, USA). See Supporting Information 1 for sample preparation procedures.

2.2.3 Instrumentation and Measurements

Prior to use, the microfluidic electrochemical cell was flushed with electrolyte solution followed by cyclic voltammetry scans (-2 to 2 V, 100 mV/s) until reproducible CVs were obtained. Analyte solutions were introduced at a total flow rate of 2 µL/min using a syringe pump (Nemesys, Cetoni, Korbussen, Germany) installed in a Lab-in-a-Suitcase.[38] Cyclic voltammetric and chronoamperometric measurements to characterize the microfluidic electrochemical cells were done using a potentiostat (SP 300, Bio-Logic, Claix, France). UV/vis absorbance measurements were done in a 2.4 µL cell with an optical path length of 10 mm (LWCC-M-10, World Precision Instruments), a deuterium lamp as light source (DH-2000, Ocean Optics) and a UV/vis spectrometer (Maya 2000 Pro, Ocean Optics).

Mass voltammograms of LWL, LYL and LFL were recorded on-line by ramping the cell potential linearly from 0 to 2500 mV at a scan rate of 2 mV/s using a portable potentiostat (SP 200, Bio-Logic, Claix, France). A metal union connected to electrical ground was placed between the chip outlet and electrospray needle to decouple the electrochemical cell from the high voltage ESI interface. For ACTH 1-10, insulin and lysozyme, the potential was ramped from 0 to 2000 mV under otherwise equal conditions. The electrochemical oxidation and cleavage products were analyzed using an LTQ-Orbitrap XL mass spectrometer (Thermo Scientific, Bremen, Germany). The transit time of 1.5 min between product formation within the electrochemical cell and mass spectrometric detection was taken into account when the cell potential was synchronized with MS signal intensities.

Cleavage at constant potentials was done under conditions identical to the on-line EC-MS experiments using 1300 mV (LWL) or 2000 mV (LYL, insulin and lysozyme). Cleavage of ACTH 1-10 was performed at two different constant potentials of 700 and 1100 mV. Oxidation of LFL by $^{\bullet}$OH radicals was shown to occur at a constant potential of 2000 mV. The reaction product mixtures were collected and diluted with water to 2.5 µM (LWL, LYL, LFL, ACTH 1-10 and insulin) and 1 µM (lysozyme) and analyzed by LC-MS/MS. The cleavage yield was calculated from the peak area of the cleavage product (A_{cl}) and the total area of the peaks of uncleaved tyrosine and tryptophan oxidation products (A_{ox}):

$$Yield = \left|\frac{A_{cl}}{A_{cl}+A_{\mathrm{ox}}}\right| \cdot 100\ \% \qquad 1$$

LC-MS/MS analyses of cleavage product mixtures were performed LC systems coupled to an LTQ-Orbitrap XL mass spectrometer. The tripeptides and ACTH 1-10 were separated using a Dionex Ultimate 3000 nano-LC system equipped with an Acclaim Pepmap column (150 mm x 75 µm (length x i.d.), Thermo Scientific, Bremen, Germany) with a 40 min gradient of 2-50 % acetonitrile in water/0.1 % formic acid at a flow rate of 300 nL/min. Electrochemically cleaved insulin and reduced and alkylated lysozyme were separated using an HPLC system equipped with a Shim-pack XR-ODS column (50 mm x 2.0 mm (length x i.d.), Shimadzu, Kyoto, Japan) with a 30 min gradient of 2-60 % acetonitrile in water/0.1 % formic acid at a flow rate of 300 µL/min. See Supporting Information 1 for MS equipment settings and SwissProt (chicken) database search engine parameters (PEAKS version 7.5, Bioinformatics Solutions Inc).

2.3 Results and Discussion

2.3.1 Microfluidic electrochemical cell design

A photo and exploded view of the three-electrode microfluidic electrochemical cell are shown in **Figure 1A** and **B**, respectively. The device consists of four layers with micro-fabricated structures, which are constituted as shown in **Figure 1C**; **I**) a BDD-on-

insulator wafer with the working electrode (WE) and counter electrode (CE) structured in BDD, **II**) the pseudo-reference electrode (pRE) and electrical contact pads made from platinum, **III**) microchannel structures in SU-8, and **IV**) a borosilicate glass wafer with powder blasted access holes and etched microfluidic structures.

Following the inlet of the electrochemical cell, a T-junction directs the flow into two separate channels-one located above the WE and the other located above the CE (see **Figure 1D**). This ensures separation of the respective reaction products. The pRE is located in close proximity to the WE (300 µm distance) just before the junction to minimize the electrolyte resistance between these two electrodes and prevent unwanted Ohmic drop.

The conversion performance of a thin-layer type electrochemical cell can be related to a dimensionless number in analogy to the performance of a separation column, which is usually described by the number of equilibrium stages (theoretical plates). For thin-layer electrochemical cells, this plate number (N_{tl}) can be defined as a function of both the residence time of a molecule above the electrode (t_{res}) and the time it takes for this molecule to diffuse to reach the electrode surface (t_d).[18] This number is therefore a function of cell geometry (channel height (h), and length of the channel in contact with the electrode (l)), the diffusion coefficient of the respective molecule (D) and the average flow velocity ($\bar{u}$). Alternatively, N_{tl} can be calculated using the liquid volume in contact with the electrode (V) and the volumetric flow rate (Q):

$$N_{tl} = \frac{t_{res}}{t_d} = \frac{2Dl}{\bar{u}h^2} = \frac{2DV}{Qh^2} \qquad 2$$

Based on these considerations related to mass transport, we designed a cell with shallow, long meandering channels having a width (w) of 200 µm, h=5 µm and l=24 mm. The cell is typically operated using a 1 µL/min flow rate over the WE and the volume above the WE is 24 nL. Using **Equation 2** with D=1.1·10^{-10} m^2/s for lysozyme,[39] we find that N_{tl}=13, indicating that a high electrochemical conversion efficiency can be expected compared to most regular thin-layer flow cells, which have a N_{tl}<1 for this

compound.[18] From a practical point of view, it is clear that the channel height is the most important length scale that determines the electrochemical cell's conversion performance, and therefore it is essential that this dimension can be accurately controlled in the microfabrication process.

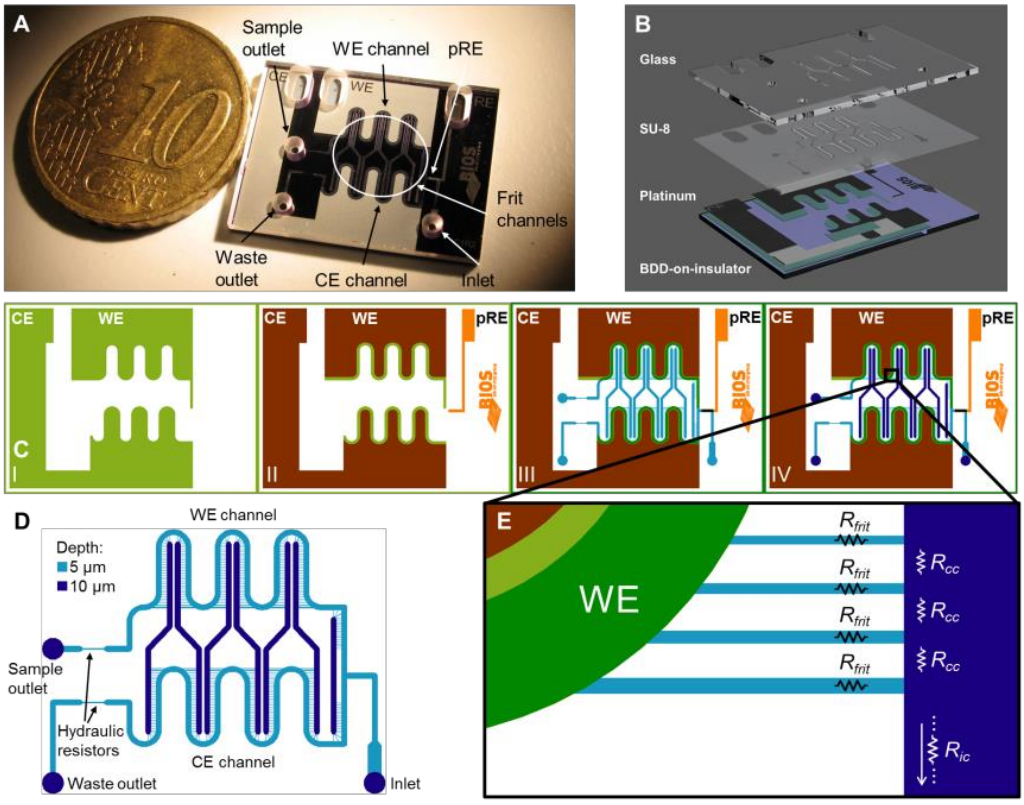

Figure 1. Schematic representation of the microfluidic electrochemical cell. A: Photo of an assembled device. B: Exploded view of the cell, showing the different layers of structures. C: Layers of structures containing a BDD working electrode (WE) and counter electrode (CE) (I), a Pt pseudo-reference electrode (pRE) and Pt contact pads (II). Microchannels were prepared in 5 µm thick SU-8 using photolithography (III) and additional 5 µm deep microfluidic structures and access holes were etched and powder blasted, respectively, in borosilicate glass (IV). D: Schematic diagram of fluidic structures, indicating the channels located on top of the WE and CE. E: Expanded view of part of the WE and frit channel network.

2.3.2 BDD material and microfluidic electrochemical cell characterization

The potential window of BDD electrodes was determined off-chip with a 0.1 M KNO_3/10 mM phosphate buffer (pH 7.4) solution. A micro-structured BDD WE (4.8 mm^2), using only the bottom part of a chip without the glass top layer (see **Figure 1B** and **C**) was compared to a platinum WE (2.5 mm^2) in a macroscopic (regular) electrochemical cell having a platinum CE and a commercially available KCl saturated Ag/AgCl RE. Cyclic voltammograms (CVs) recorded at 100 mV/s with both WEs (**Figure 2A**) show that the BDD electrode has a mainly featureless CV over a potential range of -2 to 2.2 V, providing a potential window of 4.2 V, while this is only 2.6 V for platinum due to the onset of water electrolysis. The small anodic current peak in the CV of the BDD electrode just before the onset of oxygen evolution has been reported to originate from the oxidation of non-diamond carbon impurities at the surface.[40] To take maximum advantage of the electrochemical properties of this material, both WE and CE of the microfluidic cell were made from BDD to minimize the extent of gas bubble formation in the microchannels at elevated potentials.

Electrochemical conversion efficiency was characterized by UV/vis spectroscopy using 0.45 mM/0.45 mM ferri-/ferrocyanide in a 0.1 M KNO_3/10 mM phosphate buffer (pH 7.4) solution introduced at a flow rate of 2 µL/min. Ferricyanide absorbs at 418 nm, allowing calculation of the conversion efficiency (η) from the absorbance peak heights during oxidation and reduction (A_{ox} and A_{red}, respectively) with respect to the initial absorbance (A_0):

$$\eta = \left|\frac{A_{ox/red} - A_0}{A_0}\right| \cdot 100\ \% \qquad 3$$

Figure 2B shows the absorbance measurements at 418 nm as a function of time. After absorbance has stabilized at the initial value, 1 V is applied to the WE for 5 min. Subsequently, the potential is switched back to open circuit potential (E_{ocp}) for 10 min, after which -1 V is applied for 5 min. For this redox couple, an oxidation efficiency of 97 % and a reduction efficiency of 95 % was calculated.

To be able to relate the protein cleavage potentials in the microfluidic electrochemical cell to a KCl saturated Ag/AgCl reference electrode, the Pt pRE was calibrated using 1,1'-ferrocenedimethanol. The potential of the platinum pRE was determined to be 225 mV vs. Ag/AgCl (KCl saturated) in 89/10/1 (v/v/v) water/acetonitrile/formic acid (pH 2.0) and 196 mV vs. Ag/AgCl (KCl saturated) in 85/10/5 (v/v/v) water/acetonitrile/formic acid (pH 1.5). See **Supplementary Information S2**.

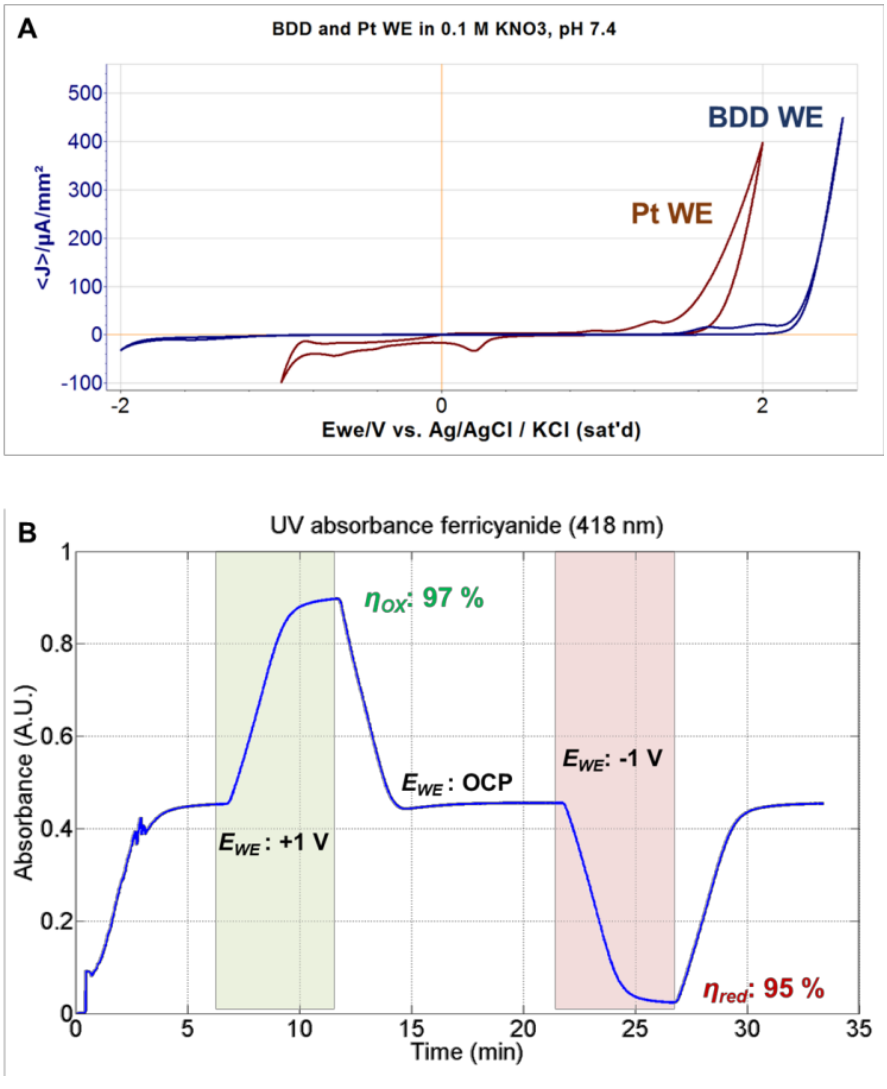

Figure 2. A: Determination of the potential window of a micro-structured BDD WE compared to a platinum WE in a regular electrochemical cell setup containing 0.1 M KNO_3/10 mM phosphate buffer solution (pH 7.4). CVs were recorded at a scan rate of 100 mV/s using a saturated Ag/AgCl

RE and a platinum CE. B: Optical absorbance measurements of ferricyanide using 0.45 mM/0.45 mM ferri-/ferrocyanide in 0.1 M KNO_3/10 mM phosphate buffer solution (pH 7.4), which was introduced at a flow rate of 2 µL/min.

2.3.3 Electrochemical cleavage of tripeptides

Two different tripeptides (LWL and LYL) were employed to study the specific electrochemical cleavage of peptide bonds C-terminal to tyrosine and tryptophan in the microfluidic electrochemical cell. First, electrochemical oxidation and cleavage products were generated from the peptides LWL and LYL using a linear potential sweep in an on-line EC-MS experiment. The measured mass voltammograms allowed determination of the potential range over which cleavage occurred. Electrochemical oxidation and cleavage mechanisms, previously published by Roeser *et al*., [4] are shown in **Scheme S3**.

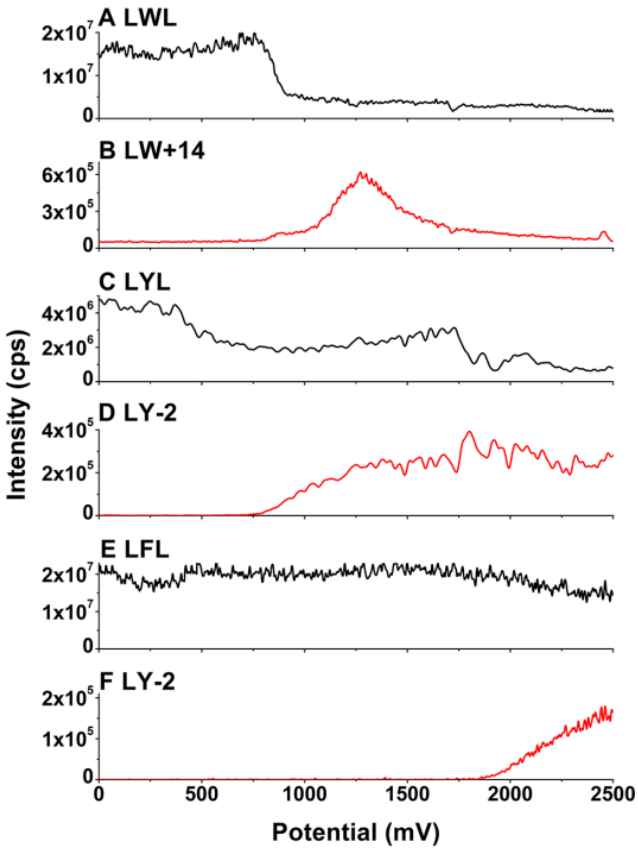

Figure 3. Electrochemical cleavage of LWL, LYL and LFL. On-line EC-MS voltammograms of LWL, LYL and LFL (10 μM in 85/10/5 (v/v/v) water/acetonitrile/formic acid) were recorded by ramping the potential from 0 to 2500 mV at a scan rate of 2 mV/s. Traces were extracted and plotted versus cell potential for A: LWL (*m/z* 431.27), B: LW+14 (*m/z* 332.16), C: LYL (*m/z* 408.25), D: LY-2 (*m/z* 293.15), E: LFL (*m/z* 392.26) and F: The LFL cleavage product LY-2 (*m/z* 293.15).

A decrease of the LWL signal in **Figure 3A** indicated the onset of electrochemical oxidation at ~800 mV. Oxidation efficiency increased further with increasing WE potential. Signal intensity for the cleavage product (LW+14) reached a maximum at 1300 mV, followed by a decrease at higher potentials (**Figure 3B**) likely due to the formation of other oxidation products. LC-MS analysis of the reaction products of LWL generated at 1300 mV revealed an oxidation yield of 95 %, which is determined from a decrease in LWL signal intensity, and a cleavage yield of 50 % (see LC-MS chromatograms in **Figure S4** and **Equation 1**).

Electrochemical oxidation of LYL started at ~450 mV (**Figure 3C**). However, compared to LWL, oxidation yield was lower and spread over a potential range from 500-1750 mV. Signal intensity for LYL decreased a second time at 1750 mV, which may be attributed to further oxidation by hydroxyl radicals (see also results obtained with LFL, **Figure 3E** and **F**). Formation of the cleavage product LY-2 started at 750 mV and increased until 1250 mV after which signal intensity remained rather stable up to the upper limit of the voltammogram at 2500 mV (**Figure 3D**). LC-MS analysis of the reaction products of LYL generated at 2000 mV revealed an oxidation yield of 100 % and a cleavage yield of 30 % (see LC-MS chromatograms in **Figure S5** and **Equation 1**).

LFL was used to monitor the formation of hydroxyl radicals at the BDD electrode. Previously, it was shown that LFL can be cleaved after conversion to LYL through hydroxylation at the para-position of the phenyl group.[16] A slight decrease in signal intensity of LFL at 1750-2500 mV indicated that it was converted (**Figure 3E**). As

proof of aromatic hydroxylation, the cleavage product LY-2 appeared at 1850 mV, and its abundance increased until the upper limit of the potential range of 2500 mV (**Figure 3F**). LC-MS analysis of the reaction products of LFL generated at 2000 mV showed an oxidation yield of ~8 % and a yield of the subsequent cleavage of LYL of ~30 % (see LC-MS chromatograms in **Figure S6** and **Equation 1**).

2.3.4 Electrochemical cleavage of ACTH 1-10

To see whether the microfluidic electrochemical cell could also be used to cleave peptide bonds in larger peptides, ACTH 1-10 (SYSMEHFRWG), which has one tyrosine and one tryptophan, was studied using on-line EC-MS. Mass voltammograms show that cleavage of the peptide bond at the C-terminal side of tryptophan occurred first, starting at a potential of 600 mV and reaching maximum signal intensity at 730 mV (see **Figure 4**). Cleavage at the C-terminal side of tyrosine started at 730 mV and reached maximum signal intensity between 1000 and 1250 mV. These results show that selectivity in peptide bond cleavage may be achieved by controlling the applied potential and notably by addressing tryptophan alone or tryptophan and tyrosine together. Cleavage products generated at 700 mV and 1100 mV were analyzed by LC-MS. The tryptophan cleavage product (SYSMEHFRW+14) was observed upon electrochemical cleavage at 700 mV, while both SYSMEHFRW+14 and the combined tryptophan and tyrosine cleavage product (SMEHFRW+14) were observed at 1100 mV (see **Figure S7** for LC-MS chromatograms).

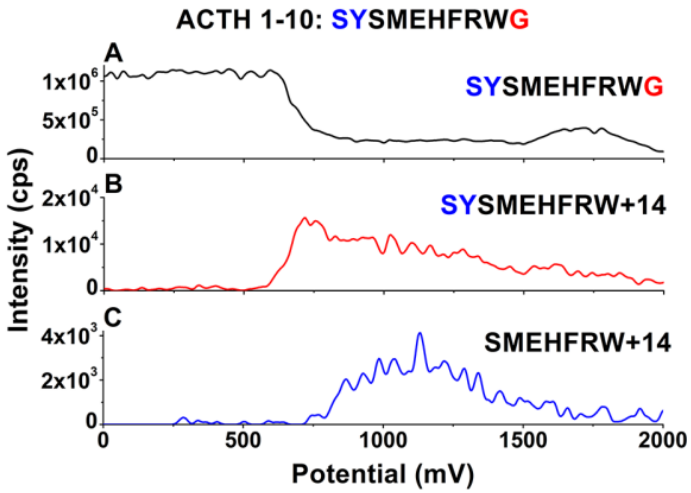

Figure 4. Electrochemical cleavage of ACTH 1-10 (SYSMEHFRWG), which has one tyrosine and one tryptophan. On-line mass voltammograms of ACTH 1-10 (10 µM in 89/10/1 (v/v/v) water/acetonitrile/formic acid) were recorded by ramping the potential from 0 to 2000 mV with a scan rate of 2 mV/s. Traces were extracted and plotted versus cell potential for A: ACTH 1-10 (*m/z* 433.86, charge 3+), B: SYSMEHFRW+14 (*m/z* 419.51, charge 3+) and C: SMEHFRW+14 (*m/z* 336.14, charge 3+).

2.3.5 Electrochemical cleavage of insulin

Electrochemical cleavage of bovine insulin was studied to see whether the approach could be extended to a significantly more complex molecule. Insulin is composed of 51 amino acids, including 4 tyrosines (numbered 1 to 4 and indicated in red in **Figure 5A**), which are assembled in 2 chains (A and B) that are linked by 2 disulfide bonds, while chain A has an additional internal disulfide bond. Mass voltammograms recorded using on-line EC-MS analysis (**Figure S8**) show that cleavage occurs over the potential range from 1200 to 2000 mV. Three cleavage products were detected: the C-terminal peptide formed upon cleavage at site 4 (TPKA), the peptide formed upon cleavage at sites 1 and 2 (QLENY-2) and the N-terminal parts of the A and B chains released upon cleavage at sites 1 and 3, which are linked together by a disulfide bond (A(1-14)+B(1-16)). The cleavage products generated at 2000 mV were analyzed and identified using LC-MS

(see **Figure 5**). These results show that peptide bonds at all 4 tyrosines in insulin were cleaved at the BDD electrode of the microfluidic electrochemical cell, in accordance with earlier work of Permentier and Bruins reporting the electrochemical cleavage of insulin in a flow-through cell equipped with a porous graphite electrode.[15]

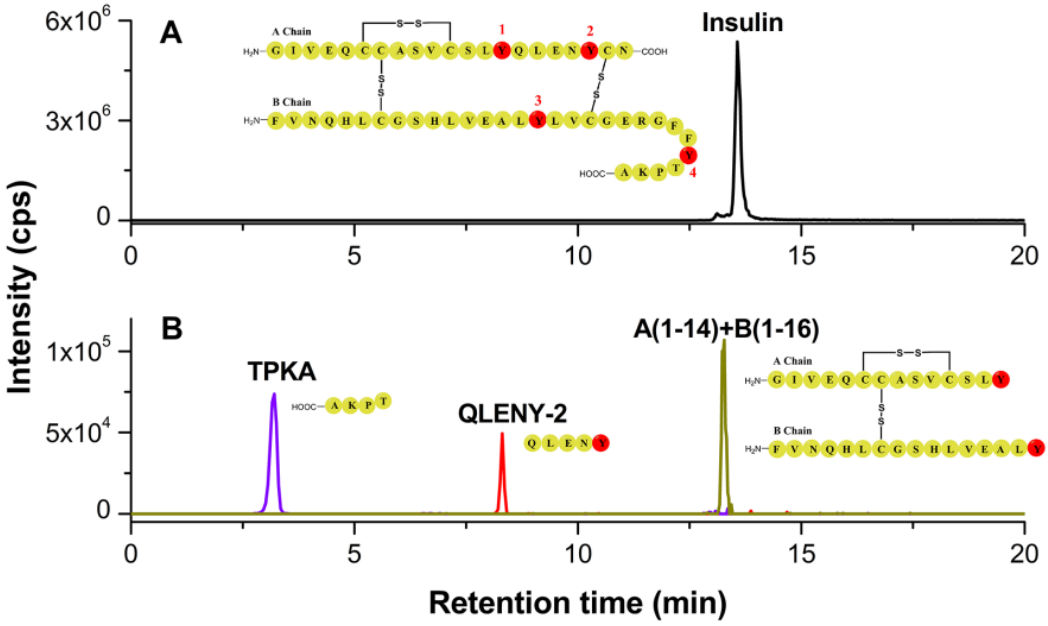

Figure 5. Electrochemical cleavage of insulin, which contains four tyrosine residues (shown in red). Insulin (10 µM in 85/10/5 (v/v/v) water/acetonitrile/formic acid) was electrochemically cleaved at 2000 mV. A: Extracted ion chromatogram of insulin (*m/z* 1146.93, charge 5+) and B: Combined extracted ion chromatograms of the cleavage products TPKA (*m/z* 208.63, charge 2+), QLENY-2 (*m/z* 664.29, charge 1+) and A (1-14)+B(1-16) (*m/z* 1099.16, charge 3+).

2.3.6 Electrochemical cleavage of lysozyme

To investigate whether electrochemically-mediated cleavage is applicable to a protein, lysozyme was studied, containing 129 amino acids with 3 tyrosines and 6 tryptophans, and 4 internal disulfide bridges. To facilitate cleavage, disulfide bonds were reduced and free SH groups alkylated with iodoacetamide prior to electrochemical oxidation.[15]

Mass voltammograms of lysozyme recorded using on-line EC-MS (**Figure S9**) indicated that two distinct potential regions exist, in which the MS signal intensity for lysozyme decreased first by 60 % followed by a further decrease towards zero at higher potentials. It appeared that electrochemical cleavage at site 3 (a tryptophan, see table 1 for numbering of cleavage sites) occurred between 800 and 1000 mV, resulting in the peptide KVFGRC(+57)ELAA-AMKRHGLDNY-RGYSLGNW+14, and that cleavage at site 9 started at 1900 mV, resulting in the peptide IRGCRL released from the C-terminus of the protein.

This potential-dependence indicates again that some selectivity can be achieved, as already observed for ACTH 1-10. Table 1 presents an overview of the eight identified cleavage products of lysozyme that were generated after peptide bond cleavage at 7 out of 9 possible sites (2 out of 3 tyrosines and 5 out of 6 tryptophans) at a potential of 1000 mV and 2000 mV. See **Figure S10** for LC-MS chromatograms. The database search algorithm PEAKS was used for protein identification using a chicken protein sequence database (*Gallus gallus* (chicken), SwissProt) resulting in a single significant match to lysozyme based on 5 identified peptides (peptides marked with validation P in **Table 1**). Manual inspection allowed the identification of 2 additional peptides (marked with M in **Table 1**), which were filtered out by PEAKS because of their short length. These results indicate that the microfluidic electrochemical cell has the potential to be used for protein and proteomics research.

The first report on the electrochemical cleavage of lysozyme described cleavage between two tryptophan residues (site 5) using a graphite rod anode.[11] In later work Permentier and Bruins observed four peptides upon electrochemical digestion of lysozyme on a porous graphite electrode.[15] Comparing our results to earlier data, we see that the same 5 out of 6 tryptophan and 2 out of 3 tyrosine residues were cleaved in both the work of Permentier and these experiments. However, a larger number of peptides of increased length were recovered from the microfluidic electrochemical cell, which is especially relevant for confident protein identification. This improvement is likely due

to reduced adsorption at BDD working electrodes compared to porous graphite electrodes used in earlier studies and a high electrochemical conversion efficiency of our thin-layer cell in microfluidic format.

Table 1. Electrochemical cleavage of chicken egg white lysozyme (reduced and alkylated with iodoacetamide). Chicken egg white lysozyme contains 3 tyrosine and 6 tryptophan residues which are numbered as cleavage sites 1 to 9. Lysozyme (2 µM in 85/10/5 (v/v/v) water/acetonitrile/formic acid) was electrochemically cleaved at 1000 and 2000 mV.

Full sequence of chicken egg white lysozyme (reduced and alkylated with IAM)

KVFGRC[a]ELAA AMKRHGLDNY[1] RGY[2]SLGNW[3]VC[a] AAKFESNFNT QATNRNTDGS

TDY[4]GILQINS RW[5]W[6]C[a]NDGRT GSRNLC[a]NIPC[a] SALLSSDITA SVNC[a]AKKIVS

DGNGMNAW[7]VA W[8]RNRC[a]KGTDV QAW[9]IRGC[a]RL

Detected cleavage products	Cleavage site	Validation[b]	Monoisotopic mass (Da)	Cleavage potential[c] (mV)
SLGNW[3]+14	2, 3	M	589.2567	2000
KVFGRC[a]ELAAAMKRHGLDNY[1]RGY[2]SLGNW[3]+14	3	P	3283.5920	1000
VC[a]AAKFESNFNTQATNRNTDGSTDY[4]-2	3, 4	P	2808.2042	2000
VC[a]AAKFESNFNTQATNRNTDGSTDY[4]GILQINSRW[5]+14	3, 5	P	3891.8066	2000
GILQINSRW[5]+14	4, 5	P	1098.5774	2000
VAW[8]+14	7, 8	M	388.1820	2000
RNRC[a]KGTDVQAW[9]+14	8, 9	(P)	1503.7005	2000
IRGC[a]RL	9	P	773.4327	2000

[a)] Cysteine(C) was alkylated with iodoacetamide after reduction of disulfide bonds with dithiothreitol.

[b)] P: validation by database search algorithm PEAKS; (P): validation by database search algorithm PEAKS with a low score; M: validation manually by MS/MS spectra.

[c)] Cleavage potential: the potential at which the highest intensity of cleavage product signals was observed.

2.4 Conclusions

In this work we demonstrate the development and use of a microfluidic electrochemical cell for protein identification studies. To this end, peptides and proteins were cleaved electrochemically in a microfluidic cell equipped with integrated BDD electrodes and a volume of 160 nL. Advantages of the cell design and the superior properties of BDD were exploited to be able to generate lysozyme cleavage products that allowed us to identify this protein by interrogating a sequence database as a proof of concept for future proteomics studies.

Tripeptides (LWL and LYL) were used to demonstrate specific electrochemical peptide bond cleavage at the C-terminal side of tyrosine and tryptophan, followed by cleavage of the decapeptide ACTH (1-10), which contains both a tyrosine and a tryptophan residue. Peptide bond cleavage was found to be potential-dependent with tryptophan being cleaved at a lower potential than tyrosine suggesting that some selectivity may be obtained by varying the potential. Next, bovine insulin was cleaved at all 4 tyrosines, and finally chicken egg white lysozyme was successfully identified in the UniProt_SwissProt database based on 5 electrochemically generated peptides. For each compound, mass voltammograms recorded using an on-line EC/MS set-up allowed rapid screening for cleavage potentials using small amounts of sample (33-42 μL), after which electrochemically generated peptides were analyzed in more detail using LC-MS/MS.

Further improvements will be needed to increase cleavage yield. The possibility of a chemical labelling approach based on the reactive spirolactone at the C-terminus of the cleaved peptides to introduce affinity tags for enrichment opens further possibilities even in the absence of complete electrochemical peptide bond cleavage. The observed dependence of peptide bond cleavage on the applied potential opens further possibilities to achieve some selectivity. In this context it is interesting to note that, while cleavage at sites 3 and 9 in lysozyme occurred C-terminal to tryptophan, the potentials required for cleavage were different. While the potential providing the highest cleavage yield at site

3 was similar to that observed for ACTH 1-10 (700-800 mV), cleavage at site 9 required more than 1900 mV. This indicates that other parameters, such as sequence context, may contribute to defining the cleavage potential in addition to whether a tryptophan or tyrosine peptide bond needs to be cleaved. Electrochemical protein cleavage in a microfluidic format could thus become an attractive, fully instrumental approach for protein digestion in proteomics research applications and the analysis of biopharmaceuticals.

2.5 References

(1) Sobott, F.; Robinson, C. V. *Curr*. *Opin*. *Struct*. *Biol*. **2002**, *12* (6), 729-734.

(2) Trauger, S. A.; Webb, W.; Siuzdak, G. *Spectroscopy*. 2002, pp 15-28.

(3) Wysocki, V. H.; Resing, K. A.; Zhang, Q.; Cheng, G. *Methods* **2005**, *35*, 211-222.

(4) Henzel, W. J.; Watanabe, C.; Stults, J. T. *J*. *Am*. *Soc*. *Mass Spectrom*. **2003**, *14* (9), 931-942.

(5) Cottrell, J. S. *J*. *Proteomics* **2011**, *74* (10), 1842-1851.

(6) Ma, B.; Johnson, R. *Mol*. *Cell*. *Proteomics* **2012**, *11* (2), 1-16.

(7) Lam, H.; Deutsch, E. W.; Eddes, J. S.; Eng, J. K.; King, N.; Stein, S. E.; Aebersold, R. *Proteomics* **2007**, *7*, 655-667.

(8) Lam, H.; Deutsch, E. W.; Eddes, J. S.; Eng, J. K.; Stein, S. E.; Aebersold, R. *Nat*. *Methods* **2008**, *5* (10), 873-875.

(9) Maleknia, S. D.; Johnson, R. In *Amino Acids, Peptides and Proteins in Organic Chemistry*; Hughes, A. B., Ed.; Wiley-VCH, 2012; Vol. 5, pp 1-50.

(10) Iwasaki, H.; Cohen, L. A.; Witkop, B. *J*. *Am*. *Chem*. *Soc*. **1963**, *85* (22), 3701-3702.

(11) Walton, D. J.; Richards, P. G.; Heptinstall, J.; Coles, B. *Electrochim*. *Acta* **1997**, *42* (15), 2285-2294.

(12) MacDonald, S. M.; Roscoe, S. G. *Electrochim*. *Acta* **1997**, *42* (8), 1189-1200.

(13) Permentier, H. P.; Jurva, U.; Barroso, B.; Bruins, A. P. *Rapid Commun*. *Mass Spectrom*. **2003**, *17* (14), 1585-1592.

(14) Roeser, J.; Permentier, H. P.; Bruins, A. P.; Bischoff, R. *Anal*. *Chem*. **2010**, *82* (18), 7556-7565.

(15) Permentier, H. P.; Bruins, A. P. *J*. *Am*. *Soc*. *Mass Spectrom*. **2004**, *15* (12), 1707-1716.

(16) Roeser, J.; Alting, N. F. A.; Permentier, H. P.; Bruins, A. P.; Bischoff, R. *Anal*. *Chem*. **2013**, *85*, 6626-6632.

(17) van den Brink, F. T. G.; Büter, L.; Odijk, M.; Olthuis, W.; Karst, U.; van den Berg, A. *Anal*. *Chem*. **2015**, *87* (3), 1527-1535.

(18) van den Brink, F. T. G.; Olthuis, W.; van den Berg, A.; Odijk, M. *TrAC Trends Anal*. *Chem*. **2015**, *70*, 40-49.

(19) Odijk, M.; Baumann, A.; Lohmann, W.; van den Brink, F. T. G.; Olthuis, W.; Karst, U.; van den Berg, A.

Lab Chip **2009**, *9* (12), 1687-1693.

(20) Odijk, M.; A.Baumann; W.Olthuis; van den Berg, A.; Karst, U. *Biosens*. *Bioelectron*. **2010**, *26* (4), 1521-1527.

(21) Odijk, M.; Olthuis, W.; van den Berg, A.; Qiao, L.; Girault, H. *Anal*. *Chem*. **2012**, *84* (21), 9176-9183.

(22) Odijk, M. Miniaturized electrochemical cells for applications in drug screening and protein cleavage, University of Twente, 2011.

(23) Fujimori, N.; Doi, A.; Inai, T. *Vacuum* **1986**, *36*, 99-102.

(24) Iwaki, M.; Sato, S.; Takahashi, K.; Sakairi, H. *Nucl*. *instruments methods Phys*. *Res*. **1983**, *209-210* (Pt 2), 1129–1133.

(25) Swain, G. M.; Ramesham, R. *Anal*. *Chem*. **1993**, *65* (4), 345–351.

(26) Xu, J.; Granger, M. C.; Chen, Q.; Strojek, J. W.; Lister, T. E.; Swain, G. M. *Anal*. *Chem*. **1997**, *69* (19), 591A-597A.

(27) Compton, R. G.; Foord, J. S.; Marken, F. *Electroanalysis* **2003**, *15* (17), 1349-1363.

(28) Kraft, A. *Int*. *J*. *Electrochem*. *Sci*. **2007**, *2*, 355-385.

(29) Luong, J. H. T.; Male, K. B.; Glennon, J. D. *Analyst* **2009**, *134*, 1965-1979.

(30) Pecková, K.; Musilová, J.; Barek, J. *Crit*. *Rev*. *Anal*. *Chem*. **2009**, *39* (16), 148-172.

(31) Joseph, M. B.; Bitziou, E.; Read, T. L.; Meng, L.; Palmer, N. L.; Mollart, T. P.; Newton, M. E.; MacPherson, J. V. *Anal*. *Chem*. **2014**, *86*, 5238-5244.

(32) Soh, K. L.; Kang, W. P.; Davidson, J. L.; Wong, Y. M.; Cliffel, D. E.; Swain, G. M. *Diam*. *Relat*. *Mater*. **2008**, *17* (4-5), 900-905.

(33) Dorsch, O.; Werner, M.; Obermeier, E. *Diam*. *Relat*. *Mater*. **1995**, *4* (c), 456-459.

(34) Otterbach, R.; Hilleringmann, U. *Diam*. *Relat*. *Mater*. **2002**, *11*, 841-844.

(35) Enlund, J.; Isberg, J.; Karlsson, M.; Nikolajeff, F.; Olsson, J.; Twitchen, D. J. *Carbon N*. *Y*. **2005**, *43*, 1839-1842.

(36) Watanabe, T.; Shibano, S.; Maeda, H.; Sugitani, A.; Katayama, M.; Matsumoto, Y.; Einaga, Y. *Electrochim*. *Acta* **2016**, *197*, 3-14.

(37) Forsberg, P.; Jorge, E. O.; Nyholm, L.; Nikolajeff, F.; Karlsson, M. *Diam*. *Relat*. *Mater*. **2011**, *20* (8), 1121-1124.

(38) Odijk, M.; Boer, H. De; Olthuis, W.; Berg, A. van den. In *14th International Conference on Miniaturized Systems for Chemistry and Life Sciences, μTAS 2010, 3-7 October 2010, Groningen, the Netherlands*; 2010; pp 399-401.

(39) Venable, R. M.; Pastor, R. W. *Biopolymers* **1988**, *27*, 1001-1014.

(40) Granger, M. C.; Witek, M.; Xu, J.; Wang, J.; Hupert, M.; Hanks, A.; Koppang, M. D.; Butler, J. E.; Lucazeau, G.; Mermoux, M.; Strojek, J. W.; Swain, G. M. *Anal*. *Chem*. **2000**, *72* (16), 3793-3804.

2.6 Supporting Information

S1. Sample preparation, data acquisition and database searching

Sample preparation

Stock solutions of LWL, LYL, LFL and ACTH 1-10 were prepared in 89/10/1 (v/v/v) water/acetonitrile/formic acid at a concentration of 1 mM. Solutions of lysozyme and insulin were prepared in 89/10/1 (v/v/v) water/acetonitrile/formic acid to a protein concentration of 100 µM. For reduction and alkylation of lysozyme, 100 µM protein was prepared in 1 mL ammonium bicarbonate buffer (100 mM, pH 8). DTT was added at a concentration of 2 mM and incubated for 30 min at 60 °C. IAM was added at a concentration of 20 mM after cooling and incubated in a dark environment at room temperature for 60 min. After alkylation, 8 mM DTT was added and incubated in a dark environment at room temperature for 30 min to quench the alkylation reaction. Lysozyme precipitated upon reduction and alkylation. The reaction mixture was centrifuged at 13000 rpm and the supernatant was removed. 1 mL 89/10/1 (v/v/v) water/acetonitrile/formic acid was added to the precipitate to prepare a 100 µM stock solution of reduced and alkylated lysozyme.

Prior to electrochemical oxidation and cleavage, the peptides and proteins were diluted to a final concentration of 10 µM (LWL, LYL, LFL, ACTH, insulin) or 2 µM (lysozyme). To prevent acid hydrolysis or formylation of the proteins during storage, the formic acid content of peptide and protein samples was increased to 5 % just before the electrochemistry experiments.

Data acquisition

MS scans from *m*/*z* 100 to 1500 (LWL, LYL and LFL and ACTH 1-10) and MS scans from *m*/*z* 200 to 2000 (insulin and lysozyme) were recorded at a resolution of 72000 and MS/MS spectra were recorded at a resolution of 17500 after fragmentation in the high-energy collisional dissociation (HCD) cell. The normalized collision energy was set at 35 V. All data was acquired in profile mode using positive polarity.

Data analysis and database searching

The LC-MS/MS data were analyzed with the database search engine PEAKS (version 7.5, Bioinformatics Solutions Inc) using the SwissProt database of (chicken) containing 2601 protein sequences. The search parameters were as follows: Parent Mass Error Tolerance: 10.0 ppm; Frag-

ment Mass Error Tolerance: 0.7 Da; Enzyme: EC (custom-defined, digestion after Y or W); Max Missed Cleavages: 5; Non-specific Cleavage: none; Variable Modifications: Oxidation (on MFWHYC): +15.99, Carbamidomethylation (C): +57.02; EC-Y-2 (custom-defined: on C-terminal Y): -2.02; EC-W+14 (custom-defined: on C-terminal W): +13.98; Maximum variable post-translational modifications per peptide: 5. The false discovery rate (FDR) threshold was set to 0.1 % on the peptide level.

S2. Calibration pseudo-reference electrode against Ag/AgCl

To be able to relate the protein cleavage potentials in the microfluidic electrochemical cell to a KCl saturated Ag/AgCl reference electrode, the Pt pRE was calibrated against Ag/AgCl in the two solutions containing 89/10/1 (v/v/v) water/acetonitrile/formic acid (pH 2.0) and 85/10/5 (v/v/v) water/acetonitrile/formic acid (pH 1.5), respectively. Cyclic voltammograms of 1 mM 1,1'-ferrocenedimethanol in these two solutions were recorded in both the regular electrochemical cell (micro-structured BDD WE, platinum CE and saturated Ag/AgCl RE) and the microfluidic electrochemical cell (BDD WE and CE, Pt pRE) and the half-wave potential from the second scan of each CV was determined in both systems (see CVs in **Figure S1**). From these measurements, the potential of the platinum pRE was determined to be on average (n=3) 225 mV vs. Ag/AgCl (KCl saturated) in the 1 % formic acid solution and on average (n=3) 196 mV vs. Ag/AgCl (KCl saturated) in the 5 % formic acid solution.

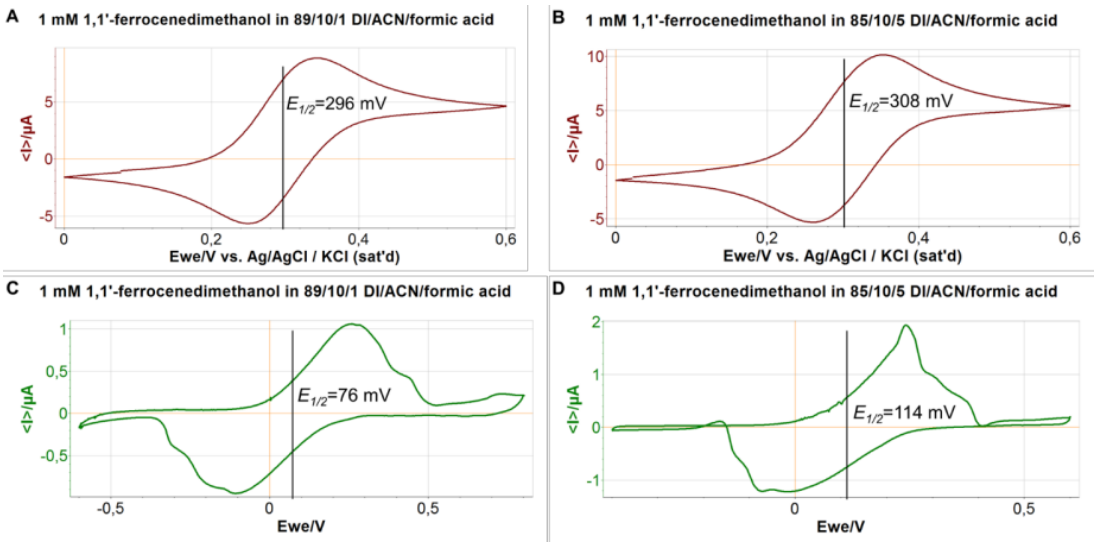

Figure S2: Cyclic voltammograms recorded using 1 mM 1,1'-ferrocenedimethanol in the two solutions used throughout the experiments (10 % acetonitrile in 1 % and 5 % formic acid). A and B: voltammograms recorded using a regular electrochemical cell with a BDD working electrode (WE), platinum counter electrode (CE) and Ag/AgCl (KCl saturated) reference electrode (RE). C and D: voltammograms recorded using a microfluidic electrochemical cell with a BDD WE and CE and a platinum pseudo-RE.

S3. Electrochemical oxidation and cleavage mechanisms of LWL and LYL

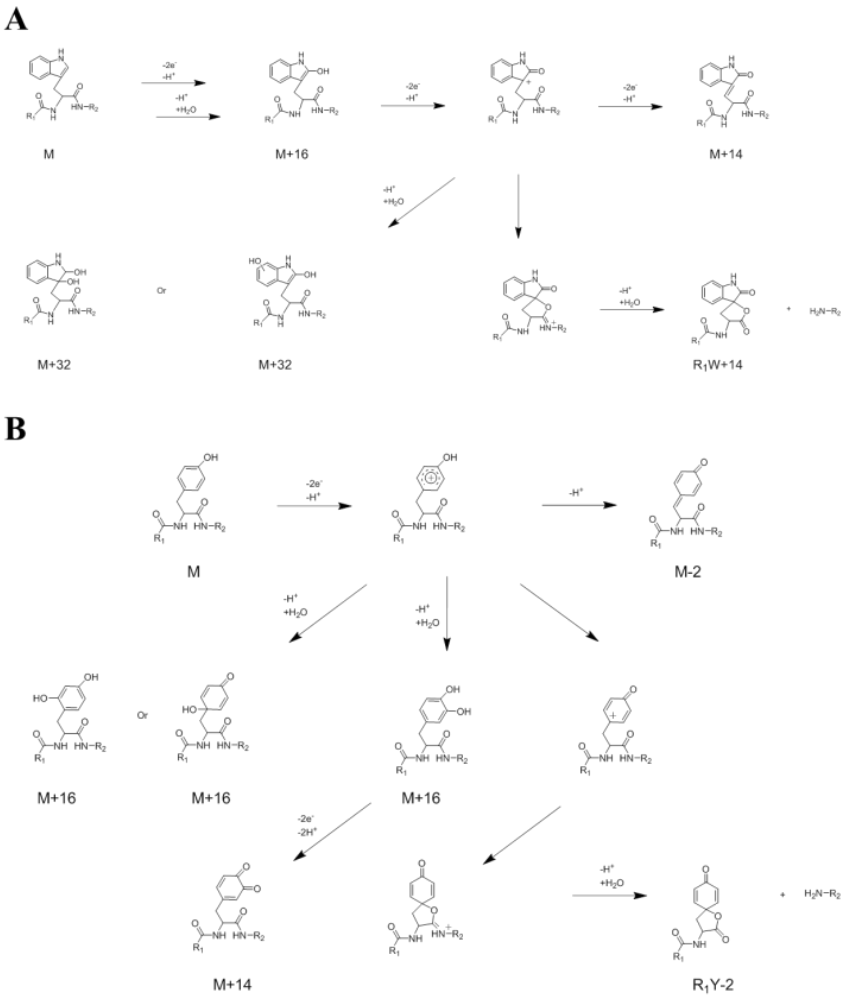

Scheme S3: Proposed electrochemical oxidation and cleavage pathways of A: tryptophan-containing peptides and proteins and B: tyrosine-containing peptides and proteins. Adapted with permission from reference 14. Copyright 2010 American Chemical Society.

S4. LC-MS extracted ion chromatograms of oxidized and cleaved LWL

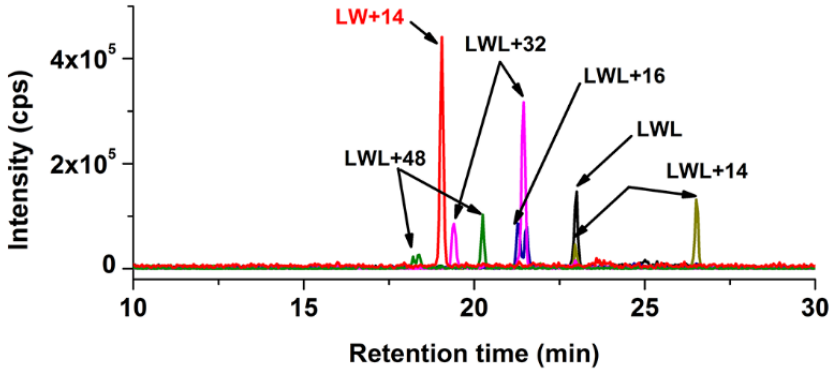

Figure S4: LC-MS extracted ion chromatograms of products collected from a microfluidic electrochemical cell after oxidation and cleavage of 10 µM LWL in 89/10/1 (v/v/v) water/acetonitrile/formic acid at a potential of 1300 mV at a BDD working electrode. Analyte was introduced at a total flow rate of 2 µL/min (1 µL/min over the WE). A number of oxidation products are observed in addition to the cleavage product LW+14.

S5. LC-MS extracted ion chromatograms of oxidized and cleaved LYL

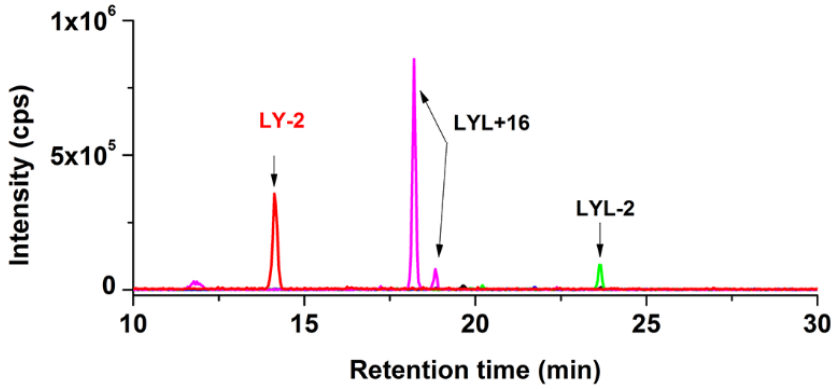

Figure S5: LC-MS extracted ion chromatograms of products collected from a microfluidic electrochemical cell after oxidation and cleavage of 10 µM LYL in 89/10/1 (v/v/v) water/acetonitrile/formic acid at a potential of 2000 mV at a BDD working electrode. Analyte was introduced at a total flow rate of 2 µL/min (1 µL/min over the WE). A number of oxidation products are observed in addition to the cleavage product LY-2.

S6. LC-MS extracted ion chromatograms of oxidized and cleaved LFL

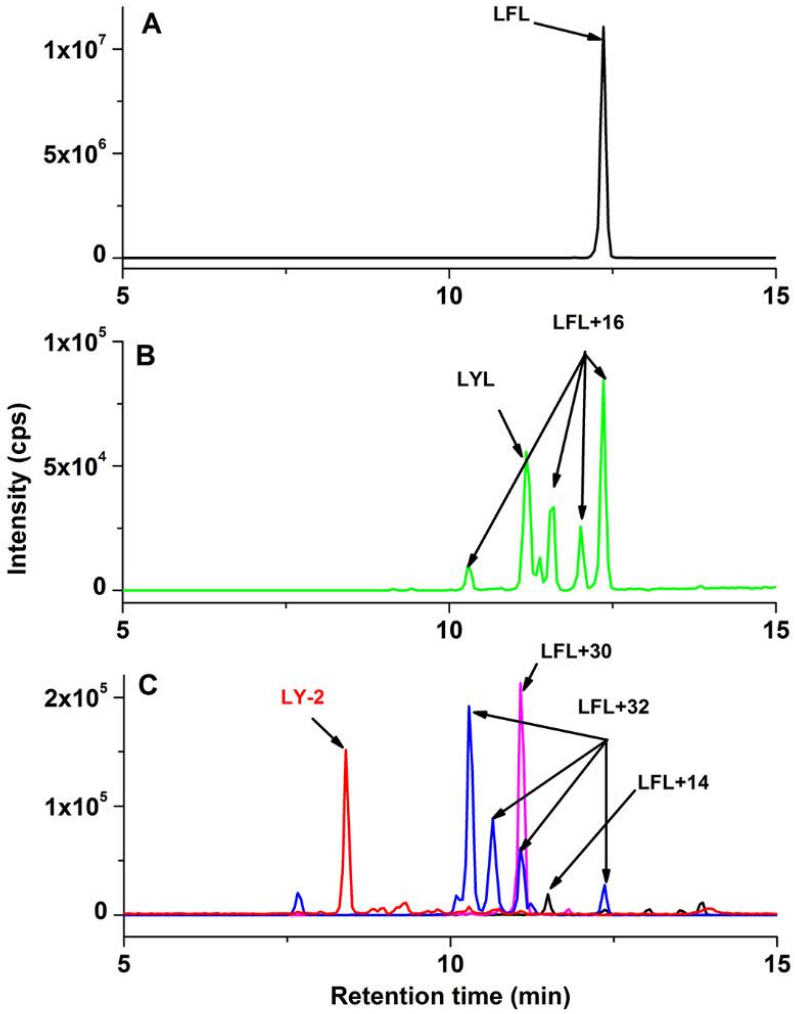

Figure S6: LC-MS extracted ion chromatograms of the products collected from a microfluidic electrochemical cell after oxidation and cleavage of 10 µM LFL in 85/10/5 (v/v/v) water/acetonitrile/formic acid at 2000 mV at a BDD working electrode. Analyte was introduced at a total flow rate of 2 µL/min (1 µL/min over the WE). A: starting material LFL; B: oxidation (aromatic hydroxylation) products LFL+16 including LYL and C: further oxidation products LFL+14, LFL+30, LFL+32 and the cleavage product LY-2.

S7. LC-MS extracted ion chromatograms of ACTH cleavage products

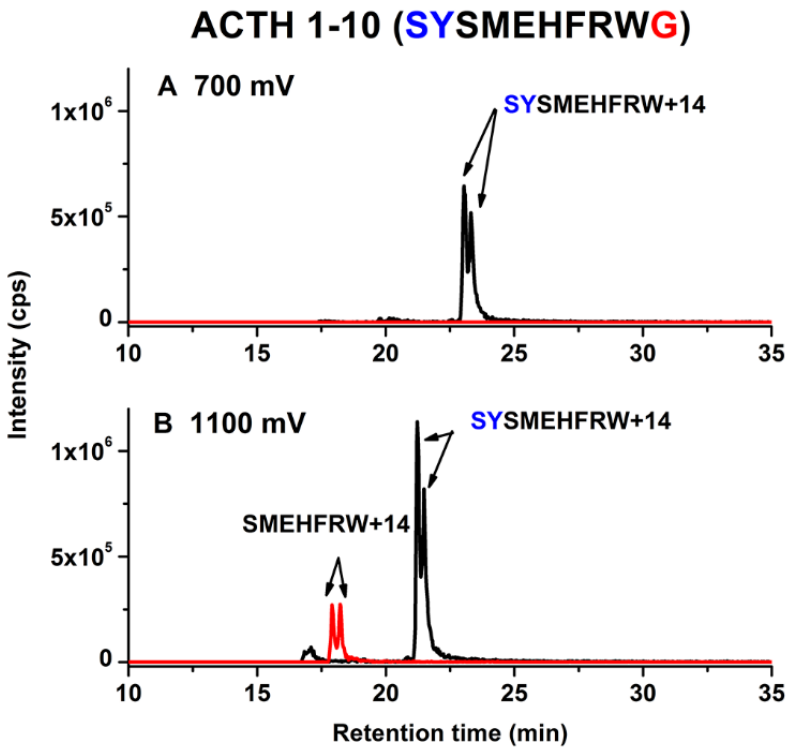

Figure S7: LC-MS extracted ion chromatograms of cleavage products of ACTH 1-10 (10 µM in 89/10/1 (v/v/v) water/acetonitrile/formic acid) generated at the BDD working electrode in a microfluidic electrochemical cell. Analyte was introduced at a total flow rate of 2 µL/min (1 µL/min over the WE). A: cleavage products generated at 700 mV and B: cleavage products generated at 1100 mV. A pair of two isobaric chromatographic peaks with identical MS and MS/MS spectra were observed for each cleavage product, and the nature of these compounds is currently under investigation.

S8. Mass-voltammograms of insulin cleavage

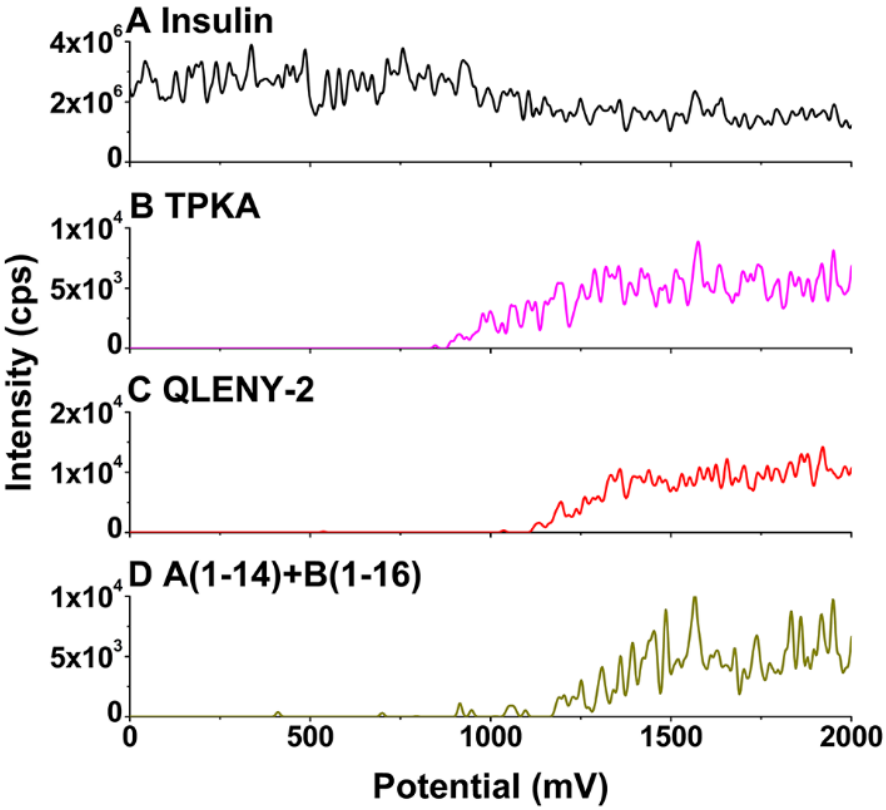

Figure S8: Mass voltammograms of 10 µM insulin in 85/10/5 (v/v/v) water/acetonitrile/formic acid. The potential was ramped from 0 to 2000 mV at a scan rate of 2 mV/s while analyte was introduced at a total flow rate of 2 µL/min (1 µL/min over the BDD WE). Traces of insulin and its cleavage products were plotted as a function of cell potential. A: Insulin (*m/z* 1146.93, charge 5+); B: TPKA (*m/z* 208.63, charge 2+); C: QLENY-2 (*m/z* 664.29, charge 1+) and D: A(1-14)+B(1-16) (*m/z* 1099.16, charge 3+). A(1-14)+B(1-16) corresponds to the N-terminal parts of the A- and B-chains released upon cleavage at sites 1 and 3, respectively, which remain linked together by a disulfide bond (see **Figure 5** in the main text for details).

S9. Mass voltammograms of lysozyme cleavage

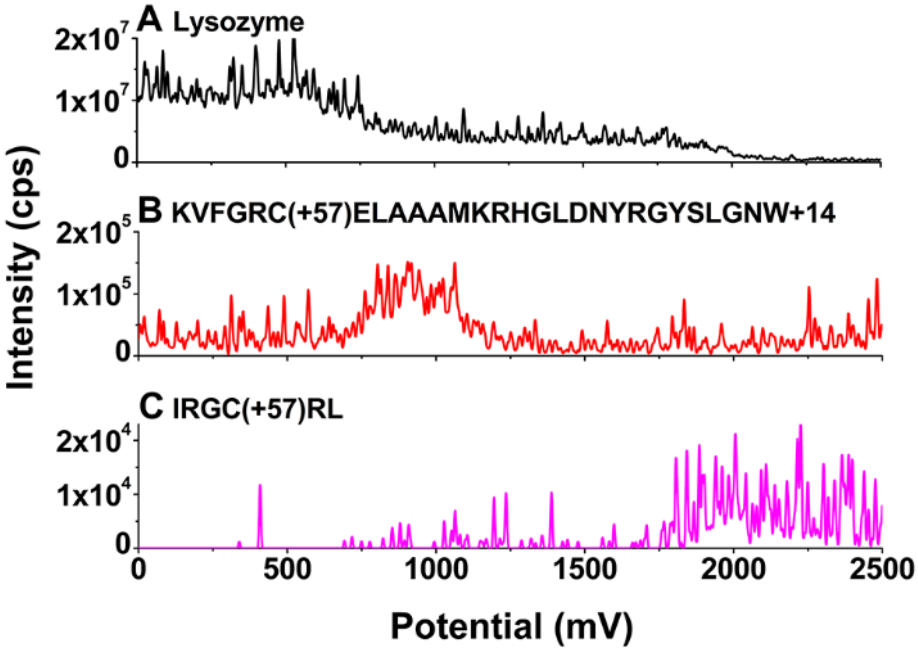

Figure S9: Mass voltammograms of 2 µM lysozyme in 85/10/5 (v/v/v) water/acetonitrile/formic acid. The potential was ramped from 0 to 2500 mV at a scan rate of 2 mV/s while analyte was introduced at a total flow rate of 2 µL/min (1 µL/min over the BDD WE). Traces for lysozyme and two products (KVFGRC(+57)ELAA-AMKRHGLDNY-RGYSLGNW+14 and IRGC(+57)RL) resulting from cleavage at the C-terminal of tryptophan (sites 3 and 9) were extracted and plotted versus cell potential. A: Lysozyme (*m/z* 739.37, charge 20+), B: KVFGRC(+57)ELAA-AMKRHGLDNY-RGYSLGNW+14 (*m/z* 657.53, charge 5+) and C: IRGC(+57)RL (*m/z* 387.72, charge 2+). See table 1 in the main text for details.

S10. LC-MS extracted ion chromatograms of lysozyme cleavage products

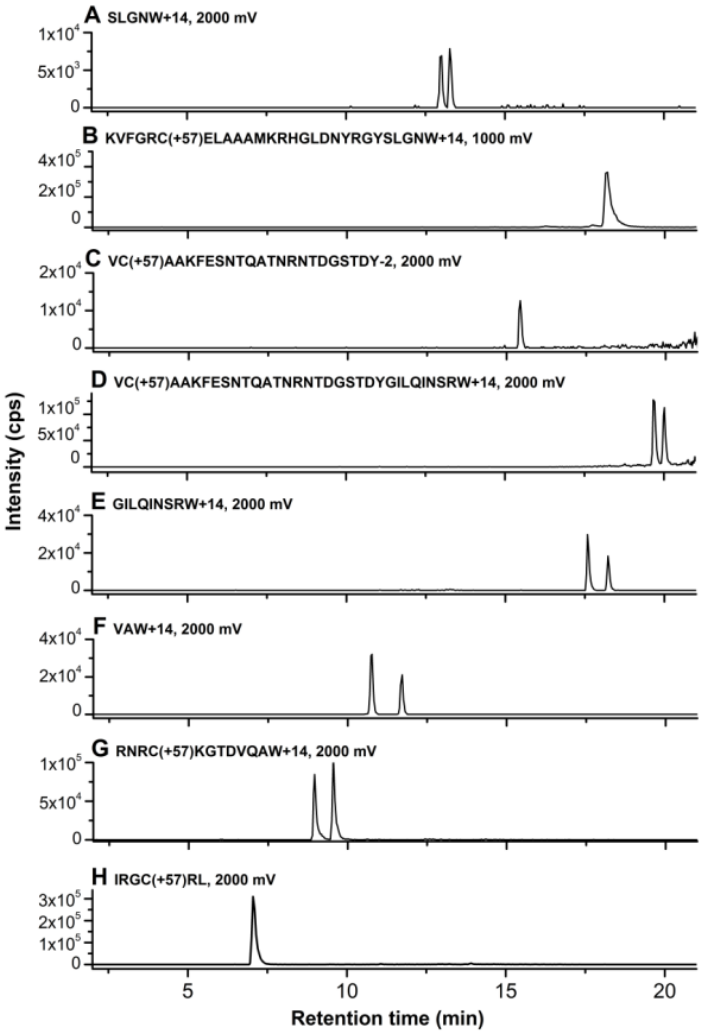

Figure S10: LC-MS extracted ion chromatograms of cleavage products of lysozyme (2 µM in 85/10/5 (v/v/v) water/acetonitrile/formic acid) generated at the BDD working electrode in a microfluidic electrochemical cell. Two different potentials were used (1000 and 2000 mV) and analyte was introduced at a total flow rate of 2 µL/min (1 µL/min over the WE). See table 1 in the main text for details. Isobaric chromatographic peak pairs were observed for all 7 spirolactone-containing peptides with two exceptions, KVFGRC(+57)ELAA-AMKRHGLDNY-RGYSLGNW+14 and VC(+57)AAKFESNF-NTQATNRNTD-GSTDY-2, which is possibly due to insufficient chromatographic separation.

Chapter 3

Efficient and selective chemical labeling of electrochemically-generated peptides based on spirolactone chemistry

Abstract: Specific digestion of proteins is an essential step for mass spectrometry-based proteomics, and the chemical labeling of the resulting peptides is often used for peptide enrichment or the introduction of desirable tags. Cleavage of the peptide bond following electrochemical oxidation of Tyr or Trp results in a spirolactone moiety at the newly formed C-terminus offering a handle for chemical labeling. In this work, we developed a highly efficient and selective chemical labeling approach based on spirolactone chemistry. Electrochemically generated peptide-spirolactones readily undergo an intramolecular rearrangement yielding isomeric diketopiperazines precluding further chemical labeling. A strategy was established to prevent intramolecular arrangement by acetylating the N-terminal amino group prior to electrochemical oxidation and cleavage allowing the complete and selective chemical labeling of the tripeptide LWL and the decapeptide ACTH 1-10 with amine-containing reagents. As examples, we show the successful introduction of a fluorescent label and biotin for detection or affinity enrichment. Electrochemical digestion of peptides and proteins followed by efficient chemical labeling constitutes a new, powerful tool in protein chemistry and protein analysis.

Published as: Tao Zhang, Xiaoyu Niu, Tao Yuan, Marco Tessari, Marcel P. de Vries, Hjalmar P. Permentier and Rainer Bischoff. Efficient and selective chemical labeling of electrochemically-generated peptides based on spirolactone chemistry. *Analytical Chemistry*, **2016**, 88, 6465-6471.

3.1 Introduction

Mass spectrometry-based proteomics plays a central role in protein identification and quantification in complex biological matrices starting with protein digestion followed by analysis of the resulting peptides by reversed-phase liquid chromatography coupled to tandem mass spectrometry (RPLC-MS/MS).[1-3] Enzymatic digestion with proteases is the most widespread method for cleavage of proteins at specific peptide bonds, and a number of proteases with different specificities are available.[4-7] Chemical cleavage is sometimes used as an alternative to enzymatic digestion if specificity for a certain amino acid sequence is required for which no protease is known.[8-10] Electrochemical oxidation of peptides and proteins has been shown to lead to specific cleavage of the peptide bond C-terminal to Tyr and Trp, which makes electrochemistry (EC) a potential instrumental alternative to chemical and enzymatic peptide bond cleavage, since EC is fast, does not require the addition of reagents and works under denaturing conditions.[11-15]

Chemical labeling with fluorescent dyes, affinity tags or other groups was developed to enrich molecules from complex mixtures, notably from biological samples, to allow for their selective and sensitive detection or to generate internal standards for mass spectrometry through incorporation of stable isotopes.[3, 16-18] An easy capture and labeling strategy for the peptides of interest based on specific reactions would further boost proteomics analysis efficiency after protein digestion. Ideally, the reaction for chemical labeling should have high selectivity and efficiency, as well as produce a single chemical moiety without side reactions or multiplicity of labeling. However, most commonly used chemical labeling reactions rely on reactions of the side chains of natural amino acids and N-terminal or C-terminal residues and are thus limited by a lack of selectivity resulting in multiple reaction products that often require tedious purification steps to arrive at single compounds.[19-22] Thus, the lack of reactions with distinct and tunable reactivity and selectivity for efficient chemical labeling remains a challenge, which we address by electrochemically-mediated cleavage of the peptide bond with subsequent chemical labeling.

An interesting aspect of electrochemically cleaved peptides is that the newly generated C-terminus is converted into a unique activated ester in the form of a spirolactone.[13] We have previously shown that this spirolactone is reactive towards amines and employed its reactivity for chemical labeling with hexylamine.[14] However, Tyr- and Trp-derived spirolactones show modest coupling yields even at a large molar excess of the amine under aqueous conditions at the slightly acidic pH values required to prevent spirolactone hydrolysis.[14, 23-25] In this work, we developed a chemical labeling approach that overcomes these limitations and allows complete and selective peptide labeling after electrochemical cleavage.

3.2 Experimental section

3.2.1 Materials and Chemicals.

The tripeptide LWL was obtained from Research Plus Inc. (Barnegat, NJ, USA). LFL was purchased from Bachem (Weil am Rhein, Germany). Adrenocorticotropic hormone (ACTH) 1-10 (SYSMEHFRWG), formic acid (HCOOH, FA, 98%), triethylamine (TEA, 99%), trifluoroacetic acid (TFA, 99%), hexylamine (99%), acetic acid anhydride (99%), dimethyl sulfoxide (DMSO, anhydrous, 99.8%), 5-((2-Aminoethyl)amino)naphthalene-1-sulfonic acid, sodium salt (EDANS) and dimethyl sulfoxide-d_6 (100%, 99.96 atom % D) were obtained from Sigma Aldrich (Steinheim, Germany). EZ-Link amine-PEG_2-biotin was purchased from Pierce Biotechnology (Rockford, USA). Acetonitrile (HPLC SupraGradient grade) was purchased from Biosolve (Valkenswaard, The Netherlands). Water was purified by a Millipore system (conductivity 18.2 MΩ cm, Millipore Corp., Billerica, MA, USA).

3.2.2 N-terminal acetylation of peptides and Ac-peptide purification.

100 µL LWL and ACTH 1-10 were prepared in DMSO at a concentration of 10 mM and 100 µL acetic acid anhydride (15 mM in DMSO) were added. Acetylation was performed at room temperature with shaking at 900 rpm in an Eppendorf Thermomixer comfort (Eppendorf, Hamburg, Germany) for 2 h. The mixture was diluted with 99/1

(v/v) water/formic acid to a final concentration of 1 mM and the reaction products purified by HPLC. The HPLC system (Shimadzu, Kyoto, Japan) was equipped with a SIL-20AC autosampler, an LC-20AT pump, an SPD-20A absorbance detector and an FRC-10A fraction collector. 100 µL samples were injected and purified on a Vydac RP-C18 column (250 mm × 4.6 mm i.d., 5 µm particles, 300 Å pore size, Grace Vydac, Lokeren, Belgium) with a 40 min gradient of 5-40% acetonitrile in water/0.1% formic acid at a flow rate of 500 µL/min. Fractions were collected and evaporated under nitrogen and dried in an Eppendorf Concentrator 5301 (Eppendorf, Hamburg, Germany) at 30 °C.

3.2.3 Electrochemical cleavage.

Stock solutions of LWL, Ac-LWL, ACTH 1-10 and Ac-ACTH 1-10 were prepared in 89/10/1 (v/v/v) water/acetonitrile/formic acid at a concentration of 1 mM shortly before electrochemical oxidation and cleavage. Stock solutions of LWL and Ac-LWL were diluted to 10 µM and 20 µM in 89/10/1 (v/v/v) water/acetonitrile/formic acid, respectively, and oxidized at a flow-rate of 10 µL/min (syringe pump, KD Scientific Inc., Holliston, MA, USA) with a Coulochem 5021 conditioning cell (ESA Inc., Bedford, MA, USA) containing a porous graphite flow-through working electrode, a palladium auxiliary electrode and a palladium reference electrode. ATCH 1-10 and Ac-ACTH 1-10 were oxidized and cleaved at a concentration of 50 µM and a flow-rate of 5 µL/min, following the same procedure. On-line EC-MS experiments of peptides were done by linearly ramping the cell potential from 300 to 1500 mV at a scan rate of 2 mV/s with a homemade potentiostat controlled by a MacLab system (ADInstruments, Castle Hill, NSW, Australia) and EChem software (eDAQ, Denistone East, NSW, Australia) to determine the optimal oxidation/cleavage potentials. LWL, Ac-LWL, ACTH 1-10 and Ac-ACTH 1-10 were oxidized at 700 mV, 710 mV, 750 mV and 750 mV vs Pd/H_2, respectively, for LC-MS analysis. Currents recorded at the working electrode were 3.0 µA, 3.2 µA, 3.5 µA and 3.2 µA, respectively. The reaction product mixtures (EC-LWL, EC-Ac-LWL, EC-ACTH 1-10, and EC-Ac-ACTH 1-10, respectively) were collected for

further reactions and analyses at different time points to assess the stability of the cleavage products.

3.2.4 Intramolecular rearrangement of spirolactone-containing peptides.

Two mL of 10 μM EC-LWL were concentrated by evaporation under nitrogen (2 h) and dried in an Eppendorf Concentrator at 30 °C. EC-LWL conversions were performed by dissolving the dried sample in DMSO at a concentration of 1 mM by pipetting for 30 s. Reactions were performed at 25 °C with shaking at 900 rpm in an Eppendorf Thermomixer. Intramolecular rearrangement was monitored at different time points, (0 h, 1 h, 2 h, 3 h, 4 h, and 6 h) by subjecting 40 μL of the reaction mixtures to LC-MS analysis after dilution to 2.5 μM with 99/1 (v/v) water/formic acid.

Conversions of EC-Ac-LWL and EC-Ac-ACTH 1-10 were done at a concentration of 1 mM in DMSO after drying following the same procedure. 40 μL samples (10 μM) at time points 0 and 6 h were prepared by dilution with 99/1 (v/v) water/formic acid and analyzed by LC-MS.

Intramolecular rearrangements under acidic and basic conditions were studied by drying 2 mL of 10 μM EC-LWL as described above. Dried samples were dissolved in DMSO/TFA (99.5/0.5) or DMSO/TEA (99.5/0.5) at a final concentration of 1 mM by pipetting for 30 s. The samples were incubated at 25 °C with shaking at 900 rpm, and the conversion reaction was monitored at different time points by LC-MS after dilution with 99/1 (v/v) water/formic acid.

3.2.5 Analysis of intramolecular rearrangements product by LC-MS analysis.

Liquid chromatography was performed on an Ultimate plus system (Dionex-LC Packings, Amsterdam, The Netherlands) equipped with a gradient pump and a Famos autosampler. A Vydac RP-C18 column (150 mm × 2.1 mm i.d., 5 μm particles, 300 Å pore size, Grace Vydac, Lokeren, Belgium) was used for chromatographic separation at

a flow rate of 300 µL/min. Mobile phase A consisted of ultra-pure water with 0.1% formic acid. Mobile phase B was acetonitrile with 0.1% formic acid.

40 µL of reaction mixtures (EC-LWL; 2.5 µM, EC-Ac-LWL; 10 µM and Ac-ACTH 1-10; 10 µM) were injected and separation was achieved with a gradient of 5-40% B at 1 %/min. The column was directly coupled to an API 365 triple quadrupole mass spectrometer (PE-Sciex) with an EP10+ upgrade (Ionics) for product detection in positive ion mode. All experiments were performed in triplicate and peak areas obtained by LC/MS analyses were normalized to the peak area of 100 nM LFL, which was added as internal standard prior to LC/MS analysis.

3.2.6 Isomer preparation and NMR analysis.

300 mL EC-LWL were collected from a Coulochem 5021 conditioning cell to prepare approximately 200 µg of spirolactone-containing peptide isomers for NMR analysis. EC-LWL solutions were evaporated under nitrogen and dried in an Eppendorf Concentrator at 30 °C. Intramolecular rearrangements were performed at a final concentration of 30 mM by adding 100 µL DMSO/TEA (99.5/0.5) to dissolve the dried EC-LWL and incubating it for 24 h at 25 °C (Eppendorf Thermomixer at 900 rpm). After reaction, the solution was diluted with 900 µL 99/1 (v/v) water/formic acid prior to purification.

The isomers were purified on the Shimadzu chromatographic system described above with a 210 min gradient of 5-15% acetonitrile in water/0.1% formic acid at a flow rate of 200 µL/min. Fractions were collected, evaporated under nitrogen and dried in an Eppendorf Concentrator at 30 °C. The samples were stored at -20 °C. Purity of the isolated isomers was checked by LC-MS immediately prior to NMR analysis.

All NMR experiments were performed at 298 K on a Varian UnityINOVA spectrometer operating at 800 MHz (^{1}H resonance frequency) equipped with a cryo-cooled probe. Each isomer was dissolved in 700 µL perdeuterated DMSO. 1D ^{1}H and 2D TOCSY experiments were acquired for both samples with identical parameter settings.

A total of 128 transients were acquired for the 1D experiments using a 30-degree excitation pulse, an acquisition time of 1.5 s and a preparation period of 8.5 s.

The 2D TOCSY data matrix consisted of 400 × 5000 complex points, with spectral widths of 9000 Hz and 10000 Hz in the indirect (t1) and acquisition (t2) dimension, respectively. A MLEV17 sequence of 40 ms was employed for TOCSY mixing. For each increment 16 transients were collected using a recycle delay of 2.5 s. All 2D data sets were processed with NMRPipe[26] using 72° shifted squared sine-bell apodization in both dimensions, prior to zero filling to 2048(t1) × 16384(t2) complex points, and Fourier transformation. The software iNMR (http://www.inmr.net) was used for 1D processing and analysis of all spectra.

3.2.7 Chemical coupling of electrochemically cleaved peptides with amine-containing reagents.

Chemical coupling of the LW+14, Ac-LW+14 and Ac-SYSMEHFRW+14 with hexylamine in DMSO/TEA (99.5/0.5) was performed according to Roeser *et al.*[14] with slight modification. 1 mL of EC-LWL (10 µM), EC-Ac-LWL (20 µM) and EC-Ac-ACTH 1-10 (50 µM) solutions were dried following the same procedure and the coupling with hexylamine was performed at a concentration of 500 µM by adding 20 µL, 40 µL and 100µL of a mixture of DMSO, TEA and hexylamine (195:1:4), respectively. Chemical coupling of the peptide-spirolactones Ac-LW+14 and Ac-SYSMEHFRW+14 with EDANS and amine-PEG_2-biotin were performed with the same procedure expect that the added mixtures were composed of DMSO, TEA and amine-containing reagent (159:1:40).

20 µL reaction mixtures (5 µM of EC-LWL, 10 µM EC-Ac-LWL and 25 µM EC-Ac-ACTH 1-10) at time points 0 and 6 h were prepared by dilution with 99/1 (v/v) water/formic acid and analyzed by LC-MS. The LC-MS analysis was performed on an HPLC system equipped with a 2.0 mm i.d. × 50 mm Shim-pack XR-ODS column (Shimadzu, Kyoto, Japan) coupled to an LTQ-Orbitrap XL mass spectrometer (Thermo

Scientific, Bremen, Germany). The separation of the hexylamine reaction mixture was achieved with a 40 min gradient of 2-60% acetonitrile in water/0.1% formic acid at a flow rate of 300 µL/min while a 65 min gradient was employed for the separation of the EDANS and amine-PEG_2-biotin reaction mixtures.

3.2.8 High-resolution MS/MS analysis.

High-resolution MS/MS experiments of the spirolactone-containing cleavage products including LW+14 (LWL), Ac-LW+14 (Ac-LWL), SYSMEHFRW+14 (ACTH 1-10, SYSMEHFRWG), Ac-SYSMEHFRW+14 (Ac-ACTH 1-10, Ac-SYSMEHFRWG) and the rearrangement product LW+14* (LW+14) were performed on a Q Exactive Plus hybrid quadrupole-orbitrap mass spectrometer (Thermo Scientific, Bremen, Germany). Separation was performed with an HPLC system equipped with a 2.0 mm i.d. × 50 mm Shim-pack XR-ODS column (Shimadzu, Kyoto, Japan). A 30 min gradient of 5-40% acetonitrile in water/0.1% formic acid was used at a flow rate of 300 µL/min.

Isomers were prepared by intramolecular rearrangements of 100 µM EC-LWL in DMSO for 6 h. 10 µL of 2.5 µM EC-LWL and 10 µM EC-Ac-LWL, EC-ACTH 1-10 and EC-Ac-ACTH 1-10 were prepared by dilution with 99/1 (v/v) water/formic acid and injected for LC-MS/MS analysis. MS scans from *m/z* 200 to 800 (LW+14, LW+14* and Ac-LW+14) and MS scans from *m/z* 200 to 1400 (SYSMEHFRW+14 and Ac-SYSMEHFRW+14) were recorded at a resolution of 72 000 and MS/MS spectra were recorded at a resolution of 17 500 after collision-induced fragmentation in the HCD cell. The normalized collision energy was set at 10 V (LW+14 and LW+14*) and 35 V (Ac-LW+14, SYSMEHFRW+14 and Ac-SYSMEHFRW+14), respectively.

High-resolution MS/MS experiments of the spirolactone-containing cleavage products (Ac-LW+14 and Ac-SYSMEHFRW+14) and the coupling products (Ac-LW+hexylamine and Ac-SYSMEHFRW+hexylamine) were performed on an LTQ-Orbitrap XL mass spectrometer. MS scans from *m/z* 100 to 2000 was recorded at a resolution of 75 000 and MS/MS spectra were recorded at a resolution of 17 500 with a

normalized collision energy at 35 V. All data was acquired in profile mode using positive polarity.

3.3 Results and Discussion

3.3.1 Molecular rearrangement of LW+14 and formation of isomers.

Reactions of peptide-spirolactones with amines under aqueous conditions have been reported to require a basic pH and a large molar excess while reaching only limited labeling efficiencies.[14] Non-aqueous conditions are preferable for spirolactone labeling, since hydrolysis of the spirolactone is prevented, and the molar excess of amine can be reduced. DMSO was selected in this work due to the good solubility of most peptides in this solvent and hexylamine was employed to study the spirolactone chemistry in more detail.[27-29] The reaction between the spirolactone-containing EC-cleavage product of the tripeptide LWL (LW+14) and hexylamine resulted in two chromatographically separated products (**Figures S1A** and **B**) which have identical MS and MS/MS spectra, as previously reported by Roeser *et al*.[14] However, a competing reaction led to the formation of a pair of isomers (LW+14*) with the same mass as LW+14 (**Figure S1C**).

The rearrangement reaction proceeded to 78% completion within 6 h in the absence of hexylamine indicating that it is independent of the actual labeling reaction (**Figure 1**). The newly generated LW+14* products lost reactivity towards primary amines suggesting that the spirolactone participated in the rearrangement. We hypothesized that LW+14* was formed by an intramolecular reaction between the N-terminal primary amino group and the spirolactone. Since this reaction requires a non-protonated amino group, we investigated the conversion of LW+14 under basic and acidic conditions in DMSO. **Figure S2** shows that conversion does not take place under acidic conditions (0.5% trifluoroacetic acid (TFA)) while it proceeds readily under basic conditions (0.5% triethylamine (TEA)), supporting the hypothesis of an intramolecular rearrangement involving the N-terminal amino group.

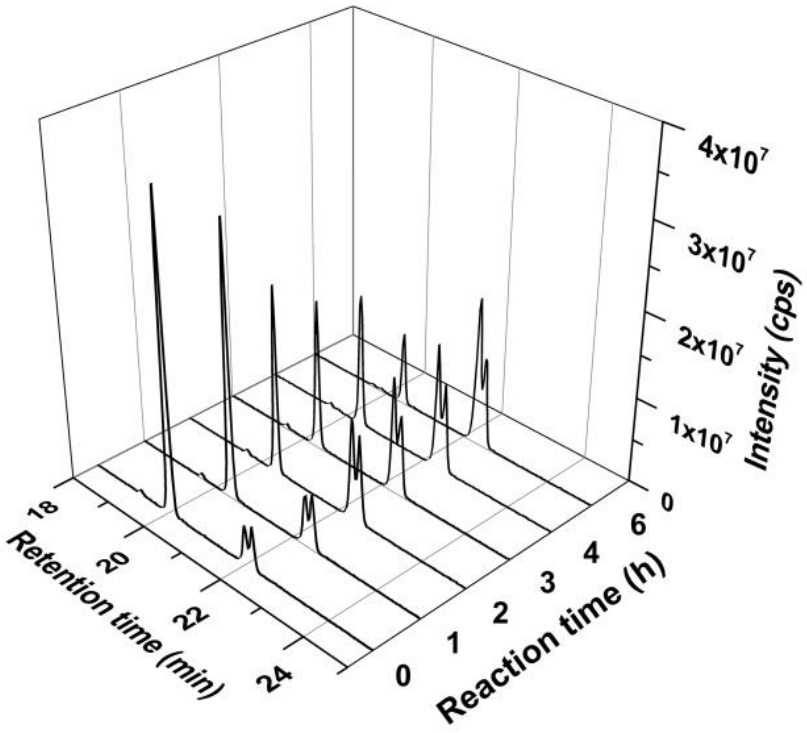

Figure 1. LC-MS analysis of the rearrangement of the spirolactone-containing LW+14 (retention time 19.5 min) in pure DMSO to a pair of isomers (LW+14*, retention times 23.6 min and 23.8 min) that no longer react with primary amines. Some LW+14* was already observed after sample preparation (0 h time point).

Based on the intramolecular aminolysis involving the primary amino group in peptide chemistry, [30-32] we assumed that a similar rearrangement of LW+14 might occur under neutral or basic conditions. The proposed mechanism (**Scheme 1**) suggests that the single bond attached to the tertiary carbocation can rotate freely to form isomers **4a** and **4b** from **3** due to formation of a new chiral center. The peptide bond in **4a** and **4b** is subsequently cleaved to form spirolactones **5a** and **5b** (LW+14) under acidic, aqueous conditions. While **5a** and **5b** are stable under acidic conditions, they undergo molecular rearrangement to the corresponding diketopiperazines **6a** and **6b** (LW+14*) under neutral or basic conditions in DMSO.

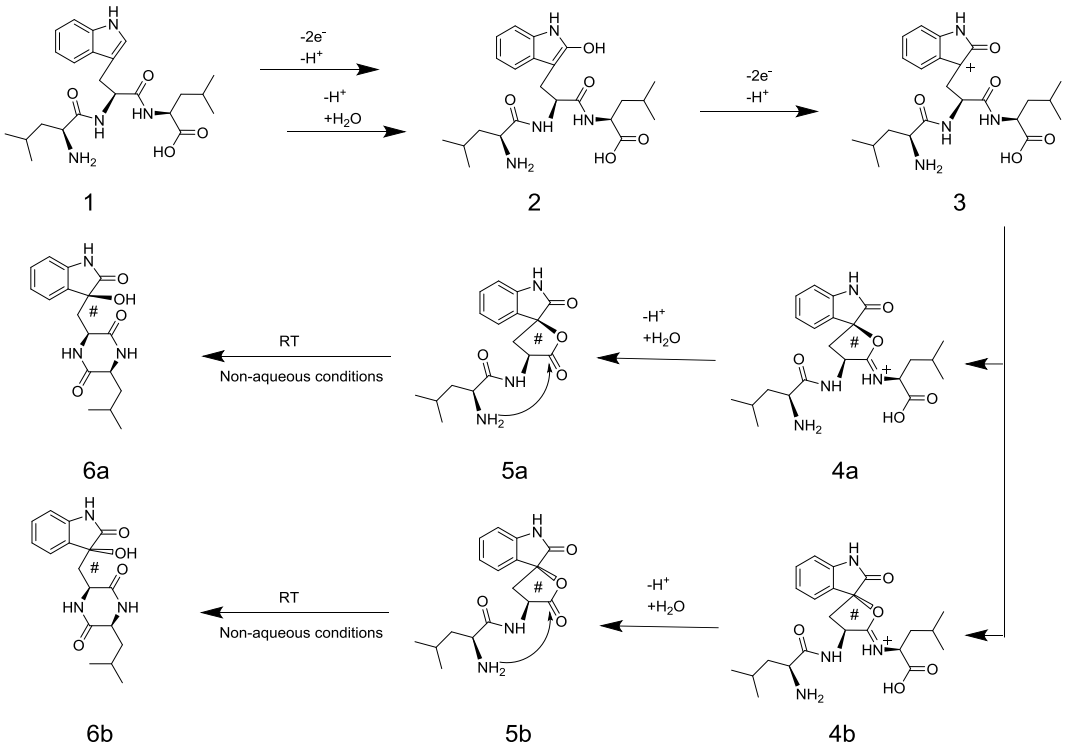

Scheme 1. Proposed electrochemical oxidation and cleavage pathway of the Trp-containing peptide LWL and the ensuing intramolecular rearrangement to the corresponding diketopiperazines containing a chiral tertiary alcohol indicated with # (**6a** and **6b**) (partially adapted from Roeser *et al.*[13]).

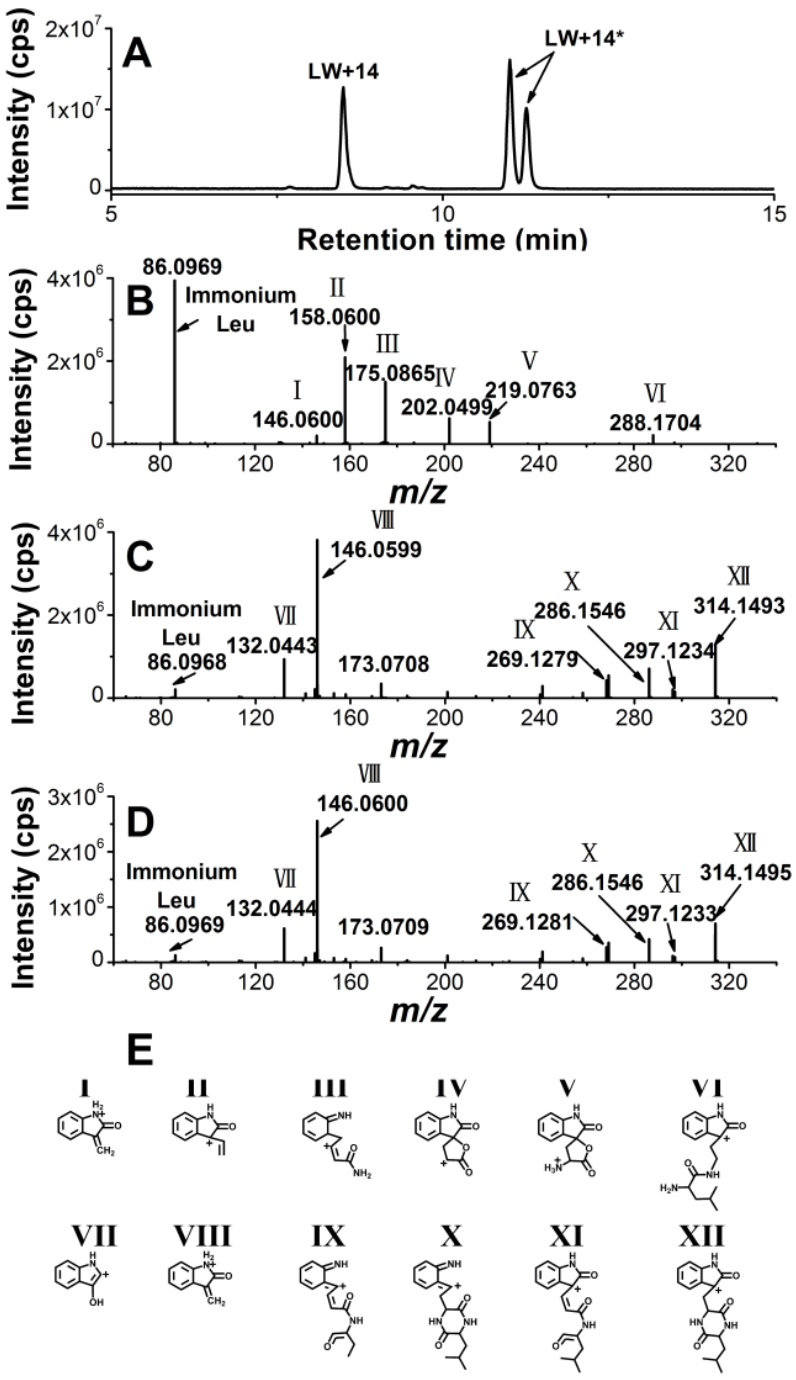

Figure 2. Extracted ion chromatogram of *m/z* 332.160 showing LW+14, the early-eluting LW+14* isomer and the late-eluting LW+14* isomer (A). MS/MS spectra of the electrochemical cleavage products of LW+14 (B), the early-eluting LW+14* isomer (C) and the late-eluting LW+14* isomer (D). Proposed structures of the fragment ions of LW+14 and LW+14* (E).

To confirm the structure of LW+14* in support of our mechanistic hypothesis, structural studies on the early-eluting and late-eluting LW+14* isomers were carried out with the aid of high-resolution LC-MS/MS, 1D ^{1}H-NMR and 2D TOCSY. High-resolution LC-MS/MS of LW+14 and LW+14* was performed on a sample obtained after reaction for 1 h at a concentration of 400 μM in DMSO containing both LW+14 and the two LW+14* isomers in comparable amounts (**Figure 2A**). The MS/MS spectrum of LW+14 was similar to the one reported by Roeser *et al*.[13] Noteworthy is the high intensity of the immonium ion of Leu (*m*/*z* 86.097) indicating the presence of an unmodified Leu residue at the N-terminus (**Figure 2B**). This peak was greatly reduced after intramolecular rearrangement in LW+14*, since the Leu residue becomes part of the diketopiperazine ring structure, which is difficult to fragment (**Figures 2C** and **D**). The two LW+14* isomers produced identical MS/MS spectra. Fragments were assigned based on ion fragmentation rules for peptides in combination with the elemental compositions derived from accurate mass measurements. The easy loss of water to form the fragment at *m*/*z* 314.149 even at the low collision energy of 10 V is consistent with the presence of a tertiary hydroxyl group.[33, 34] The fragment at *m*/*z* 286.154 was generated from the loss of CO from the fragment at *m*/*z* 314.149 followed by a further loss of ammonia to yield the fragment at *m*/*z* 269.128. The fragment at *m*/*z* 297.123 was generated from loss of ammonia due to ring opening of the diketopiperazine. None of these fragments was detectable in the LW+14 spectrum. The intense peak at *m*/*z* 146.060 in LW+14* corresponds to a Trp-related fragment ion, which was also observed in LW+14 but at a much lower intensity. These results are consistent with the proposed tertiary hydroxyl group and diketopiperazine structure as a result of the molecular rearrangement proposed in **Scheme 1**. The obtained ^{1}H-NMR spectra of the LW+14* isomers in DMSO-d_6 as well as 2D-TOCSY spectra results were in agreement with the proposed structures of the LW+14* isomers supporting the proposed mechanism of rearrangement (see supporting information, **Figures S3-S6**, for details).

3.3.2 Stabilization of peptide-spirolactones against intramolecular rearrangement.

The proposed reaction mechanism (**Scheme 1**) implies that a free, non-protonated N-terminal amino group is needed for the intramolecular rearrangement. Acetylation of the N-terminus should thus prevent rearrangement and stabilize the spirolactone-containing reaction products to prevent the side reaction that leads to the formation of the diketopiperazines **6a** and **6b**. The tripeptide LWL and the decapeptide adrenocorticotropic hormone (ACTH) fragment 1-10 (SYSMEHFRWG) were acetylated to Ac-LWL and Ac-ACTH 1-10, respectively, prior to electrochemical oxidation and cleavage. As expected, Ac-LW+14 and Ac-SYSMEHFRW+14 were stable and did not undergo intramolecular rearrangement even after incubation at room temperature for 6 h in DMSO containing 0.5% TEA (**Figure 3A** and **B**). In both cases, Ac-LW+14 and Ac-SYSMEHFRW+14 produced a pair of isomers in analogy to **5a** and **5b** (see **Scheme 1**) with the same MS/MS fragmentation patterns (supporting information, **Figures S7-S8**) which further supports the proposed mechanism.

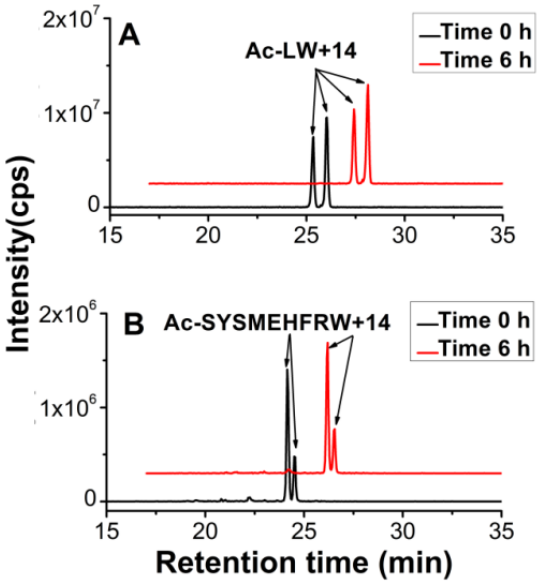

Figure 3. Stability of the spirolactone-containing cleavage products Ac-LW+14 (A) and Ac-SYSMEHFRW+14 (B) in DMSO containing 0.5 % TEA after incubation for 6 h at room temperature. For clarity, the 6 h trace in (A) was offset by 2 min and 3×10^6 cps and in (B) by 2 min and 3×10^5 cps.

3.3.3 Chemical labeling of electrochemically-generated peptide-spirolactones.

Based on these results, we established a three-step strategy resulting in the efficient labeling of peptide-spirolactones (**Scheme 2**). Peptides were first acetylated with acetic acid anhydride followed by electrochemical cleavage and labelling of the spirolactone. LWL and ACTH 1-10 were used to assess the feasibility of this strategy with hexylamine (see supporting information, **Figures S9-S11**) followed by reaction with the amine-containing tags amine-PEG_2-biotin and the fluorescent dye EDANS (**Figure 4**).

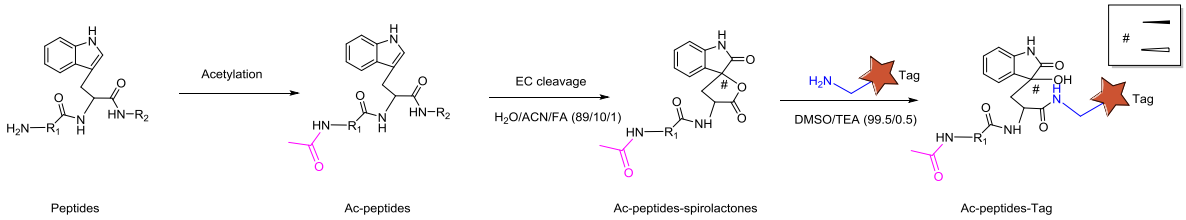

Scheme 2. Three-step labeling scheme of acetylated, electrochemically cleaved peptides via their spirolactone moieties with amine-containing tags under non-aqueous conditions.

Biotinylation of peptides and proteins is commonly exploited for purification and enrichment based on its affinity for avidin.[3, 35-37] Fluorescent labeling is widely used to modify peptides and proteins for sensitive and selective detection.[38-41] **Figure 5** shows biotinylation of Ac-LW+14 to Ac-LW-amine-PEG_2-biotin (**Figure 5A** and **B**) and of Ac-SYSMEHFRW+14 to Ac-SYSMEHFRW-amine-PEG_2-biotin (**Figure 5C** and **D**) after reaction of the electrochemical cleavage products Ac-LW+14 (*m/z* 374.17) and Ac-SYSMEHFW+14 (*m/z* 649.77 (2+)) in DMSO containing 0.5% TEA at room temperature for 6 h. Both cleavage products were completely biotinylated to Ac-LW-amine-PEG_2-biotin (*m/z* 748.37) and Ac-SYSMEHFRW-amine-PEG_2-biotin (*m/z* 836.87 (2+))

with a mass increment of 374.20 Da. Complete coupling of Ac-LW+14 and Ac-SYSMEHFRW+14 with the amine-containing fluorescent dye EDANS was also achieved under the same conditions (see **Figure S12**) resulting in a mass increment of 266.04 Da (Ac-LW-EDANS (*m/z* 640.24) and Ac-SYSMEHFRW-EDANS (*m/z* 782.80 (2+)).

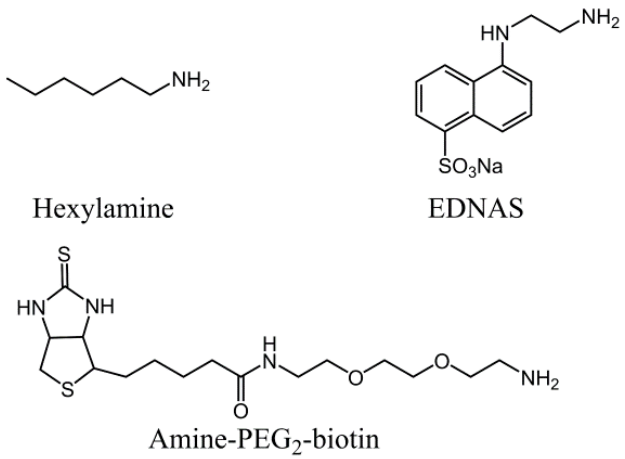

Figure 4. Structure of amine-containing reagents used for chemical labeling of spirolactones.

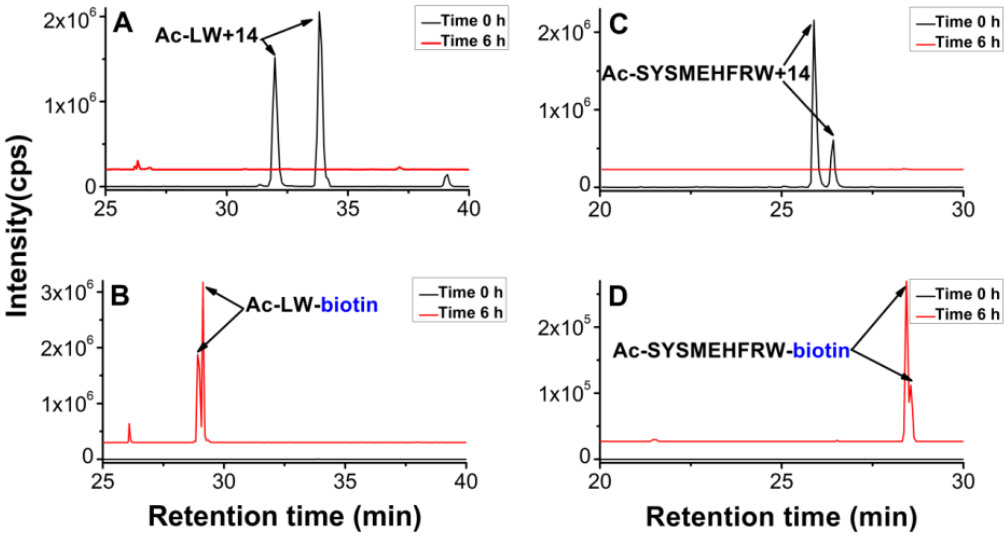

Figure 5. Chemical labeling of Ac-LW+14 and Ac-SYSMEHFRW+14 with amine-PEG_2-biotin. Extracted ion chromatogram of Ac-LW+14 (A) (*m/z* 374.171), Ac-SYSMEHFRW+14 (C) (*m/z* 649.767, (2+)) and the chemical labeling products Ac-LW-amine-PEG_2-biotin (B) (*m/z* 748.373)

and Ac-SYSMEHFRW-amine-PEG_2-biotin (D) (*m*/*z* 836.871, (2+)) before and after reaction with a 4000-fold molar excess of amine-PEG_2-biotin in DMSO containing 0.5 % TEA for 6 h at room temperature. For clarity, the y axis of 6 h trace in (A) was offset by 2×10^5 cps, in (B) by 3×10^5 cps, in (C) by 3×10^5 cps and in (D) by 3×10^4 cps.

3.4 Conclusions

The electrochemical, oxidative cleavage of peptide bonds at Trp and Tyr opens possibilities for specific chemical labeling by introducing a reactive spirolactone moiety at the C-terminus of the cleavage products. To make full use of this reaction for peptide and protein analysis, it is crucial to prevent side reactions that inactivate the spirolactone. To advance along these lines, we studied the intramolecular rearrangement of spirolactone-containing peptides and characterized the observed isomeric products. The proposed reaction mechanism (**Scheme 1**) explains the existence of a pair of spirolactone-containing isomers and their subsequent rearrangement to non-reactive diketopiperazines. Acetylation of the N-terminal amino group prevents this rearrangement and stabilizes the spirolactone for further reaction with amine-containing tags (**Scheme 2**). Selective chemical coupling of acetylated, electrochemically cleaved spirolactone-containing peptides to the amine-containing reagents amine-PEG_2-biotin and the fluorescent dye EDANS in DMSO containing TEA went to completion without any competing side reactions. These results open new possibilities of chemical peptide and protein labeling via electrochemically-generated spirolactones with desirable tags as tools in protein chemistry and protein analysis.

3.5 References

(1) Zhang, Y.; Fonslow, B. R.; Shan, B.; Baek, M. C.; Yates, J. R., III *Chem*. *Rev*. **2013**, *113*, 2343-2394.

(2) Abu-Farha, M.; Elisma, F.; Zhou, H.; Tian, R.; Zhou, H.; Asmer, M. S.; Figeys, D. *Anal*. *Chem*. **2009**, *81*, 4585-4599.

(3) Yates, J. R., III *J*. *Am*. *Chem*. *Soc*. **2013**, *135*, 1629-1640.

(4) Shevchenko, A.; Tomas, H.; Havlis, J.; Olsen, J. V.; Mann, M. *Nat*. *Protoc*. **2006**, *1*, 2856-2860.

(5) Vandermarliere, E.; Mueller, M.; Martens, L. *Mass Spectrom*. *Rev*. **2013**, *32*, 453-465.

(6) Walmsley, S. J.; Rudnick, P. A.; Liang, Y.; Dong, Q.; Stein, S. E.; Nesvizhskii, A. I. *J*. *Proteome Res*. **2013**, *12*, 5666-5680.

(7) Olsen, J. V.; Ong, S.; Mann, M. *Mol*. *Cell*. *Proteomics* **2004**, *3*, 608-614.

(8) Crimmins, D. L.; Mische, S. M.; Denslow, N. D. *Curr*. *Protoc*. *Protein*. *Sci*. **2005**, *11*. 1-11.

(9) Li, A.; Sowder, R. C.; Henderson, L. E.; Moore, S. P.; Garfinkel, D. J.; Fisher, R. J. *Anal*. *Chem*. **2001**, *73*, 5395-5402.

(10) Tanabe, K.; Taniguchi, A.; Matsumoto, T.; Oisaki, K.; Sohma, Y.; Kanai, M. *Chem*. *Sci*. **2014**, *5*, 2747-2753.

(11) Permentier, H. P.; Jurva, U.; Barroso, B.; Bruins, A. P. *Rapid*. *Commun*. *Mass*. *Spectrom*. **2003**, *17*, 1585-1592.

(12) Permentier, H. P.; Bruins, A. P. *J*. *Am*. *Soc*. *Mass*. *Spectrom*. **2004**, *15*, 1707-1716.

(13) Roeser, J.; Permentier, H. P.; Bruins, A. P.; Bischoff, R. *Anal*. *Chem*. **2010**, *82*, 7556-7565.

(14) Roeser, J.; Alting, N. F. A.; Permentier, H. P.; Bruins, A. P.; Bischoff, R. *Rapid*. *Commun*. *Mass*. *Spectrom*. **2013**, *27*, 546-552.

(15) Roeser, J.; Alting, N. F. A.; Permentier, H. P.; Bruins, A. P.; Bischoff, R. *Anal*. *Chem*. **2013**, *85*, 6626-6632.

(16) Lue, R. Y.; Chen, G. Y.; Hu, Y.; Zhu, Q.; Yao, S. Q. *J*. *Am*. *Chem*. *Soc*. **2004**, *126*, 1055-1062.

(17) Koehler, C. J.; Strozynski, M.; Kozielski, F.; Treumann, A.; Thiede, B. *J*. *Proteome Res*. **2009**, *8*, 4333-4341.

(18) Arnaudoand, A. M.; Garcia, B. A. *Epigenetics Chromatin*. **2013**, *6*, 24.

(19) Baslé, E.; Joubert, N.; Pucheault, M. *Chem*. *Biol*. **2010**, *17*, 213-227.

(20) Spicer, C. D.; Davis, B. G. *Nat*. *Commun*. **2014**, *5*, 4740.

(21) Witus, L. S.; Moore, T.; Thuronyi, B. W.; Esser-Kahn, A. P.; Scheck, R. A.; Iavarone, A. T.; Francis, M. B. *J*. *Am*. *Chem*. *Soc*. **2010**, *132*, 16812-16817.

(22) Boutureira, O.; Bernardes, G. J. L. *Chem*. *Rev*. **2015**, *115*, 2174-2195.

(23) Liu, W.; Xu, D. D.; Repič, O.; Blacklock, T. J. *Tetrahedron Lett*. **2001**, *42*, 2439-2441.

(24) Shi, T.; Weerasekera, R.; Yan, C.; Reginold, W.; Ball, H.; Klslinger, T.; Ulms, G. S. *Anal*. *Chem*. **2009**, *81*, 9885-9895.

(25) Hutinec, A.; Ziogas, A.; Rieker, A. *Amino Acids* **1996**, *11*, 345-366.

(26) Delaglio, F.; Grzesiek, S.; Vuister, G. W.; Zhu, G.; Pfeiferand, J.; Bax, A. *J*. *Biomol*. *NMR*. **1995**, *6*, 277-293.

(27) Chin, J. T.; Wheeler, S. L.; Klibanova, M. *Biotechnol*. *Bioeng*. **1994**, *44*, 140-145.

(28) Mattos, C.; Ringe, D. *Curr*. *Opin*. *Struct*. *Biol*. **2001**, *11*, 761-764.

(29) Rariy, R. V.; Klibanov, A. M. *Biotechnol*. *Bioeng*. **1999**, *62*, 704-710.

(30) Gisinand, B. F.; Merrifield, R. B. *J*. *Am*. *Chem*. *Soc*. **1972**, *94*, 3102-3106.

(31) Fife, T. H.; Duddy, N. W. *J*. *Am*. *Chem*. *Soc*. **1983**, *105*, 74-79.

(32) Fray, A. H. *Tetrahedron Asymmetry* **1998**, *9*, 2777-2781.

(33) Zhang, Z. *Anal*. *Chem*. **2004**, *76*, 3908-3922.

(34) Kumar, M.; Chatterjee, A.; Khedkar, A. P.; Kusumanchi, M.; Adhikary, L. *J*. *Am*. *Soc*. *Mass*. *Spectrom*. **2013**, *24*, 202-212.

(35) MacCoss, M. J.; Matthews, D. E. *Anal*. *Chem*. **2005**, *77*, 294-302.

(36) Pan, Y.; Ye, M.; Zheng, H.; Cheng, K.; Sun, Z.; Liu, F.; Liu, J.; Wang, K.; Qin, H.; Zou, H. *Anal*. *Chem*. **2014**, *86*, 1170-1177.

(37) Shannon, D. A.; Banerjee, R.; Webster, E. R.; Bak, D. W.; Wang, C.; Weerapana, E. *J*. *Am*. *Chem*. *Soc*. **2014**, *136*, 3330-3333.

(38) Engfeldt, T.; Renberg, B.; Brumer, H.; Nygren, P.; KarlstrÖm, A. E. *ChemBioChem* **2005**, *6*, 1043-1050.

(39) Zou, J.; Zhang, R.; Zhu, F.; Liu, J.; Madison, V.; Umland, S. P. *Biochemistry* **2005**, *44*, 4247-4256.

(40) Chen, S.; Chen, L.; Luo, H.; Sun, T.; Chen, J.; Ye, F.; Cai, J.; Shen, J.; Shen, X.; Jiang, H. *Acta*. *Pharmacologica*. *Sinica*. **2005**, *26*, 99-106.

(41) Clements, A.; Johnston, M. V.; Larsen, B. S.; McEwen, C. N. *Anal*. *Chem*. **2005**, *77*, 4495-4502.

3.6 Supporting Information

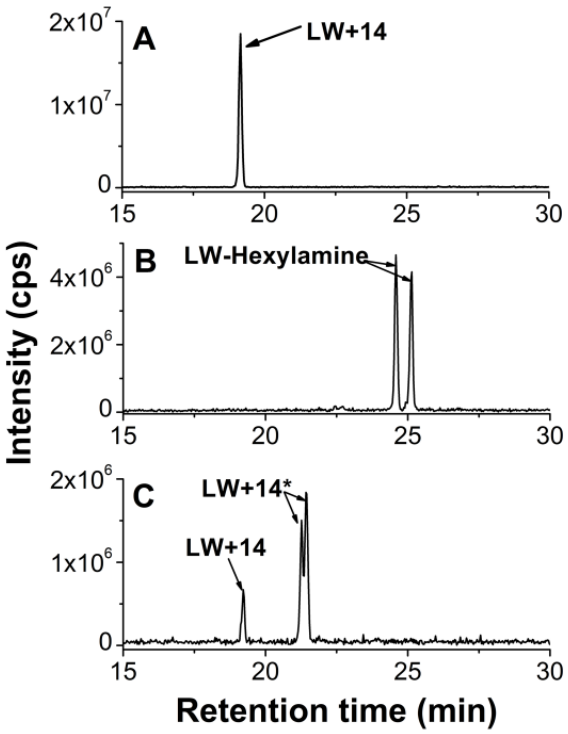

Figure S1. Extracted ion chromatogram of LW+14 (m/z 332.2) after electrochemical oxidation and cleavage (A). Extracted ion chromatogram of the coupling products between LW+14 and hexylamine (m/z 433.2) generated during reaction with a 400-fold molar excess of hexylamine under non-aqueous conditions in DMSO (3 h at room temperature) (B). Extracted ion chromatogram of unreacted LW+14 (m/z 332.2) and the rearrangement products LW+14* (m/z 332.2) under non-aqueous conditions in DMSO (3 h at room temperature) (C).

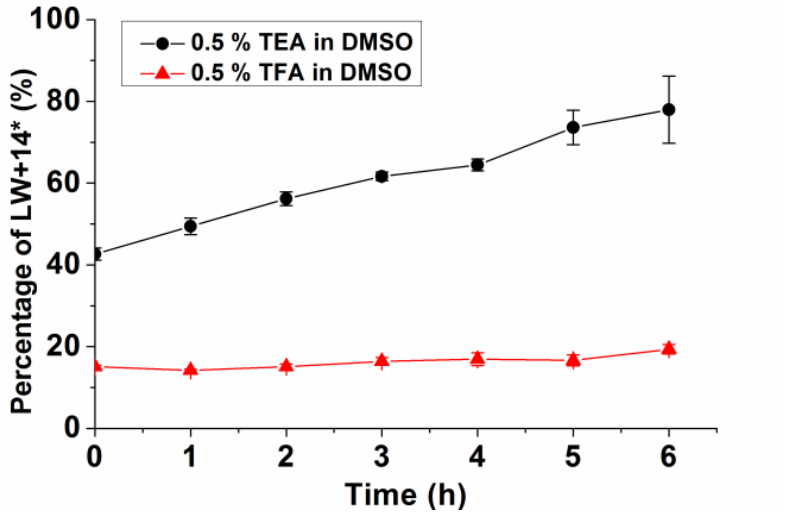

Figure S2. Percentage of peak areas of the LW+14* isomers relative to the sum of the peak areas of LW+14* and LW+14 in DMSO with 0.5 % (v/v) TFA (lower trace) or 0.5% (v/v) TEA (upper trace) upon incubation at room temperature (n = 3). Some LW+14* was generated during sample preparation.

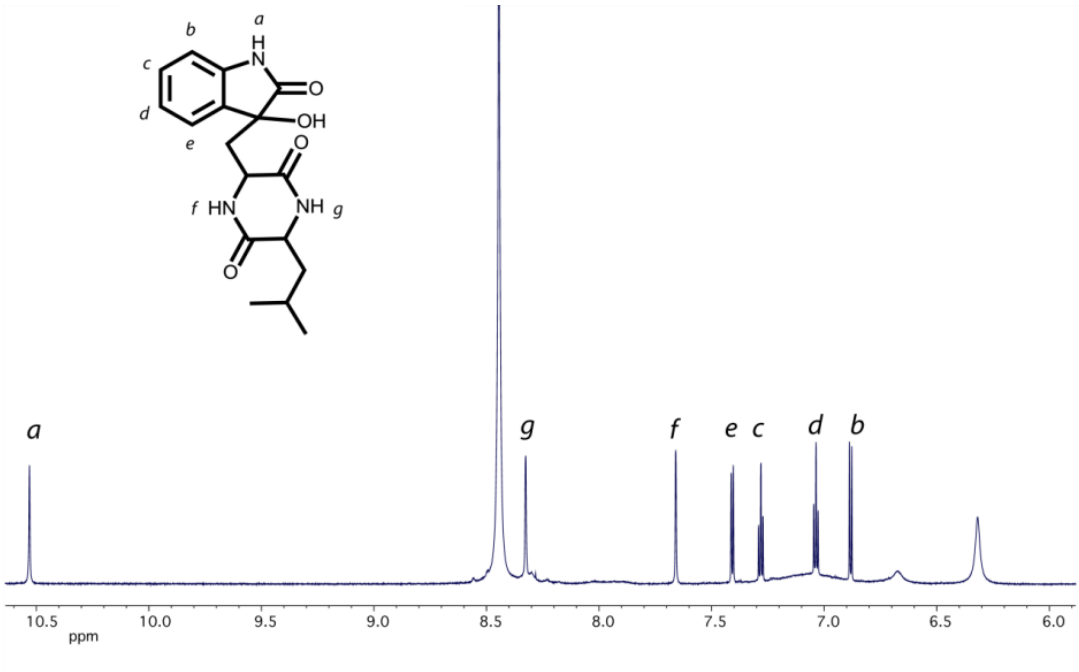

Figure S3. Low field region of a 1D 1H-NMR spectrum of the early-eluting LW+14* acquired at 800 MHz 1H resonance frequency. Resonance assignments are indicated in the structure. The following abbreviations are used to indicate signal multiplicity: s, singlet; d, doublet; t, triplet; m, multiplet; br, broad. 1H-NMR (800 MHz, DMSO-d_6); δ (ppm): 10.534 (s, 1H), 8.329 (s, 1H), 7.661 (s, 1H), 7.410 (d, J = 7.7 Hz, 1H), 7.284 (t, J = 7.5 Hz, 1H), 7.039 (td, J = 7.5, 0.9 Hz, 1H), 6.884 (d, J = 7.7 Hz, 1H).

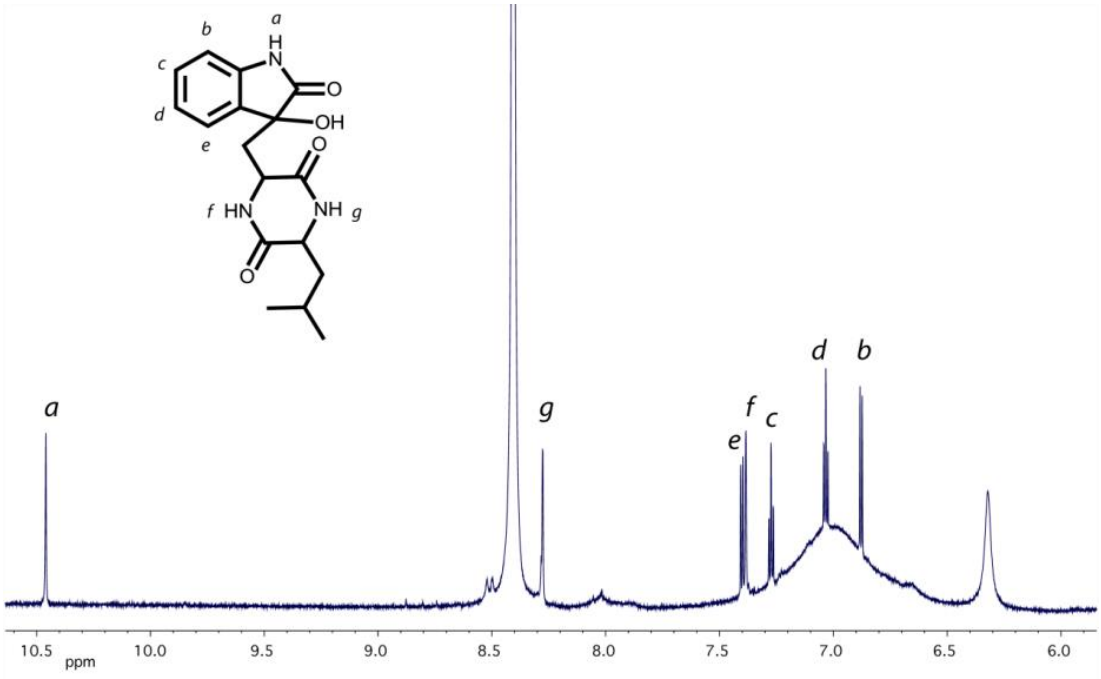

Figure S4. Low field region of a 1D 1H-NMR spectrum of the late-eluting LW+14* acquired at 800 MHz 1H resonance frequency. Resonance assignments are indicated in the structure. The following abbreviations are used to indicate signal multiplicity: s, singlet; d, doublet; t, triplet; m, multiplet; br, broad. 1H-NMR (800 MHz, DMSO-d_6): δ (ppm) =10.46 (s, 1H), 8.277 (s, 1H), 7.402 (d, J = 7.5 Hz, 1H), 7.384 (s, 1H), 7.273 (td, J = 7.7, 0.9 Hz, 1H), 7.033 (t, J = 7.5 Hz, 1H), 6.878 (d, J = 7.7 Hz, 1H).

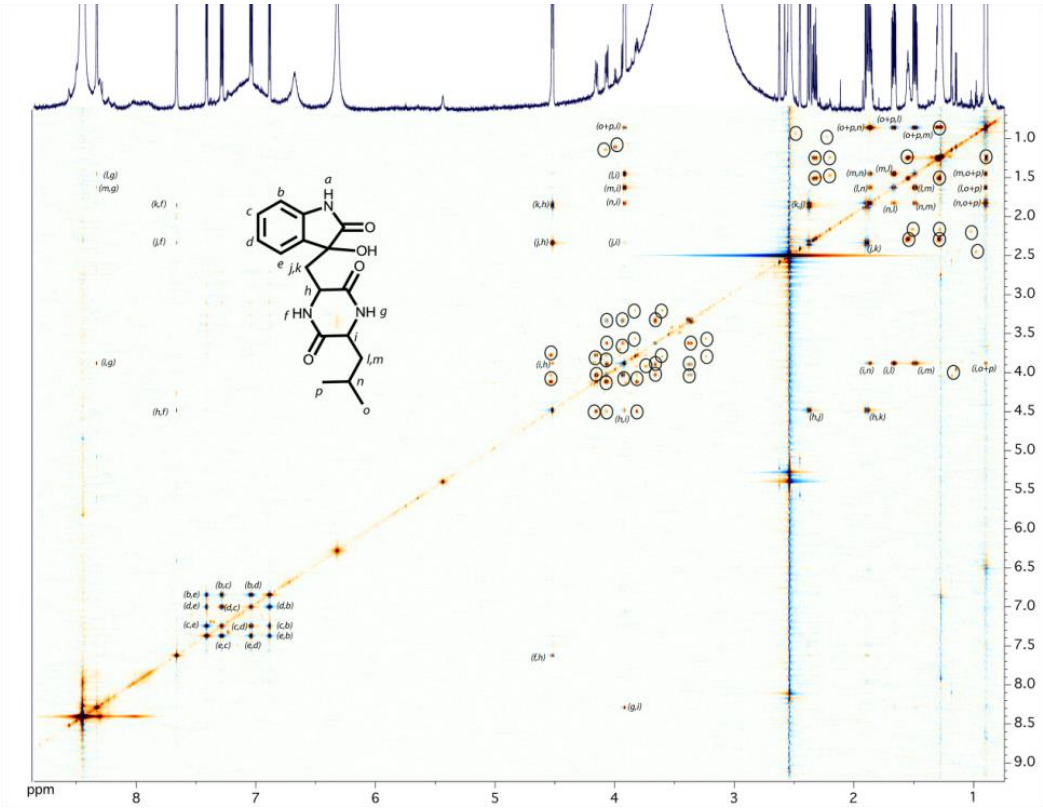

Figure S5. 2D TOCSY spectrum of the early-eluting LW+14* isomer. The assignment of the connectivities is indicated. Circles indicate signals from sample impurities. The following abbreviations are used to indicate signal multiplicity: s, singlet; d, doublet; t, triplet; m, multiplet; br, broad. 1H-NMR (800 MHz, DMSO-d_6); δ (ppm): 10.534 (s, 1H), 8.329 (s, 1H), 7.661 (s, 1H), 7.410 (d, J = 7.7 Hz, 1H), 7.284 (t, J = 7.5 Hz, 1H), 7.039 (td, J = 7.5, 0.9 Hz, 1H), 6.884 (d, J = 7.7 Hz, 1H), 4.512-4.528 (m, 1H), 3.910-3.926 (m, 1H), 2.375 (dd, J = 14.7, 3.4 Hz, 1H), 1.892 (dd, J = 14.7, 9.0 Hz, 1H), 1.842-1.884 (m, 1H), 1.667 (ddd, J = 13.6, 8.5, 4.8 Hz, 1H), 1.489 (ddd, J = 13.6, 7.8, 5.9 Hz, 1H), 0.905 (d, 3H), 0.893 (d, 3H).

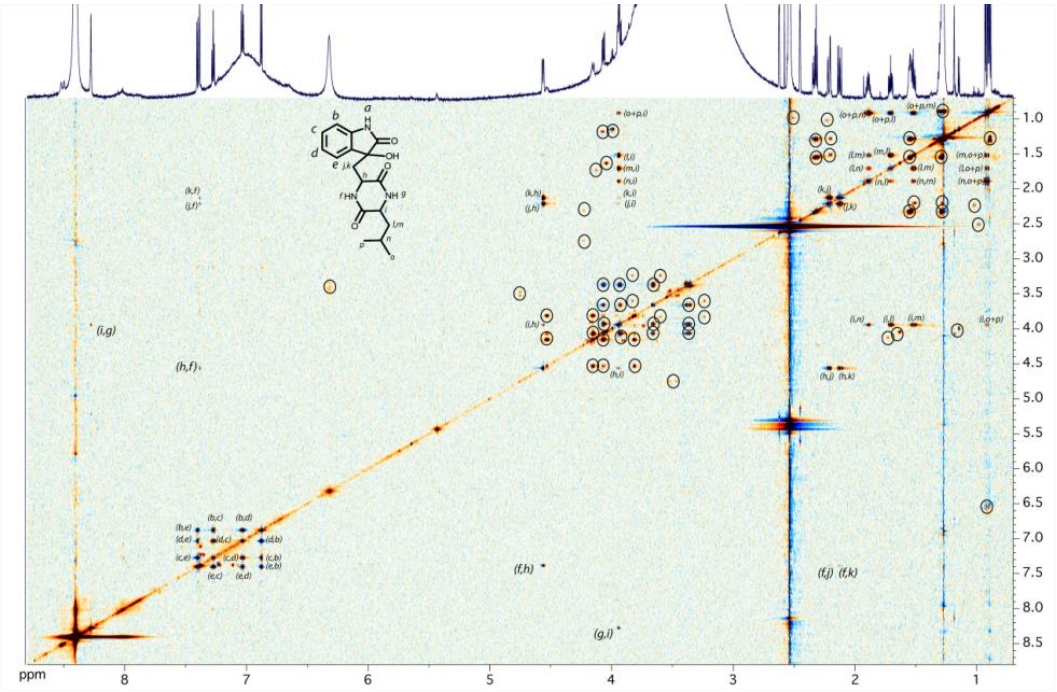

Figure S6. 2D TOCSY spectrum of the late-eluting LW+14* isomer. The assignment of the connectivities is indicated. Circles indicate signals from sample impurities. The following abbreviations are used to indicate signal multiplicity: s, singlet; d, doublet; t, triplet; m, multiplet; br, broad. 1H-NMR (800 MHz, DMSO-d_6): δ (ppm) =10.46 (s, 1H), 8.277 (s, 1H), 7.402 (d, J = 7.5 Hz, 1H), 7.384 (s, 1H), 7.273 (td, J = 7.7, 0.9 Hz, 1H), 7.033 (t, J = 7.5 Hz, 1H), 6.878 (d, J = 7.7 Hz, 1H), 4.556-4.571 (m, 1H), 3.934-3.951 (m, 1H), 2.202-2.225 (m, 1H), 2.112-2.141 (m, 1H), 1.866-1.917 (m, 1H), 1.708 (ddd, J = 13.6, 8.3, 4.9 Hz, 1H), 1.520 (ddd, J = 13.6, 7.5, 5.9 Hz, 1H), 0.927 (d, 3H), 0.906 (d, 3H).

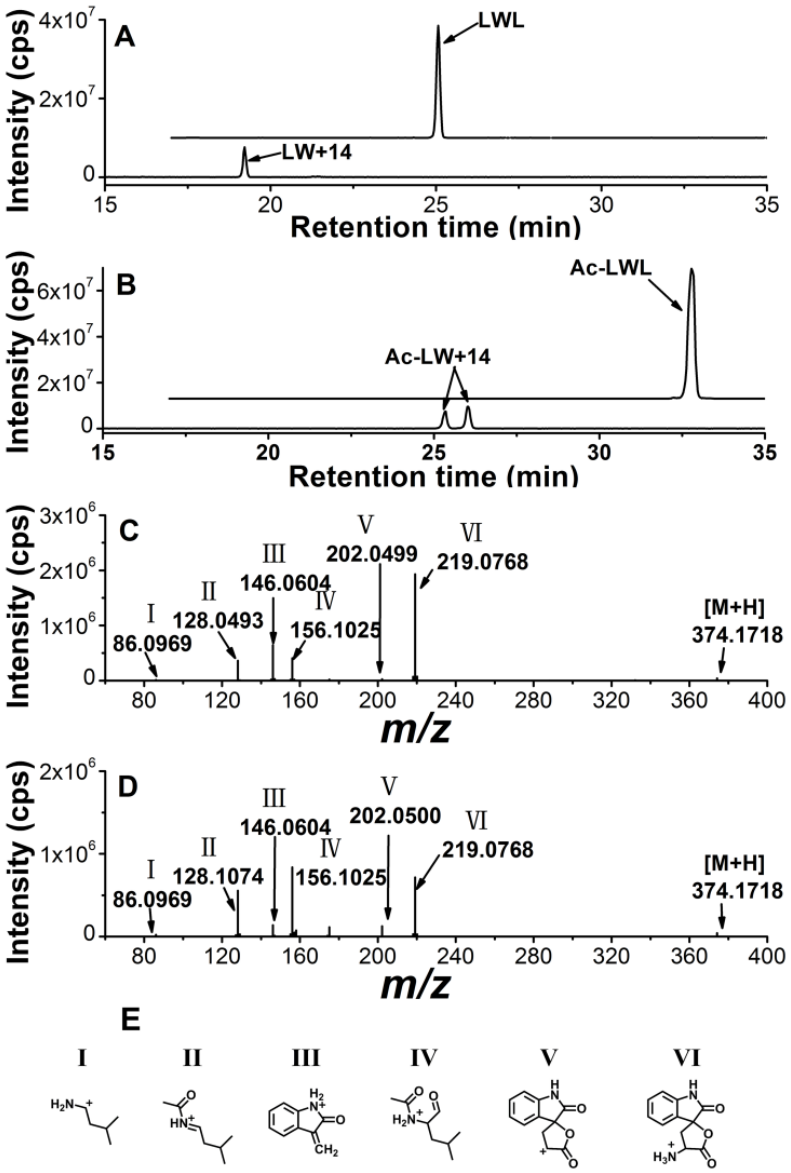

Figure S7. Extracted ion chromatograms of the electrochemical oxidation and cleavage products of LWL (LWL m/z 431.2640; LW+14 m/z 332.1599) (A) and Ac-LWL (Ac-LWL m/z 473.2740 and Ac-LW+14 m/z 374.1681) (B) (the LWL trace in A was offset by 2 min and 1×10^7 cps and the Ac-LWL trace in B was offset by 2 min and 1.2×10^7 cps for clarity). MS/MS spectra of the electrochemical cleavage products of Ac-LWL. Product ion spectra of the early-eluting (C) and the late-eluting (D) Ac-LW+14 isomer. Proposed structures of the fragments of Ac-LW+14 (E).

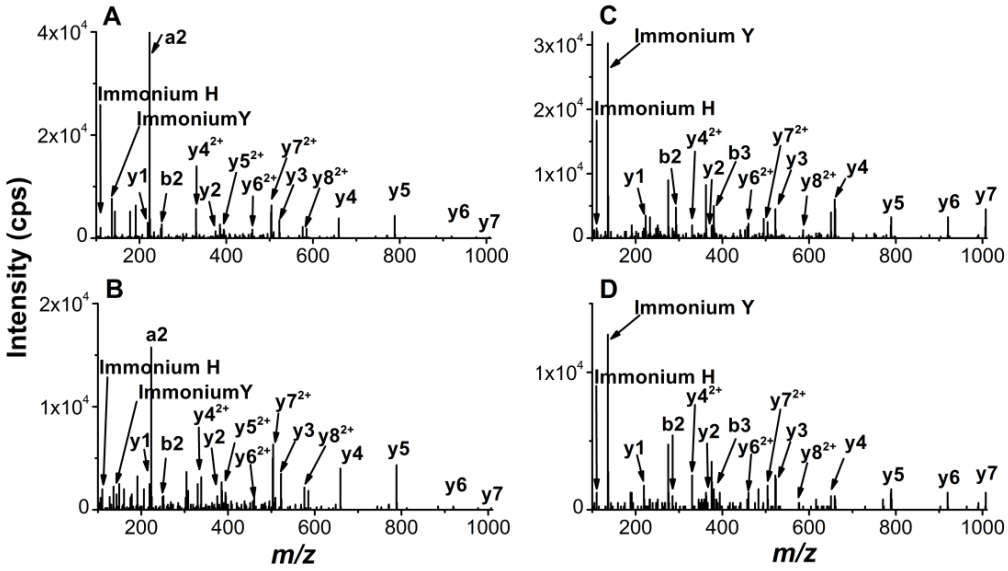

Figure S8. Representative MS/MS spectra of the electrochemical cleavage products SYSMEHFRW+14 (A & B, precursor ion at m/z 628.760 (2+)) of ACTH 1-10 and Ac-SYSMEHFRW+14 (C & D, precursor ion at m/z 649.767 (2+)) of Ac-ACTH 1-10. In both cases, early-eluting and late-eluting SYSMEHFRW+14 and Ac-SYSMEHFRW+14 isomers have the same mass and MS/MS spectra.

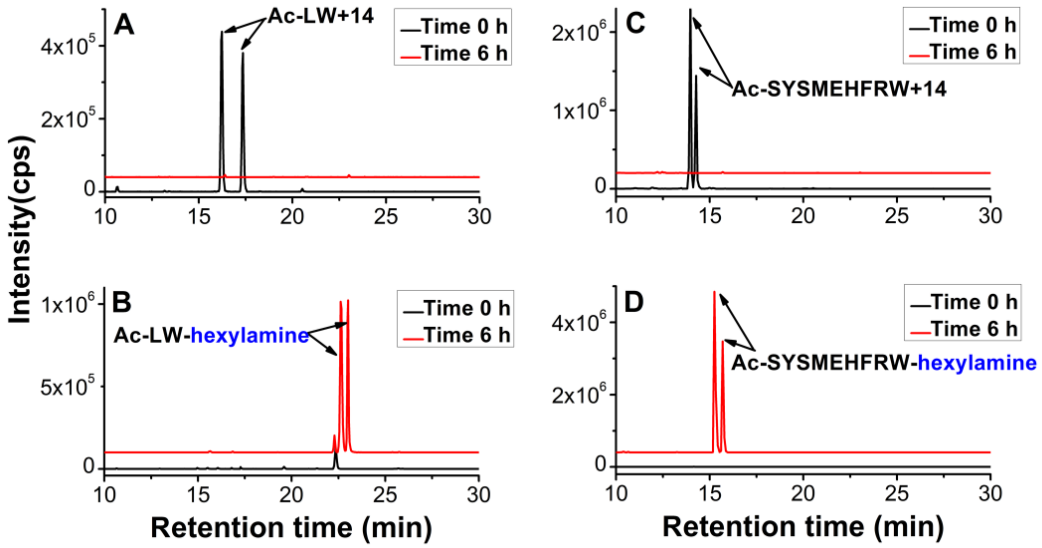

Figure S9. Chemical labeling of Ac-LW+14 and Ac-SYSMEHFRW+14 with hexylamine. Extracted ion chromatogram of Ac-LW+14 (A) (m/z 374.171), Ac-SYSMEHFRW+14 (C) (m/z 649.767, (2+)), the chemical labeling products Ac-LW-hexylamine (B) (m/z 475.296) and Ac-SYSMEHFRW-hexylamine (D) (m/z 700.328, (2+)) before and after reaction with a 400-fold molar excess of hexylamine in DMSO containing 0.5 % TEA for 6 h at room temperature. For clarity, the y axis of 6 h trace in (A) was offset by 5×10^4 cps, in (B) by 1×10^5 cps, in (C) by 2×10^5 cps and in (D) by 5×10^5 cps.

The cleavage product Ac-LW+14 (m/z 374.17) was fully converted to the corresponding hexylamide with a mass increment of 101.12 Da (m/z 475.29). Ac-LW-hexylamine was characterized by MS/MS showing that both isomers had the same fragmentation pattern (**Figure S10**). For peptide ACTH 1-10, efficient chemical coupling with hexylamine was also observed at the same condition (**Figure S9C** and **D**). Both isomers of Ac-SYSMEHFRW-hexylamine were analyzed by MS/MS and had the same fragmentation pattern (**Figure S11**).

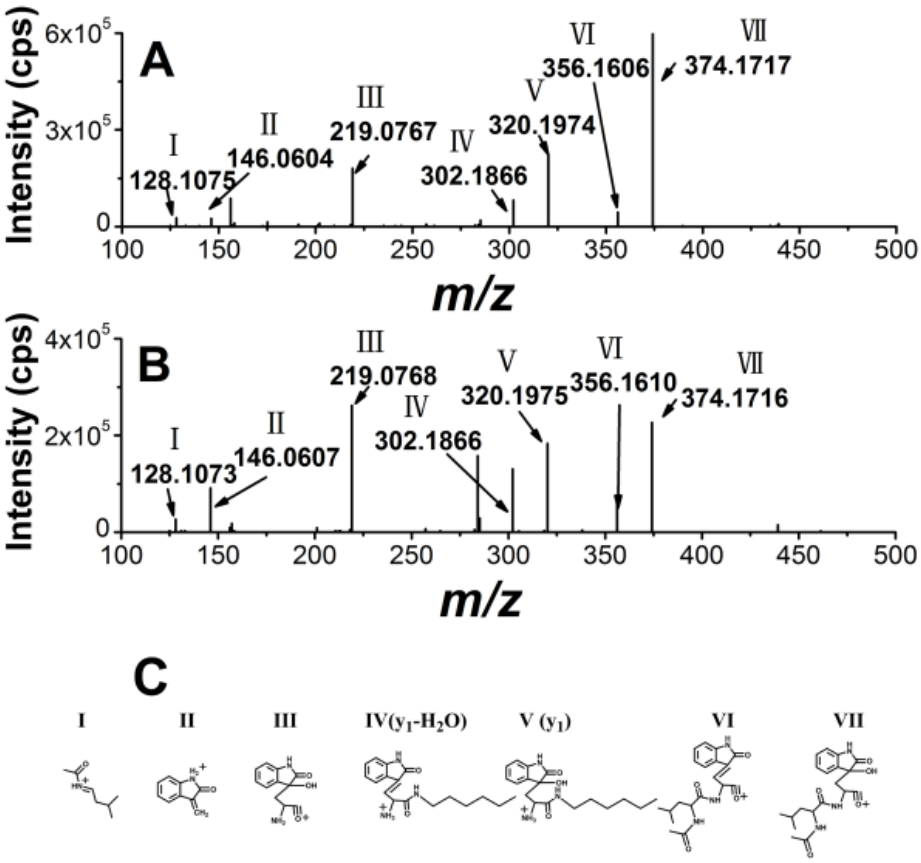

Figure S10. Representative MS/MS spectra of the early-eluting (A) and late-eluting (B) hexylamine-labeled spirolactones of electrochemically cleaved Ac-LWL. Proposed structures of the fragment ions of the coupling product of Ac-LW+14 with hexylamine (Ac-LW-hexylamine) (C). The early-eluting and late-eluting Ac-LW-hexylamine isomers have the same MS and MS/MS spectra. Specifically the y_1 fragment ion at m/z 320.20 and the y_1-H_2O ion at m/z 302.19 generated from water loss of y_1 confirmed chemical labeling of the peptide-spirolactone with hexylamine at the C-terminus. All other fragments were in agreement with the proposed structure of the labeled compound.

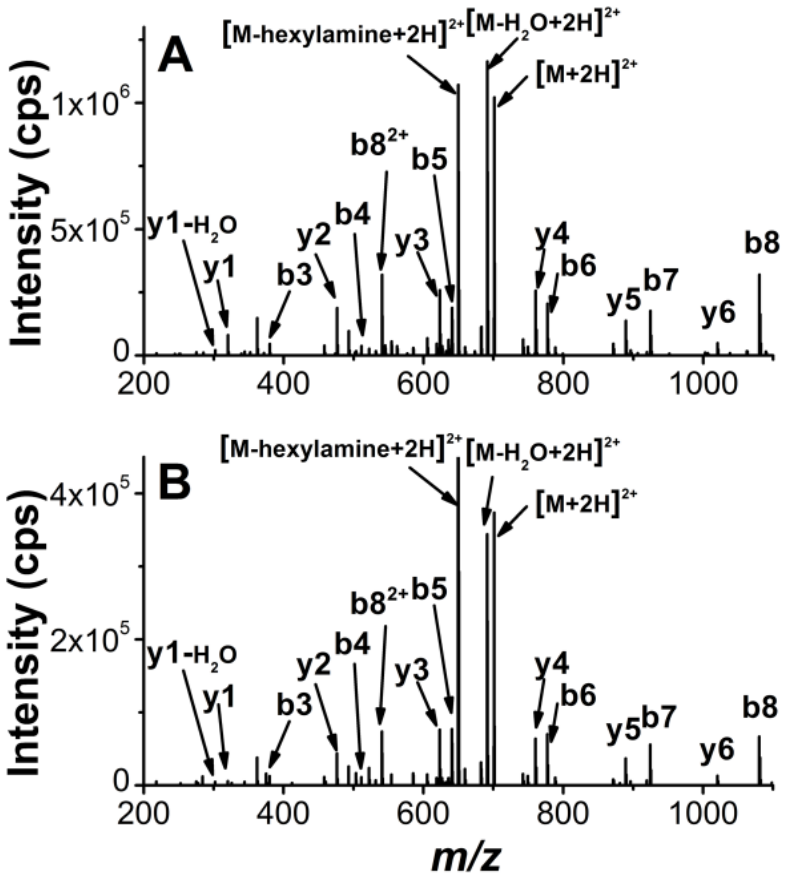

Figure S11. Representative MS/MS spectra of the early-eluting (A) and late-eluting (B) hexylamine-labeled spirolactones of electrochemically cleaved Ac-ACTH 1-10 (Ac-SYSMEHFRW-hexylamine, precursor ion at m/z 700.328 (2+)). The early-eluting and late-eluting Ac-SYSMEHFRW -hexylamine isomers have the same MS and MS/MS spectra. The same y1 fragment ion at m/z 320.20 and the y_1-H_2O ion at m/z 302.19 were generated from fragmentation of C-terminus. A mass increment of 101.12 in y_1 to y6 ions of Ac-SYSMEHFRW-hexylamine (m/z 320.20, 476.33, 625.41, 760.46, 889.51 and 1107.58) comparing with the corresponding y_1 to y_6 ions of Ac-SYSMEHFRW+14 (m/z 219.10, 375.21, 522.29, 659.34, 788.39 and 919.46) was observed which further supports chemical labeling of Ac-SYSMEHFRW+14 by hexylamine. In addition, the b ions (b_3 to b_8), water loss ion (m/z 691.32) and hexylamine loss ion (m/z 649.77) of Ac-SYSMEHFRW-hexylamine were assigned supporting the chemical labeled peptides.

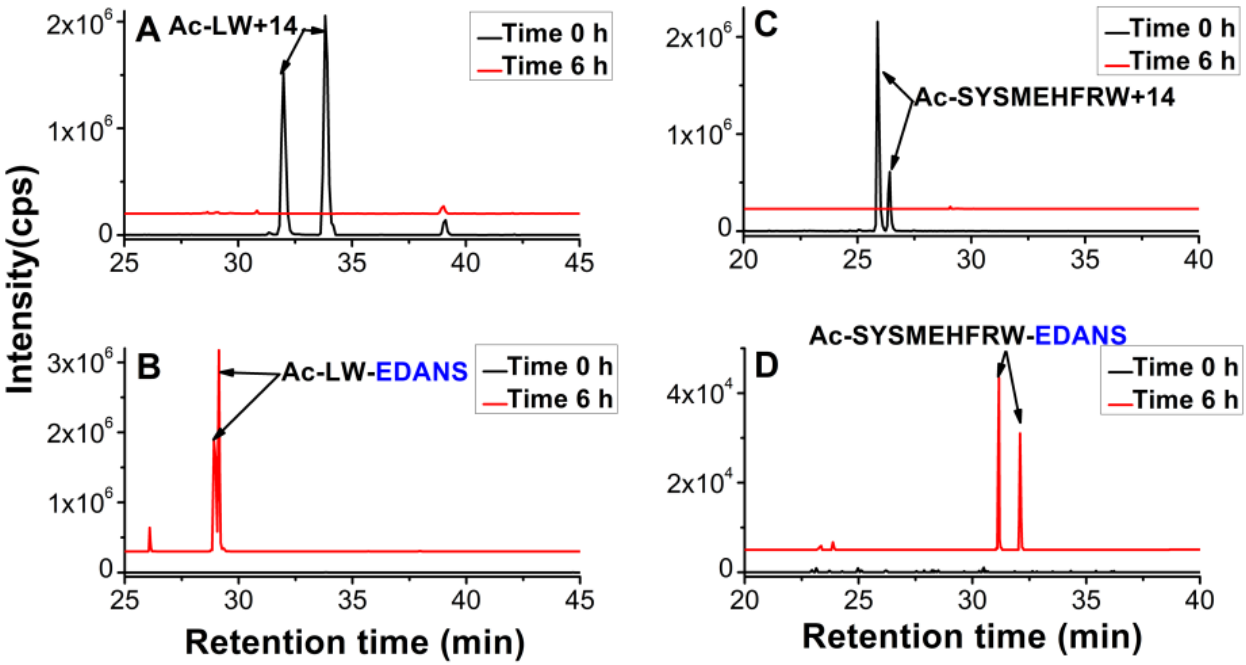

Figure S12. Chemical labeling of Ac-LW+14 and Ac-SYSMEHFRW+14 with EDANS. Extracted ion chromatogram of Ac-LW+14 (A) (m/z 374.171), Ac-SYSMEHFRW+14 (C) (m/z 649.767, (2+)), the chemical labeling products Ac-LW-EDANS (B) (m/z 640.244) and Ac-SYSMEHFRW-EDANS (D) (m/z 782.803, (2+)) before and after reaction with a 4000-fold molar excess of EDANS in DMSO containing 0.5 % TEA for 6 h at room temperature. The separation of EDANS labeling reaction mixture was achieved with a 65 min gradient of 2-60% acetonitrile in water/0.1% formic acid at a flow rate of 300 µL/min. For clarity, the y axis of 6 h trace in (A) was offset by 2×10^5 cps, in (B) by 4×10^5 cps, in (C) by 3×10^5 cps and in (D) by 5×10^3 cps.

Chapter 4

Specific affinity enrichment of electrochemically cleaved peptides based on Cu (II)-mediated spirolactone tagging

Abstract: Specific digestion of proteins is an essential step for mass spectrometry-based proteomics, and the chemical labeling of the resulting peptides is often used for peptide enrichment or the introduction of desirable tags. Electrochemical oxidation yielding specific cleavage C-terminal to tyrosine (Tyr) and tryptophan (Trp) residues provides an alternative to enzymatic digestion, and a possibility for further chemical labeling by introducing reactive spirolactone moieties. However, spirolactone-containing peptides suffer from low stability due to hydrolysis and intramolecular side reactions. We found that Cu (II) ions stabilize the spirolactone and prevents intramolecular side reactions during chemical labeling, allowing efficient chemical tagging with a reduced excess of labelling reagent without intramolecular side reactions. Based on this reaction, we developed an analytical procedure combining electrochemical digestion, Cu (II)-mediated spirolactone biotinylation and enrichment by avidin affinity chromatography with mass spectrometry. The method was optimized with the tripeptide LWL and subsequently applied to chicken egg white lysozyme, in which one biotinylated EC-cleaved peptide was identified after affinity enrichment. This proof-of-principle shows that specific enrichment of electrochemically cleaved spirolactone-containing peptides can be used for protein identification and notably that inclusion of Cu (II) ions is essential for stabilizing spirolactones for subsequent biotinylation.

Published as: Tao Zhang, Marcel P. de Vries, Hjalmar P. Permentier and Rainer Bischoff. Specific affinity enrichment of electrochemically cleaved peptides based on Cu (II)-mediated spirolactone tagging. *Analytical Chemistry*, 2017, 89, 7123-7129.

4.1 Introduction

Mass spectrometry-based proteomics is a powerful and indispensable tool for the analysis of complex samples, [1-4] and the specific digestion of proteins plays a key role in their identification and quantification. [4-6] Enzymes with different specificities are the cornerstone reagents for the digestion of proteins at specific peptide bonds [7-9] while chemical cleavage is sometimes used as an alternative when a different specificity is required. [10-13] Specific cleavage of the peptide bond C-terminal to Tyr and Trp residues occurs after electrochemical oxidation of peptides and proteins, which makes electrochemistry (EC) a potential instrumental alternative to chemical and enzymatic peptide bond cleavage. [14-20] However, EC oxidation yields complex mixtures due to the generation of non-cleavage oxidation products in addition to cleaved peptides, which poses a problem for proteomics applications.

Selective enrichment of proteins and peptides via affinity-based isolation has increasingly contributed to MS-based proteomics, serving to reduce sample complexity prior to LC-MS analysis. [21-24] An efficient enrichment strategy for the peptides of interest via specific labeling would significantly reduce sample complexity and increase the depth of proteomics analyses. [21, 25, 26] Biotinylation is a widely used strategy to prepare peptides and other molecules for enrichment by avidin affinity chromatography. [25-27] Electrochemical cleavage of the peptide bond of Tyr or Trp yields a spirolactone moiety at the newly formed C-terminus providing a handle for specific chemical labeling. [17, 20] In previous work, we used this unique spirolactone to introduce affinity tags but encountered problems with spirolactone stability and intramolecular rearrangement. [20]

A number of chemical agents and biocatalysts are known to catalyze reactions between activated esters and primary amines including Lewis bases (*e.g.* pyridine, 2-hydroxypyridine), [28-29] Lewis acids (*e.g.* sodium cyanide, and salts of zinc, nickel, iron, lanthanum, and zirconium) [30-36] and enzymes (*e.g.* Candida antarctica lipase B) [37-39]. For example, La (III) trifluoromethanesulfonate was developed as catalyst for synthesizing a variety of amides directly from esters and amines under mild conditions. [34] We therefore investigated a range of potential catalysts in view of their ability to reduce side reactions and to obtain efficient coupling with a reduced excess of the often costly labelling reagents. Addition of Cu (II) ions proved to be highly efficient in preventing spirolactone hydrolysis as well as intramolecular diketopiperazine formation. Based on this improvement, we developed a specific affinity enrichment method combining electrochemical digestion, Cu (II)-mediated spirolactone biotinylation and affinity chromatography with LC-MS to identify proteins after electrochemical digestion. The method was first optimized with the tripeptide LWL and subsequently applied to chicken egg lysozyme.

4.2 Experimental section

4.2.1 Materials and Methods

Formic acid (HCOOH, FA, 98%), dimethyl sulfoxide (DMSO, anhydrous, 99.8%), acetic acid anhydride (99%), chicken egg white lysozyme, iodoacetamide (IAM), dithiothreitol (DTT), ammonium bicarbonate (99.5%), Cu (II) chloride dihydrate (99.9%), hexylamine (99%), sodium phosphate (96%), sodium chloride (99.0%), pyridine (99.8%), 2-hydroxypyridine (97.0%), sodium cyanide (97.0%), Cu (I) chloride (99.99%), nickel (II) chloride hexahydrate (98%), zinc acetate dihydrate (99.99%), iron (II) perchlorate hydrate (98%), iron (III) perchlorate hydrate (crystalline) and D-biotin (analytical standard) were purchased from Sigma Aldrich (Steinheim, Germany). LWL was obtained from Research Plus Inc. (Barnegat, NJ, USA). Amine-PEG_2-biotin and monomeric avidin agarose were obtained from Pierce Biotechnology (Rockford, USA). Acetonitrile (HPLC SupraGradient grade) was acquired from Biosolve (Valkenswaard, The Netherlands). Ultrapure water was obtained from a Milli-Q Advantage A10 water

purification system at a resistivity of 18.2 MΩ cm (Millipore Corporation, Billerica, MA, USA).

4.2.2 Peptide and protein preparation

LWL at a concentration of 1 mM was prepared in 89/10/1 (v/v/v) water/acetonitrile/formic acid as stock solution. A stock solution of reduced and alkylated lysozyme was prepared in 89/10/1 (v/v/v) water/acetonitrile/formic acid at a protein concentration of 100 µM. For reduction and alkylation, lysozyme (100 µM), was prepared in 100 mM ammonium bicarbonate buffer (pH 8). Two mM DTT in 100 mM ammonium bicarbonate buffer were added, and the mixture was incubated with shaking at 500 rpm at 60 °C for 30 min. IAM was added at a concentration of 20 mM after cooling and reacted at room temperature in a dark environment for 40 min. After alkylation, 8 mM DTT was added to quench the alkylation reaction for 30 min. Lysozyme precipitated upon reduction and alkylation. The reaction mixture was centrifuged at 13000 rpm and the supernatant was removed. Water/acetonitrile/formic acid 89/10/1 (v/v/v) was added to dissolve the precipitated lysozyme and prepare a 100 µM stock solution of reduced and alkylated lysozyme. LWL was diluted to a final concentration of 10 µM (LWL) and lysozyme to 5 µM prior to electrochemical cleavage. To prevent formylation or acid hydrolysis, the formic acid content of lysozyme was increased to 5 % just before the electrochemistry experiments. [40-43]

4.2.3 Electrochemical cleavage

Electrochemical oxidation and cleavage was performed in a µ-PrepCell electrochemical cell (thin-layer cell, Antec, Zoeterwoude, NL) with a boron-doped diamond (BDD, 12 × 30 mm × 1 mm) working electrode (Antec), a titanium counter electrode and a palladium reference electrode (Pd/H_2). A flow rate of 10 µL/min was employed to introduce analyte solutions via a syringe pump (KD Scientific Inc., Holliston, MA, USA). The electrochemical potentials were controlled with a ROXY potentiostat (Antec) operating in Scan and DC mode. Cathodic pretreatment of BDD electrodes at a negative

potential of -3000 mV was used to regenerate the electrode surface prior to all experiments by pumping 0.5 M nitric acid in water at a flow rate of 50 µL/min for 1 h. Prior to use, the cell was flushed with electrolyte solution at a potential of -2000 mV for 1 h.

The optimal cleavage potentials of peptides and proteins were first determined via on-line EC-MS experiments by ramping the cell potential from 0 to 3000 mV linearly at a scan rate of 10 mV/s. The detection of electrochemical cleavage products in on-line EC-MS was achieved in an API 365 triple quadrupole mass spectrometer (PE-Sciex, Concord, Ontario, Canada) with an EP10+ upgrade (Ionics, Bolton, Ontario, Canada) in positive ion mode. LWL and lysozyme were oxidized at 1000 mV and 2000 mV vs Pd/H_2, and the product mixtures (EC-LWL and EC-lysozyme) were collected for LC-MS analysis and further reactions.

4.2.4 Effect of Cu (II) on stability of cleavage products and chemical tagging

Cu (II) chloride dehydrate at a concentration of 100 µM was prepared in 89/10/1 (v/v/v) water/acetonitrile/formic acid as stock solution. EC-LWL with Cu (II) was prepared by adding 4 µL Cu (II) chloride dehydrate (100 µM) into 2 mL solution and dried following the same procedure as described in our previous work. [20] EC-LWL without Cu (II) was dried following the same procedure as a control.

To study the effect of Cu (II) on the stability of the spirolactone in peptides, 2 mL EC-LWL with or without Cu (II) were concentrated by evaporation under nitrogen (2 h) and dried in an Eppendorf Concentrator at 30 °C. EC-LWL was prepared at a concentration of 400 µM by dissolving the dried sample in 50 µL DMSO/TEA (99.9/0.1, v/v) by pipetting for 30 s. Reactions were performed at 25 °C with shaking at 900 rpm in an Eppendorf Thermomixer. Ten µL of reaction product mixtures at time point 0 h and 6 h were prepared at a concentration of 5 µM by dilution with 390 µL 99/1 (v/v) water/formic acid, and 40 µL EC-LWL were subjected to LC-MS analysis. LC-MS analyses were performed on an Ultimate plus system (Dionex-LC Packings, Amsterdam, The Netherlands) coupled to an API 365 triple quadrupole mass spectrometer (PE-

Sciex) with an EP10+ upgrade (Ionics). The separation of the reaction mixtures was achieved on a Vydac RP-C18 column (150 mm × 2.1 mm i.d., 5 µm particles, 300 Å pore size, Grace Vydac, Lokeren, Belgium) with a 35 min gradient of 2-50% acetonitrile in water/0.1% formic acid at a flow rate of 250 µL/min.

Chemical tagging with hexylamine was performed at a concentration of 500 µM by adding 20 µL of a mixture of DMSO, TEA and hexylamine (99.65:0.1:0.25) to 1 mL dried EC-LWL mixture in presence or absence of Cu (II), respectively, with a 50-fold molar excess of hexylamine. The reaction mixtures were incubated with shaking at 900 rpm at 25 °C for 6 h and analyzed by LC-MS. Biotinylation of EC-LWL was performed at a concentration of 500 µM for peptides in the presence or absence of Cu (II). Prior to use, 2 mg amine-PEG_2-biotin was prepared in 1 mL water and purified on an Oasis HLB extraction cartridge (1cc, 30mg, Waters Corporation, Milford, Massachusetts, USA) by elution with 15 mL 10% ACN. After evaporating under nitrogen and drying in an Eppendorf Concentrator 5301 (Eppendorf, Hamburg, Germany), amine-PEG_2-biotin was dissolved in 50 µL DMSO/TEA (99.9/0.1). 20 µL amine-PEG_2-biotin in solution was added to the sample in the presence or absence of Cu (II), and shaken at 900 rpm at 25 °C for 16 h, with a 200-fold molar excess of hexylamine. Biotinylated EC-LWL (Bio-EC-LWL) was diluted to 5 µM by adding 99/1 (v/v) water/formic acid, and 40 µL of the reaction mixtures were analyzed by LC-MS. Liquid chromatography was performed on a Waters UPLC I-class system (Waters Corporation, Milford, USA) with a Waters Acquity Peptide BEH C18 column (100 mm × 2.1 mm *i.d.*, 1.7 µm particles, 300 Å pore size, Waters Corporation, Milford, USA) at 400 µL/min using a linear gradient from 5-40% acetonitrile in water/0.1% formic acid in 25 min. For mass spectrometry, a Maxis plus quadrupole time-of-flight mass spectrometer (QTOF, Bruker, Bremen, Germany) in positive electrospray ionization mode was used.

4.2.5 Biotinylation of EC-lysozyme with amine-PEG_2-biotin

For biotinylation of EC-lysozyme with amine-PEG_2-biotin, a reaction was performed in the presence of Cu (II). EC-lysozyme with Cu (II) was prepared by adding 4 µL Cu

(II) chloride dehydrate (100 µM) into 2 mL EC-lysozyme (5 µM) and dried following the same procedure as described in our previous work. [20] Two mg amine-PEG_2-biotin was purified, dried and dissolved in 50 µL DMSO/TEA (99.9/0.1) as described above in the same condition. Twenty µL of amine-PEG_2-biotin in DMSO/TEA (99.9/0.1) were added to the dried EC-lysozyme followed by pipetting for 30 s, and the mixture was incubated for 16 h with shaking at 900 rpm at 25 °C.

4.2.6 Removal of excess biotin by SPE after biotinylation

The biotinylation reaction mixture was diluted with 1 mL water/formic acid (99.9/0.1) and loaded on a Strata C18-E cartridge (55 µm, 70 Å, Phenomenex, Utrecht, The Netherlands). Twenty mL of 10% ACN and 3 mL 15% ACN in H_2O/FA (99.9/0.1) were used to remove the excess of amine-PEG_2-biotin (200-fold) followed by elution of the biotinylated peptide by adding 3 mL of 50% ACN to the cartridge. Elution fractions were collected and concentrated by evaporation under nitrogen (2 h, 15 µL) at 30 °C. Bio-EC-LWL and bio-EC-lysozyme were diluted with 100 mM phosphate-buffered saline (PBS, 100 mM sodium phosphate, 150 mM sodium chloride, pH 7) to a final volume of 500 µL prior to affinity enrichment.

4.2.7 Affinity enrichment of biotinylated peptides

One mL monomeric avidin agarose was packed and prepared in a disposable column according to the supplier's instructions. The biotinylated electrochemically cleaved peptides were captured with 1 mL monomeric avidin agarose in the column by incubation for 30 min at room temperature. The immobilized monomeric avidin agarose column was washed with 2 mL of PBS. Biotinylated peptides were eluted with 2 mL of D-biotin at a concentration of 2 mM in 100 mM PBS and concentrated by evaporation using nitrogen at 30 °C for 2 h. The elution fractions of bio-EC-LWL and bio-EC-lysozyme were prepared to a final volume of 5 mL and 2 mL, respectively, by adding 99/1 (v/v) water/formic acid prior to LC-MS/MS analysis.

4.2.8 Analysis by LC-MS/MS

LC-MS/MS analyses of the EC-cleaved peptide mixture, the biotinylation reaction mixture and the affinity-enriched biotinylated peptides were performed on a UPLC I-Class system (Waters) coupled to a quadrupole time-of-flight mass spectrometer (Maxis plus, Bruker) as described above. MS scans from *m/z* 200 to 1000 were recorded in profile mode using positive polarity.

The LC-MS/MS analyses of complex peptide mixtures obtained after avidin purification of EC-lysozyme were performed on a Dionex Ultimate 3000 nano-LC system equipped with an Acclaim Pepmap column (75 µm i.d. × 150 mm, Thermo Scientific, Bremen, Germany) coupled to a Q-Exactive Plus quadrupole-Orbitrap mass spectrometer (Thermo Scientific). To separate peptides, a linear gradient of 2-60 % acetonitrile in water/0.1 % formic acid in 50 min at a flow rate of 300 nL/min was employed. MS scans from *m/z* 200 to 1750 were recorded at a resolution of 75000. MS/MS spectra were recorded at a resolution of 17500 with a normalized collision energy of 35 V in data-dependent mode. The top 10 highest intensity peaks were chosen for MS/MS.

4.2.9 Data analysis and database searching

The database search engine PEAKS (version 8.0, Bioinformatics Solutions Inc.) was used to analyze LC-MS/MS data using the chicken Uniprot protein sequence database (*Gallus gallus*, updated 06-12-2016, SwissProt reviewed entries only) containing 2601 proteins . The search parameters were as follows: Parent Mass Error Tolerance: 10.0 ppm; Fragment Mass Error Tolerance: 0.05 Da; Enzyme: EC (custom-defined, digestion after Y or W); Max Missed Cleavages: 5; Non-specific Cleavage: one; Variable Modifications: Oxidation (on MFWHYC): +15.99, Carbamidomethylation (C): +57.02; EC-Y-2 (custom-defined: on C-terminal Y): -2.02; EC-W+14 (custom-defined: on C-terminal W): +13.98; EC-Y+372.16 (custom-defined: on C-terminal Y): +372.16; EC-W+388.18 (custom-defined: on C-terminal W): +388.18; Maximum variable post-translational modifications per peptide: 5.

4.3 Results and discussion

4.3.1 Stabilization of peptide-spirolactones against intramolecular rearrangement in the presence of Cu (II) ions

Specific cleavage after Tyr and Trp in peptides and proteins upon electrochemical oxidation yields a complex mixture of peptides with a reactive spirolactone moiety at the C-terminus of the N-terminal cleavage fragment in addition to other peptide and protein modifications. [18-20] We previously developed an approach to label electrochemically cleaved peptides via spirolactone chemistry to introduce affinity tags [20] for subsequent enrichment by immobilized avidin chromatography and characterization by mass spectrometry. In this approach, acetylation of the amino group at the N-terminus was essential to prevent intramolecular rearrangement to non-reactive diketopiperazines. However, this approach has limitations when it comes to the electrochemical cleavage of larger peptides or proteins, because of the unavoidable generation of neo-N-termini and the increasing difficulty to achieve complete acetylation of all amino groups. Another limitation of this approach is that a large molar excess (2000-fold) of the affinity tag amine-PEG_2-biotin [20] was required for efficient tagging. To prevent this unwanted side reaction and to increase coupling efficiency at lower molar excess of affinity tags, an alternative strategy is required that does not rely on acetylation.

To investigate a range of catalysts that have been described to facilitate the reaction between an activated ester and a primary amine, we screened the nucleophilic catalysts pyridine, 2-hydroxypyridine and NaCN as well as the following transition metal ions: Ni (II), Cu (I), Cu (II), Zn (II), Fe (II) and Fe (III). [28-31] To study the effect of the selected catalysts, we followed the stability of LW+14 in DMSO containing 0.1% TEA as well as the reaction of LW+14 with a 50-fold molar excess of hexylamine. The presence of 0.5% pyridine or 2-hydroxypyridine in the reaction mixture had no effect on the chemical coupling yield and accelerated the undesirable intramolecular rearrangement (data not shown). NaCN and most of the transition metal ions had no effect on either coupling yield or the stability of the spirolactone-containing peptides with respect to

intramolecular rearrangement. Out of all tested reagents, we found that only addition of 2 µM Cu (II) ions prevented the intramolecular rearrangement reaction and significantly increased coupling yields with hexylamine. **Figure 1A** shows that the spirolactone-containing peptide LW+14 rearranges to a pair of isomeric diketopiperazines (LW+14*) in the absence of Cu (II), as previously described, [20] while this was prevented by the addition of Cu (II). Rearrangement of LW+14 proceeded to 75% completion within 6 h in the absence of Cu (II), while LW+14 was stable in the presence of Cu (II) even under basic conditions in DMSO containing 0.1% TEA (**Figure 1B**). The small amount of diketopiperazines observed in the chromatogram was formed during the electrochemical cleavage reaction prior to adding Cu (II) ions.

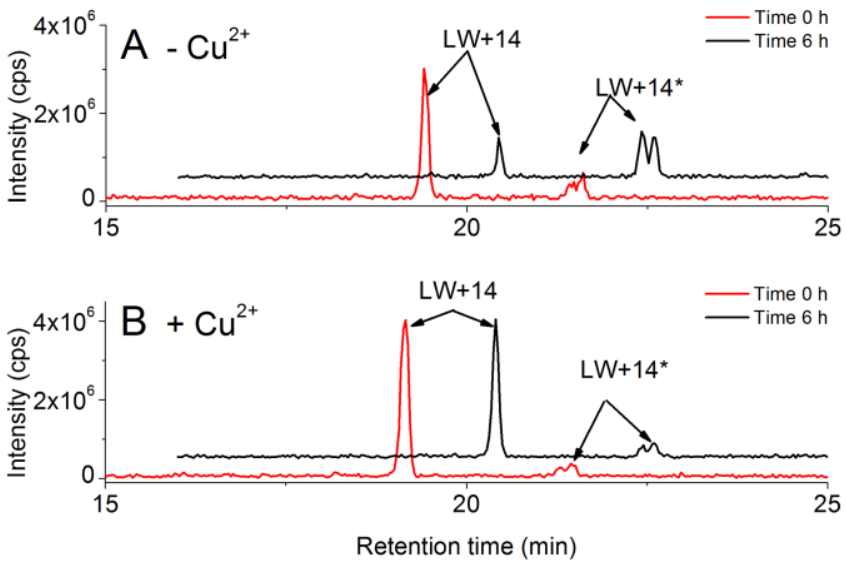

Figure 1. Stability of the electrochemical cleavage product LW+14 in the absence of Cu (II) (A) and in the presence of Cu (II) (B) after incubation for 6 h in DMSO/TEA (99.9/0.1) at room temperature. For clarity, the 6 h traces in both (A) and (B) were offset by 1 min on the x-axis and by 5×10^5 cps on the y-axis.

4.3.2 Cu (II)-mediated spirolactone chemical tagging

As shown above, Cu (II) stabilized the spirolactone-containing peptide and prevented rearrangement to diketopiperazines without having to resort to acetylation. Consequently, the chemical coupling of LW+14 to hexylamine was studied in the absence and in the presence of Cu (II) in DMSO containing 0.1% TEA. Efficient chemical tagging was only observed in the presence of Cu (II) at a 50-fold molar excess of hexylamine (**Figure 2**).

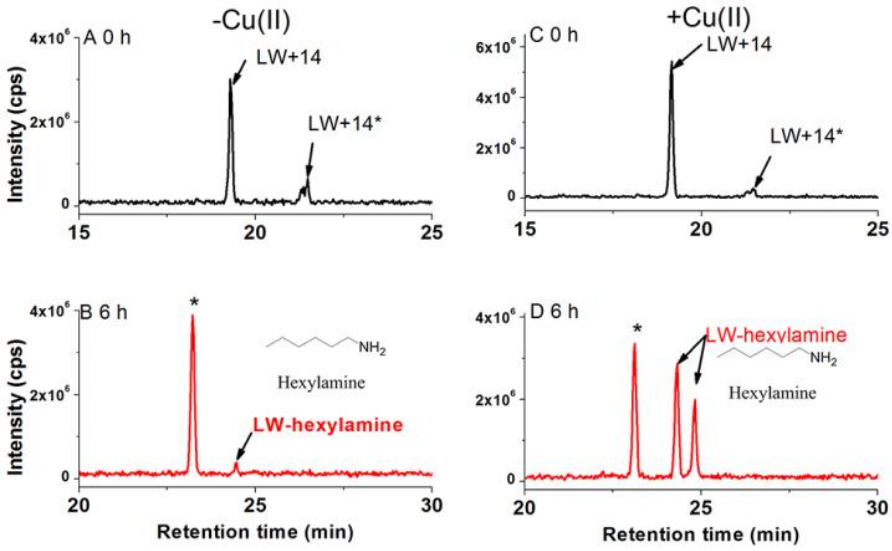

Figure 2. Chemical labeling of LW+14 with a 50-fold molar excess of hexylamine in the absence (A and B) and in the presence (C and D) of Cu (II). Extracted ion chromatograms of the electrochemically cleaved tripeptide LWL (LW+14, *m/z* 332.150) (A) before reaction, and of the chemical labeling product LW-hexylamine (433.256) (B) after reaction in DMSO containing 0.1% TEA for 6 h at room temperature in the absence of Cu (II). In the same order, panels C and D show extracted ion chromatograms of LW+14 (C) and the chemical labeling products LW-hexylamine (D) after reaction under the same conditions in the presence of Cu (II). Peaks marked with * depict the ion of LWL containing one ^{13}C atom, which has the same mass as LW-hexylamine.

Reaction of LW+14 with amine-PEG_2-biotin at a 200-fold molar excess was investigated next. **Figures 3A** and **B** show that only trace amounts of biotinylated LW+14

(Biotin-LW) were observed in the absence of Cu (II) ions since LW+14 underwent intramolecular rearrangement as the main reaction. Addition of Cu (II) prevented this side reaction resulting in complete biotinylation of LW+14 with amine-PEG_2-biotin under otherwise identical conditions (**Figures 3C** and **D**). These results confirmed that addition of Cu (II) is critical for efficient chemical tagging of spirolactone-containing peptides.

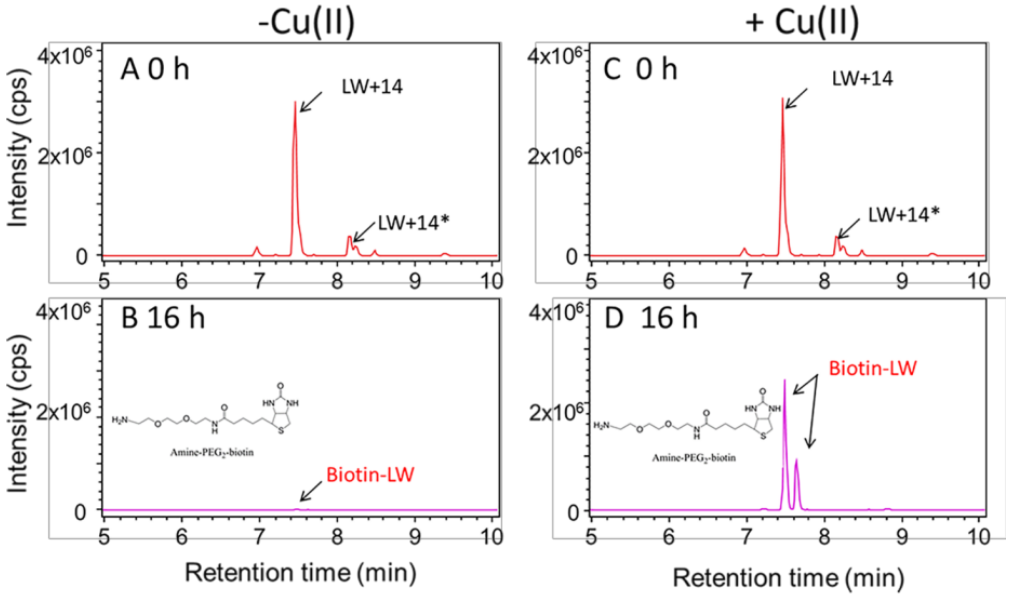

Figure 3. Biotinylation of LW+14 with amine-PEG_2-biotin in the absence (A and B) or in the presence (C and D) of Cu (II). Extracted ion chromatograms of the electrochemically cleaved tripeptide LWL (LW+14, *m/z* 332.16) (A) before reaction, and the biotinylated product Biotin-LW (*m/z* 706.37) (B) after reaction with amine-PEG_2-biotin in DMSO containing 0.1% TEA for 16 h at room temperature in the absence of Cu (II). In the same order, panels C and D show extracted ion chromatograms of LW+14 (*m/z* 332.16) (C) and the biotinylated products Biotin-LW (*m/z* 706.37) (D) after reaction under the same conditions in the presence of 2 µM Cu (II). LW+14* symbolizes the intramolecular rearrangement products (diketopiperazines) as described previously. [20]

4.3.3 Affinity enrichment of biotinylated peptides

Since electrochemical peptide bond cleavage does not only generate the spirolactone-containing peptides, we investigated whether Cu (II)-mediated biotinylation can be used to enrich cleavage products from more complex mixtures. To this end we combined Cu (II)-mediated biotinylation with selective affinity enrichment on monomeric avidin beads as shown in **Figure 4A**. **Figure 4B** shows the conversion of a Trp-containing peptide from electrochemical cleavage to biotinylation of the C-terminus of the N-terminal fragment.

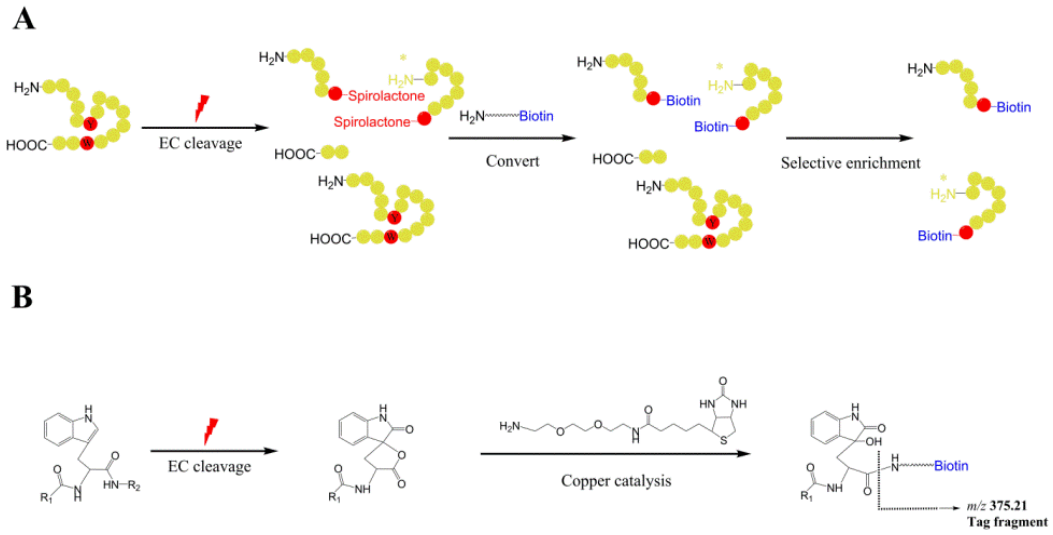

Figure 4. (A) Scheme for enriching electrochemically generated peptide fragments after electrochemical cleavage of peptides and proteins via Cu (II)-mediated biotinylation of the spirolactone-containing peptide fragments and selective affinity enrichment. (B) Scheme showing the chemical conversion of a Trp-containing peptide from electrochemical cleavage to a biotinylated residue using amine-PEG_2-biotin. R_1 and R_2 represent the peptide chains N-terminal and C-terminal to the Trp residue, respectively. The dashed line indicates the main MS/MS fragmentation site producing the characteristic fragment ion at m/z = 375.21 (see **Figure 5**).

We first tested this approach on the tripeptide LWL. LWL was electrochemically cleaved at 1100 mV in an electrochemical cell with a BDD working electrode, yielding a mixture containing LWL, uncleaved oxidation products (LWL+32) and the spirolactone-containing cleavage product LW+14 (**Figure 5A**). LW+14 was completely biotinylated to LW-amine-PEG_2-biotin (Biotin-LW) in DMSO containing 0.1% TEA in the presence of Cu (II) resulting in a mass increment of 374.21 Da (**Figure 5B**). Excess amine-PEG_2-biotin was removed by SPE on a C18 catridge, and the biotinylated peptide was captured on monomeric avidin agarose. After washing, biotinylated peptides were eluted with 2 mL D-biotin (2 mM) in PBS. **Figure 5C** shows that biotinylated LW+14 (Biotin-LW) was effectively enriched from the complex mixture.

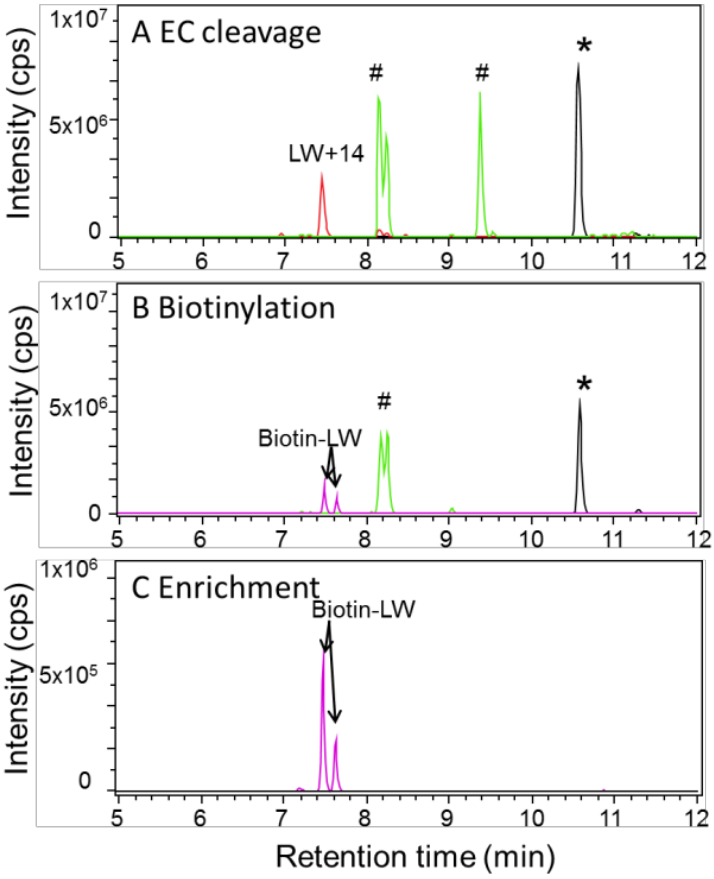

Figure 5. LC-MS analysis of the electrochemical cleavage products of LWL (EC-LWL) (A), the reaction mixture after biotinylation and solid-phase extraction (SPE) (B) and the biotinylated LW+14 (Biotin-LW) after enrichment on monomeric avidin agarose (C). (A) Combined extracted ion chromatograms of the electrochemical cleavage products of LWL. The asterisk * indicates unoxidized LWL (*m/z* 431.26). The symbol # represents uncleaved isomeric oxidation products LWL+32 (*m/z* 463.26) next to LW+14 (*m/z* 332.16). (B) LC-MS analysis of the biotinylation products of EC-LWL after SPE purification to remove excess amine-PEG_2-biotin showing complete biotinylation of LW+14 (*m/z* 332.16) to LW-amine-PEG_2-biotin (Biotin-LW, *m/z* 706.37) (mass increment of 374.21 Da). The more hydrophobic, later-eluting isomer of LWL+32 was also removed during SPE. (C) LC-MS analysis of biotinylation products of EC-LWL after enrichment on monomeric avidin agarose.

4.3.4 Affinity enrichment of biotinylated spirolactone-containing peptides from EC-cleaved lysozyme

To study whether Cu (II)-mediated biotinylation after electrochemical peptide bond cleavage can be used to enrich spirolactone-containing peptides from proteins, we applied the procedure to lysozyme (chicken egg), a protein of 14.6 kDa. Lysozyme was electrochemically cleaved at 2000 mV and the complex peptide mixture was biotinylated, enriched and subjected to nanoLC-MS/MS. Data were subjected to searching the chicken UniProt protein sequence database (*Gallus gallus*, updated 06-12-2016, SwissProt reviewed entries only) containing 2601 proteins. Modifications such as biotinylation (mass increment of 374.2062 Da) at the C-termini of predicted Tyr and Trp cleavage sites (resulting in an EC-Y+372.16 and an EC-W+388.18) were taken into account. The biotinylated peptide ^{54}GILQINSRW^{62}+388.18, which derives from the spirolactone-containing peptide ^{54}GILQINSRW^{62}+14, was identified as a unique sequence for identification of lysozyme. The MS/MS spectrum of the doubly-charged precursor ion (*m/z* at 737.8960) shows the characteristic, abundant fragment ion of the coupled biotin tag at *m/z* 375.2062, together with Fragments 1 to 4, which are smaller fragments of the amine-PEG_2-biotin tag providing a signature of a biotin-tagged compound (**Figure 6**). This result provides proof-of-principle that it is possible to identify a protein by combin-

ing electrochemical peptide bond cleavage followed by Cu (II)-mediated biotinylation and selective affinity enrichment on monomeric avidin agarose. This approach will be further optimized and evaluated on more complex protein mixtures in view of future proteomics applications.

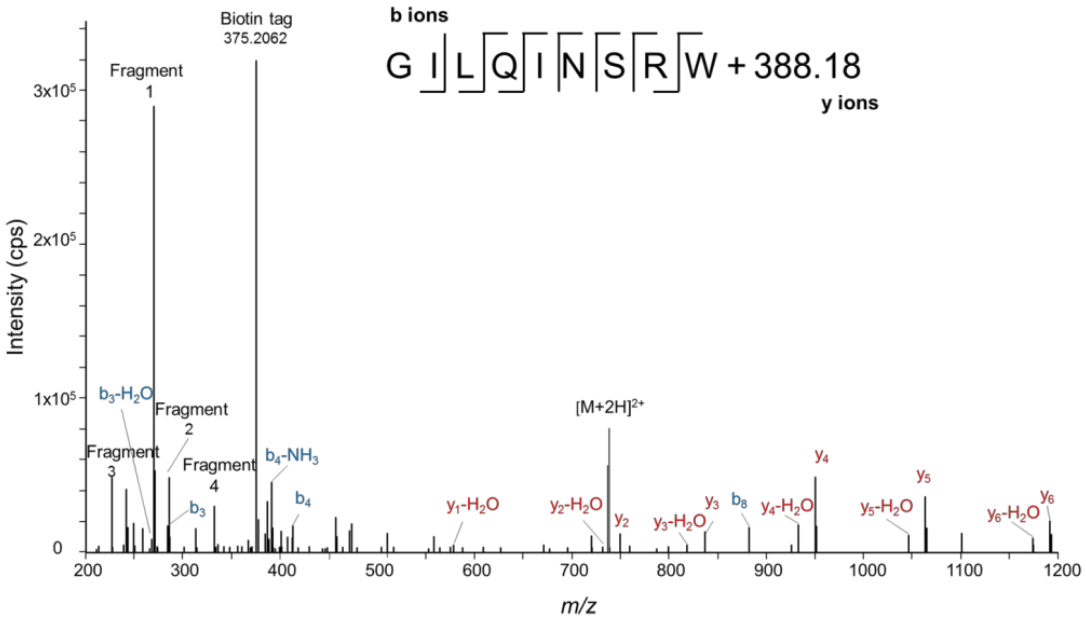

Figure 6. MS/MS spectrum of the biotinylated peptide (^{54}GILQINSRW^{62}+388.18) resulting from electrochemical cleavage of chicken egg lysozyme. The peptide was enriched by monomeric avidin agarose after Cu (II)-mediated biotinylation. The fragment at *m/z* 375.2062 comprises the entire amine-PEG_2-biotin tag, whereas Fragments 1 to 4 are parts thereof (see the proposed structures and *m/z* values of the fragments in **Figure S2**). The y and b fragment ions match the amino acid sequence.

4.4 Conclusions

Electrochemical cleavage of peptide bonds C-terminal to Trp and Tyr opens the possibility for chemical labeling and enrichment via reactive spirolactone moieties at the C-terminus of the N-terminal cleavage products. However, side reactions such as hydrolysis and intramolecular rearrangement during sample handling and chemical labeling proved to be challenges that needed to be overcome before this approach could be considered a potential instrumental alternative to chemical and enzymatic peptide bond cleavage in MS-based proteomics. In this work, we show that addition of Cu (II) ions stabilizes the spirolactone moiety towards intramolecular rearrangement to diketopiperazines and with respect to hydrolysis. This allowed efficient chemical tagging of spirolactones in the presence of free N-terminal amino groups. Based on this finding, we developed a method combining electrochemical peptide bond cleavage, Cu (II)-mediated spirolactone biotinylation and affinity chromatography with LC-MS/MS. This approach was optimized with the tripeptide LWL and applied to lysozyme from chicken egg. We identified a unique biotinylated peptide (^{54}GILQINSRW^{62}+388.18) in an unbiased 'proteomics-like' approach using the algorithm PEAKS to search the sequence database of chicken (*Gallus gallus*). Despite this proof-of-principle study, there is need for further improvements, since we observed that spirolactones may already hydrolyze or rearrange during electrochemical cleavage and further sample handling, especially when positioned C-terminal to Tyr. We will investigate in future experiments whether Cu (II) ions can be added prior to electrochemical cleavage to prevent these side reactions. This refinement of the method should increase the recovery of electrochemically cleaved peptides significantly and facilitate subsequent biotinylation. In summary, we describe an approach for enriching electrochemically cleaved peptides from a mixture of electrochemical cleavage products that may serve as starting material for LC-MS/MS-based protein identification.

4.5 References

(1) Aebersold, R.; Mann, M. *Nature* **2003**, 13, 198-207.

(2) Gingras, A. C.; Gstaiger, M.; Raught, B.; Aebersold, R. *Nat*. *Rev*. *Mol*. *Cell Biol*. **2007**, 8, 645-654.

(3) Walther, T. C.; Mann, M. *J*. *Cell Biol*. **2010**, 190, 491-500.

(4) Domon, B.; Aebersold, R. *Science* **2016**, 14, 212-217.

(5) Choudhary, G.; Wu, S.; Shieh, P.; Hancock, W. S. *J*. *Proteome Res*. **2003**, *2*, 59-67.

(6) Gundry, R. L.; White, M. Y.; Murray, C. I.; Kane, L. A.; Fu, Q.; Stanley, B. A.; Eyk, J. E. V. *Curr*. *Protoc*. *Mol*. *Biol*. **2009**, 10.25.1-10.25.23.

(7) Biringer, R. G.; Amato, H.; Harrington, M. G.; Fonteh, A. N.; Riggins, J. N.; Hühmer, A. F. R. *Brief*. *Funct*. *Genomic*. *Proteomic*. **2006**, 5, 144-153.

(8) Saveliev, S. V.; Woodroofe, C. C.; Sabat, G.; Adams, C. M.; Klaubert, D.; Wood, K.; Urh, M. *Anal*. *Chem*. **2013,** 85, 907-914.

(9) Shevchenko, A.; Tomas, H.; Havlis, J.; Olsen, J. V.; Mann, M. *Nat*. *Protoc*. **2006**, 1, 2856-2860.

(10) Crimmins, D. L.; Mische, S. M.; Denslow, N. D. *Curr*. *Protoc*. *Protein*. *Sci*. **2005**, 11. 1-11.

(11) Crimmins, D. L.; Mische, S. M.; Denslow, N. D. *Curr*. *Protoc*. *Protein*. *Sci*. **2000**, 11. 1-13.

(12) Nalbone, J. M.; Lahankar, N.; Buissereth, L.; Raj, M. *Org*. *Lett*. **2016**, 18, 1186-1189.

(13) Elashal, H. E.; Raj, M. *Chem*. *Commun*. **2016**, 52, 6304-6307.

(14) Permentier, H. P.; Jurva, U.; Barroso, B.; Bruins, A. P. *Rapid*. *Commun*. *Mass*. *Spectrom*. **2003**, 17, 1585-1592.

(15) Permentier, H. P.; Bruins, A. P. *J*. *Am*. *Soc*. *Mass*. *Spectrom*. **2004**, 15, 1707-1716.

(16) Roeser, J.; Permentier, H. P.; Bruins, A. P.; Bischoff, R. *Anal*. *Chem*. **2010**, 82, 7556-7565.

(17) Roeser, J.; Alting, N. F. A.; Permentier, H. P.; Bruins, A. P.; Bischoff, R. *Rapid*. *Commun*. *Mass*. *Spectrom*. **2013**, 27, 546-552.

(18) Roeser, J.; Alting, N. F. A.; Permentier, H. P.; Bruins, A. P.; Bischoff, R. *Anal*. *Chem*. **2013**, 85, 6626-6632.

(19) van den Brink, F.T. G.; Zhang,T.; Ma, L.; Bomer, J.; Odijk, M.; Olthuis, W.; Permentier, H. P.; Bischoff, R.; van den Berg. A. *Anal*. *Chem*. **2016**, 88, 9190-9198.

(20) Zhang, T.; Niu, X.; Yuan, T.; Tessari, M.; de Vries, M. P.; Permentier, H. P.; Bischoff, R. *Anal*. *Chem*. **2016**, 88, 6465-6471.

(21) Medvedev, A.; Kopylov, A.; Buneeva, O.; Zgoda, V.; Archakov, A. *Proteomics* **2012**, 12, 621-637.

(22) Oda, Y.; Nagasu, T.; Chait, B. T. *Nat*. *Biotech*.. **2001**, 19, 379-382.

(23) Daub, H.; Olsen, J. V.; Bairlein, M.; Gnad, F.; Oppermann, F. S.; Körner, R.; Greff, Z.; Kéri, G.; Stemmann, O.; Mann, M. *Mol*. *Cell* **2008**, 31, 438-448,

(24) Hoeppe, S.; Schreiber, T. D.; Planatscher, H.; Zell, A.; Templin, M. F.; Stoll, D.; Joos, T. O.; Poetz, O. *Mol*. *Cell*. *Proteomics* **2011**, 10, M110.002857.

(25) Abello, N.; Barroso, B.; Kerstjens, H. A. M.; Postma, D. S.; Bischoff, R. *Talanta* **2010**, 80, 1503-1512.

(26) Qiao, X.; Qin, X.; She, D.; Wang, R.; Zhang, X.; Zhang, L.; Zhang, Y. *Talanta* **2014**, 126, 91-102.

(27) Spicer, C. D.; Davis, B. G. *Nat*. *Commun*. **2014**, 5, 5740.

(28) Foley, M. A.; Jamison, T. F. *Org*. *Process Res*. *Dev*. **2010**, 14, 1177-1181.

(29) Vigante, B.; Rucins, M.; Plotniece, A.; Pajuste, K.; Luntena, I.; Cekavicus, B.; Bisenieks, E.; Smits, R.; Duburs, G.; Sobolev, A. *Molecules* **2015**, 20, 20341-20354.

(30) Allen, C. L.; Williams. J. M. J. *Chem*. *Soc*. *Rev*. **2011**, 40, 3405-3415.

(31) Högberg, T.; Ström, P.; Ebner, M.; Rämsby, S. *J*. *Org*. *Chem*. **1987**, 52, 2033-2036.

(32) Gnanaprakasam, B.; Milstein, D. *J*. *Am*. *Chem*. *Soc*. **2011**, 133, 1682-1685.

(33) Morimoto, H.; Fujiwara, Risa.; Shimizu, Y.; Morisaki, K.; Ohshima, T. *Org*. *Lett*. **2014**, 16, 2018-2021.

(34) Han, C.; Lee, J. P.; Lobkovsky, E.; Porco, J. A. Jr. *J*. *Am*. *Chem*. *Soc*. **2005**, 127, 10039-10044.

(35) Han, C.; Porco, J. A. Jr. *Org*. *Lett*. **2007**, 9, 517-1520.

(36) Bertucci, M. A.; Leeb, S. J.; Gagné, M. R. *Chem*. *Commun*. **2013**, 49, 2055-2057.

(37) Goswami, A; van Lanen, S. G. *Mol*. *BioSyst*. **2015**, 11, 338-353.

(38) Davis, B. G.; Boyer, V. *Nat*. *Prod*. *Rep*. **2001**, 18, 618-640.

(39) Yang, B.; Zhang, Y.; Zhang, S.; Izumi, T. *Indian J*. *Chem*. **2005**, 44, 1312-1316.

(40) Fountoulakis, M.; Lahm, H. W. *J*. *Chromatogr*. *A* **1998**, 826, 109-134.

(41) Remily-Wood, E.; Dirscherl, H.; Koomen, J. M. *J*. *Am*. *Soc*. *Mass Spectrom*. **2009**, 20, 2106-2115.

(42) Zheng, S.; Doucette, A. A. *Proteomics* **2016**, 16, 1059-1068.

(43) Day, A. R.; Muthukumaraswamy, N.; Freer, R. J. *Peptides* **1980**, 1, 187-188.

4.6 Supporting information

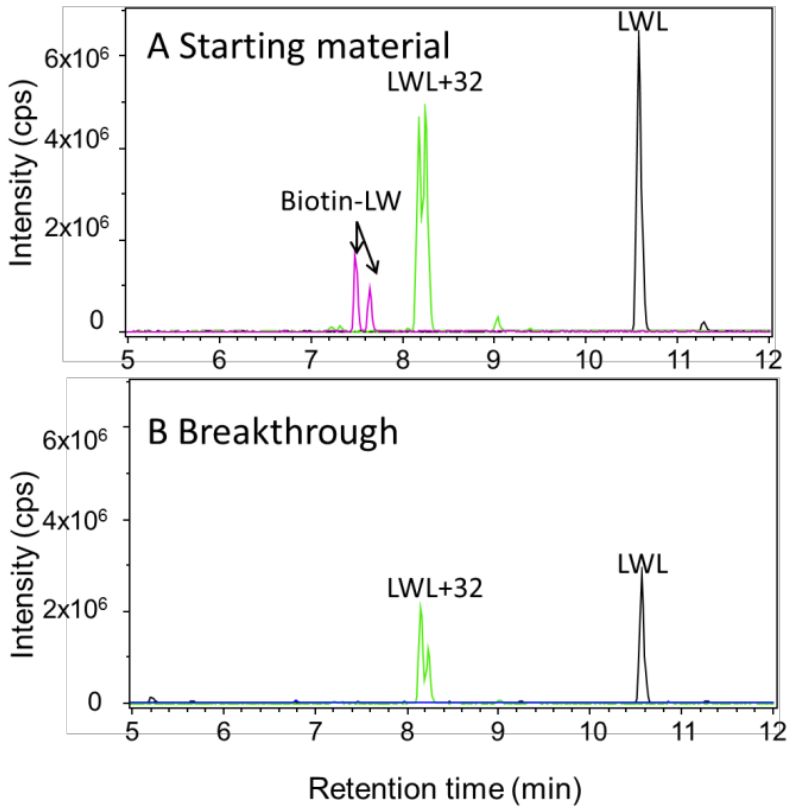

Figure S1. Specific capture of biotinylated peptides from a mixture of electrochemically cleaved, biotinylated LWL on monomeric avidin agarose. LC-MS analysis of the biotinyled electrochemical cleavage products after SPE (A) and the breakthrough (B) after loading the mixture on monomeric avidin agarose. A mixture of unoxidized LWL (*m/z* 431.2250), uncleaved oxidation products (LWL+32, *m/z* 463.2650) and biotinylated LW+14 (Biotin-LW, *m/z* 706.2250) were observed in the biotinylated product mixture of electrochemically cleaved LWL, while only LWL and LWL+32 were detected in the breakthrough of the monomeric avidin column.

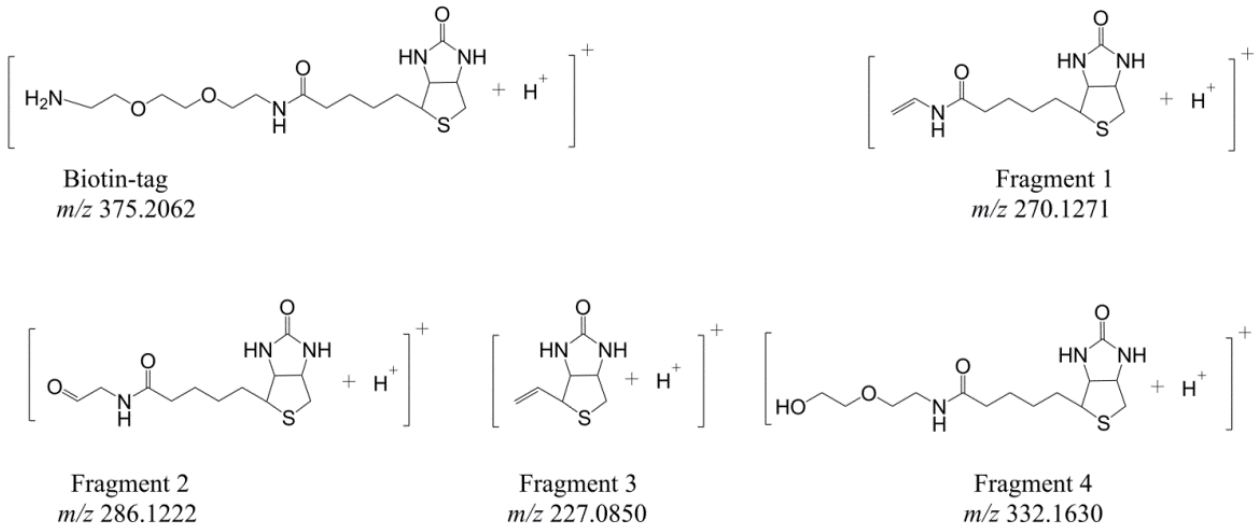

Figure S2. Proposed structures of the MS/MS fragment ions that are related to the amine-PEG_2 biotin tag.

Chapter 5

Products of Gly-Met-Gly after radiolytical and electrochemical oxidation in oxygenated aqueous solution

Abstract: Important chemical modifications of peptides and proteins under oxidative stress conditions are related to the oxidation of methionine (Met), including oxidation by hydroxyl radicals ($HO^{\bullet}$). Mimicking *in vivo* conditions by studying *in vitro* oxidation reactions followed by product identification helps understanding the underlying mechanisms and can be used to produce oxidized peptides and proteins for further research. Gamma-ray radiolysis and electrochemistry were employed for generation of $HO^{\bullet}$, and their reactivity with Gly-Met-Gly was compared to study the feasibility of mimicking oxidation reactions. Detailed analysis by LC-MS and high resolution MS/MS revealed a number of unexpected reaction products upon radiolysis which help to clarify the reaction mechanism. In addition, this study demonstrates that reaction products after gamma-ray radiolysis and electrochemical oxidation on a BDD electrode overlap to some extent but that some radiolysis products are not observed upon electrochemical oxidation.

Published as part of: Sebastian Barata-Vallejo, Carla Ferreri, Tao Zhang, Hjalmar P. Permentier, Rainer Bischoff, Krzysztof Bobrowski and Chryssostomos Chatgilialoglu. Radiation chemical studies of Gly-Met-Gly in aqueous solution. *Free Radical Research*, 2016, 50, S24-S39.

5.1 Introduction

Important biological processes are related to the oxidation of proteins due to oxidative stress leading to excessive chemical modifications. [1-3] The study of protein modifications, resulting from the attack by different types of radical species, including reactive oxygen species (ROS), is of great importance for understanding oxidation mechanisms in a broad spectrum of diseases, biological processes and during treatment by radiotherapy. [3-5]

Mimicking *in vivo* conditions by studying *in vitro* oxidation reactions helps understanding the underlying mechanisms and can be used to produce oxidized peptides and proteins for further research. Radiolysis of water, as one of the most important external sources of ROS, is used in mimicking oxidation of peptides and proteins *in vivo*. [6-7] Electrochemistry (EC) is another way of generating ROS in aqueous solutions and may be a useful approach to complement radiolysis in view of characterizing direct and indirect effects of oxidation reactions on peptides and proteins. As a purely instrumental approach to promote oxidations by direct electron transfer or through electrochemically-generated hydroxyl radicals, interest has increased in electrochemical mimicry of biological oxidation reactions. In an electrochemical cell, electrochemical reduction of molecular oxygen was used to generate hydrogen peroxide while electrochemical oxidation of water, particularly on a boron-doped diamond (BDD) electrode, was employed for hydroxyl radical ($HO^{\bullet}$) production at sufficiently high potentials. [8-9] This ability to generate ROS in an electrochemical approach makes EC an attractive analytical tool for oxidation studies in comparison to radiolysis.

The oxidation of methionine (Met) is an important reaction in the biological milieu. The major oxidation products of Met residues in peptides and proteins by ROS are two epimeric forms of methionine sulfoxide that can be reduced back to Met by methionine sulfoxide reductase (Msr). [10-11] Therefore, Met residues in proteins are suggested to act as an antioxidant pool and several studies support this hypothesis. [12-13] The reaction of oxidants like H_2O_2, HOONO or HOCl with Met occurs in a site-specific manner with

formation of methionine sulfoxide, [14-16] whereas oxidation by $HO^{\bullet}$ radicals is believed to lead to complex product mixtures.[17]

Barata-Vallejo *et al*. recently reported detailed studies of the reaction between hydroxyl radicals generated by gamma-radiolysis and free methionine **(1)**. [18] This study showed that (i) $HO^{\bullet}$ radicals attack the sulfur atom with high specificity under anoxic and aerobic conditions, (ii) $HO^{\bullet}$ radicals do not oxidize methionine to the corresponding sulfoxide Met (O) either in the presence or absence of oxygen, and (iii) H_2O_2 formed either from the radiolysis of water or from the disproportionation of the by-product $O_2^{\bullet-}$ is responsible for Met (O) formation.

Although the reaction of $HO^{\bullet}$ radicals with free Met is well understood, [18] several fundamental aspects remain to be elucidated in the reaction of the $HO^{\bullet}$ radical with Met residues in peptides and proteins. Functional groups (neighboring groups) adjacent to the sulfur center, the primary site of initial oxidation, clearly have a key influence. Such neighboring group participation in the oxidation of Met not only stabilizes the corresponding radical cation, but may also render the reduction potential of Met less positive, and therefore facilitate its oxidation.[21]

So far, the formation of sulfoxides in the radiolytic study of model peptides under anaerobic conditions was attributed to $HO^{\bullet}$ radical attack at the sulfur of the Met residue.[22-25] The present study focuses on the hydroxyl-radical-mediated oxidation of Gly-Met-Gly (**5**, **Figure 1**) under aerobic conditions, the simplest model peptide where a Met residue is located internally, to investigate differences with oxidation of free Met. Both radiolytic and electrochemical approaches were employed to generate $HO^{\bullet}$ radicals in oxygenated aqueous solution in this work to investigate whether radiolytic conditions can be mimicked electrochemically.

5.2 Experimental section

5.2.1 Materials.

Gly-Met-Gly (trifluoroacetate salt) was obtained from Peptide 2.0 Inc. (Chantilly, USA) and used as received. Ortho-phthaldialdehyde (OPA) perchloric acid ($HClO_4$), formic acid (HCOOH, FA, 98%), 2-mercaptoethanol (99.0%), sodium hydroxide (NaOH, 97%), boric acid (H_3BO_3, 99.5%) and phosphoric acid (H_3PO_4, 85%) were purchased from Fluka-Sigma Aldrich Co. (Milan, Italy and Steinheim, Germany) and used without any further purification. Acetonitrile (HPLC SupraGradient grade) was purchased from Biosolve (Valkenswaard, The Netherlands). Other solvents (HPLC grade) were purchased from Merck Millipore (Darmstadt, Germany) and used without further purification. All solutions were made with deionized water provided by a Millipore MilliQ system (conductivity 18.2 MΩ cm, Millipore Corp., Billerica, MA, USA). All aqueous peptide solutions were prepared immediately before use.

5.2.2 Reaction of Gly-Met-Gly with H_2O_2.

500 μL of 0.2 M aqueous H_2O_2 were introduced by a syringe pump (flow rate 167 μL/h) to an aqueous solution of Gly-Met-Gly (25 mL, 10.1 mM, pH 6.8) under stirring for 3 h (H_2O_2 final concentration = 3.9 mM). Samples were withdrawn each hour, followed by OPA (ortho-phthaldialdehyde) derivatization and HPLC analysis. OPA derivatization was performed following a protocol previously published by Barata-Vallejo *et al*. [18] In short, 100 μL of the sample were diluted in 250 μL of borate solution (0.4 M H_3BO_3, pH 10.2, adjusted with 4M NaOH) and 50 μL of the freshly prepared OPA reagent (10 mg/mL OPA and 10 mg/mL 2-mercaptoethanol) were added. The solution was vortexed for 2 min and finally diluted with 320 μL of 1.5% v/v concentrated H_3PO_4. The same samples were also analyzed by ESI-MS prior to derivatization by direct infusion into a Q-Trap 4000 triple quadrupole mass spectrometer (AB Sciex INC., Concord, Ontario, Canada) in positive mode.

5.2.3 Steady-state gamma-radiolysis.

Irradiations were performed at room temperature using a ^{60}Co-Gammacell at different dose rates. The exact absorbed radiation dose was determined with the Fricke chemical dosimeter.[27] Mixtures of gases were obtained by an appropriate mixer, controlled by a flow meter connected to the line, reaching the vessel through a needle. The flow was adjusted to get continuous bubbling during irradiation. Four mL of a N_2-purged aqueous solution of Gly-Met-Gly (all experiments were run at 1 mM peptide concentration) were saturated with a gas mixture of N_2O:O_2 (90:10 v/v) prior to gamma-irradiation. Aliquots of the irradiated Gly-Met-Gly solutions were withdrawn at the specified doses for immediate conversion to the OPA derivatives.

5.2.4 OPA derivatization of irradiated samples and HPLC analysis.

After OPA derivatization following the same procedure, 20 µL of the reaction mixture were subjected to HPLC analysis. HPLC analyses were recorded on an Agilent 1100 liquid chromatograph, equipped with a quaternary pump delivery system, a column thermostat, and a variable-wavelength UV-Vis detector. RP18 5 µm columns were used to separate the derivatized reaction products and the detection was performed at 365 nm.

5.2.5 Electrochemical oxidation and EC-MS analysis.

20 µM Gly-Met-Gly was prepared in 89/10/1 (v/v/v) ultrapure water/acetonitrile/formic acid and oxidized in a thin-layer cell (Flexcell, Antec, Zoeterwoude, The Netherlands) with a boron-doped diamond (BDD) working electrode (8 mm diameter, surface area 50.3 mm^2) and a palladium (Pd/H_2) reference electrode (Hy-REF) at a flow rate of 5 µL/min. Pretreatment of BDD electrodes was performed according to Roeser *et al*. [8] Mass voltammograms of Gly-Met-Gly were recorded on-line by ramping the cell potential linearly from 0 to 3000 mV at a scan rate of 20 mV/s using a homemade potentiostat controlled by a MacLab system (ADInstruments, Castle Hill, NSW, Australia) and EChem software (eDAQ, Denistone East, NSW, Australia).

The electrochemical oxidation products were analyzed using an API365 triple quadrupole mass spectrometer (MDS-Sciex, Concord, Ontario, Canada) upgraded to EP10+ (Ionics, Bolton, Ontario, Canada).

5.2.6 HPLC-MS/MS measurements.

Liquid chromatography was performed on an Acquity UPLC system (Waters, Milford, MA, USA) equipped with an Alltima HP HILIC column (cyano-modified, 150 mm × 2.1 mm *i.d.*, 3 μm particles, 120 Å pore size, Grace Alltech, Lokeren, Belgium) at a flow rate of 400 μL/min. Mobile phase A consisted of ultra-pure water with 0.1% formic acid. Mobile phase B was acetonitrile with 0.1% formic acid. 25 μL of 100 μM samples were injected, and separation was achieved with a gradient of 2-50% A in 25 min. The column was directly coupled to a Maxis plus quadruple time-of-flight mass spectrometer (QTOF) (Bruker, Billerica, MA, USA) for product detection in positive ion mode. High-resolution MS/MS experiments of reaction products of Gly-Met-Gly were performed in auto MS/MS mode (2 GHz) with a maximum of 7 precursors per cycle and an active exclusion of 0.1 min using a mass range of 100-300 amu with a capillary voltage of 3500 V.

5.3 Results and Discussion

5.3.1 Reaction of Gly-Met-Gly with H_2O_2.

The reaction of Gly-Met-Gly with H_2O_2, simulating the steady-state formation of H_2O_2 during gamma-irradiation, was examined in order to have a better understanding of the radiolysis outcome and the reactive species involved in the formation of each product. Two approaches to analyze the reaction mixtures were followed: a) OPA derivatization, taking into account that this reagent is able to react with amino-containing moieties, [28-29] followed by HPLC analysis with UV/Vis detection; b) LC/MS analysis combined with high-resolution MS/MS to determine product structures without OPA derivatization. It is worth noting that product analysis of Met-containing peptides

has never been performed in radiolytic studies, and so far mechanistic schemes have been proposed without further evidence from product identification.

The oxidation of Gly-Met-Gly to Gly-Met(O)-Gly (**6**) occurs readily and quantitatively with respect to consumed starting tripeptide (**Figure 1**). ESI-MS analysis of samples withdrawn after every hour showed the presence of two compounds in the reaction mixture: *m*/*z* 264.1 corresponding to protonated Gly-Met-Gly and *m*/*z* 280.1 corresponding to protonated Gly-Met(O)-Gly.

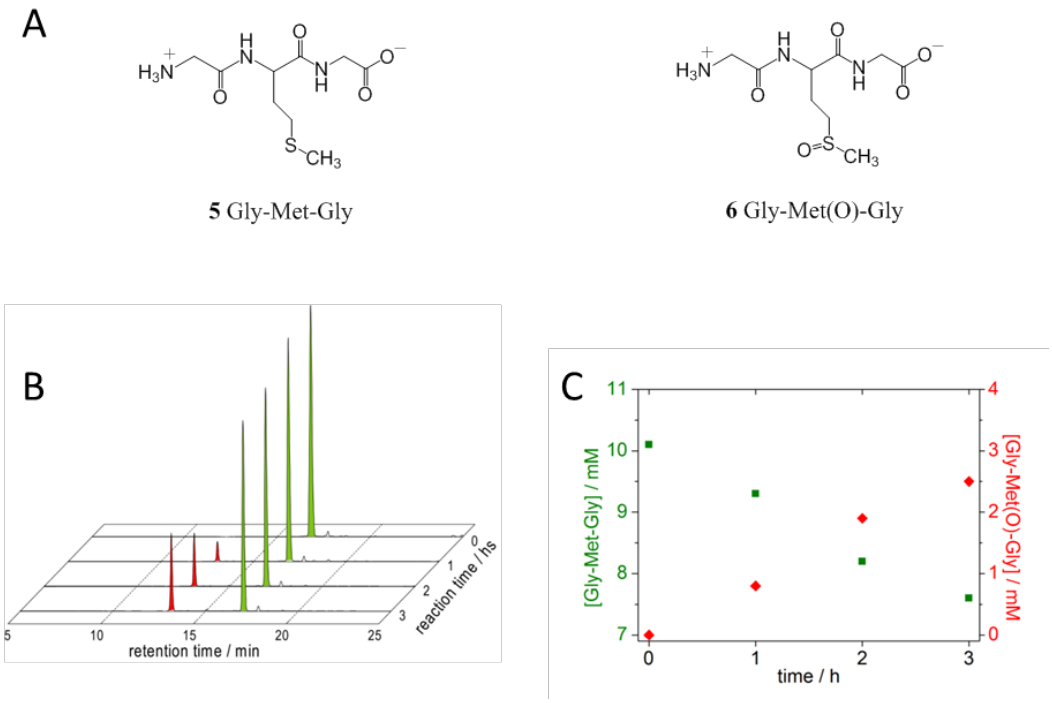

Figure 1. (A) HPLC traces showing the oxidation of Gly-Met-Gly (green peak) to Gly-Met(O)-Gly (red peak) by H_2O_2. Samples were withdrawn every hour, followed by OPA derivatization (detecting amino-group-containing compounds) and HPLC analysis. (B) Time course of the conversion of Gly-Met-Gly (green) into Gly-Met(O)-Gly (red).

5.3.2 Reaction of $HO^{\bullet}$ radicals with Gly-Met-Gly in oxygenated aqueous solution upon gamma-radiolysis.

The products resulting from the continuous gamma-radiolysis of aqueous solutions of Gly-Met-Gly in the presence of oxygen were investigated. Radiolysis of water leads to the reactive species e_{aq}^-, $HO^{\bullet}$, and $H^{\bullet}$ together with H^+ and H_2O_2 as shown in **reaction 1**. In the presence of N_2O and H_2O, e_{aq}^- will further convert to $HO^{\bullet}$ and other products following **reaction 2**. The values in parentheses represent the radiation chemical yields (G) in units of μmol J^{-1}. At 1 atm of N_2O:O_2 (90:10 v/v) e_{aq}^- are efficiently transformed into $HO^{\bullet}$ radicals via **reaction 2**, affording G ($HO^{\bullet}$) = 0.55 μmol J^{-1}. [30-31]

$$H_2O \xrightarrow{\sim\sim} e_{aq}^-(0.27), HO^{\bullet}(0.28), H^{\bullet}(0.06), H^+(0.27), H_2O_2(0.07) \quad \textbf{(1)}$$

$$e_{aq}^- + N_2O + H_2O \rightarrow HO^{\bullet} + N_2 + HO^- \quad \textbf{(2)}$$

N_2O:O_2 (90:10 v/v) saturated solutions containing Gly-Met-Gly (1.1 mM) at pH 7 were irradiated under steady state conditions with a dose rate of approximately 5.5 Gy min^{-1}, continuously bubbling the gas mixture throughout the irradiation time. Aliquots were taken at specified doses followed by OPA derivatization and HPLC analysis. The consumption of Gly-Met-Gly (green peaks, **Figure 2**) led to the formation of five products, two major and three minor ones. The second product that eluted from the column (R_t = 12.9 min, red peaks) was identified as Gly-Met(O)-Gly by comparison with the corresponding OPA derivatives obtained from Gly-Met-Gly oxidation by H_2O_2.

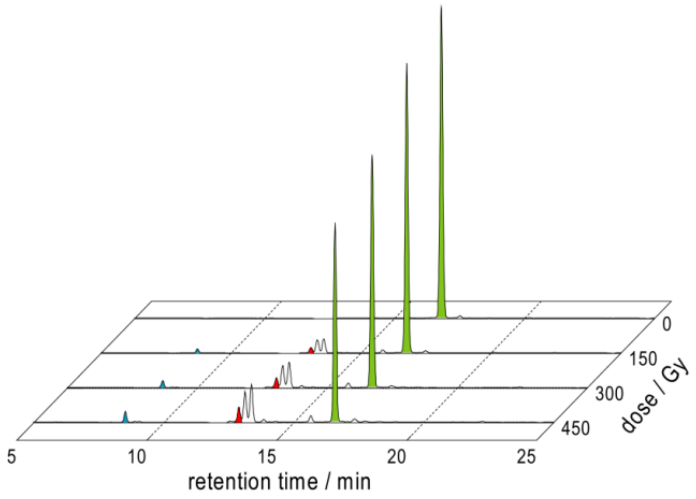

Figure 2. HPLC traces of gamma-irradiated of N_2O:O_2 (90:10 v/v)-saturated solutions of 1.1 mM Gly-Met-Gly at pH 6.8 (dose rate ~ 5.5 Gy min^{-1}) after OPA derivatization.

5.3.3 Product identification by LC-MS and high-resolution MS/MS.

HPLC analyses of the irradiated samples in the presence of oxygen at a dose of 450 Gy are shown in **Figure 3**. In agreement with the OPA derivatization, there are a number of compounds including the starting material. The peaks were identified as the structures in **Figure 4** by their high resolution mass together with their characteristic fragmentation patterns (**Figures 5** and **6**).

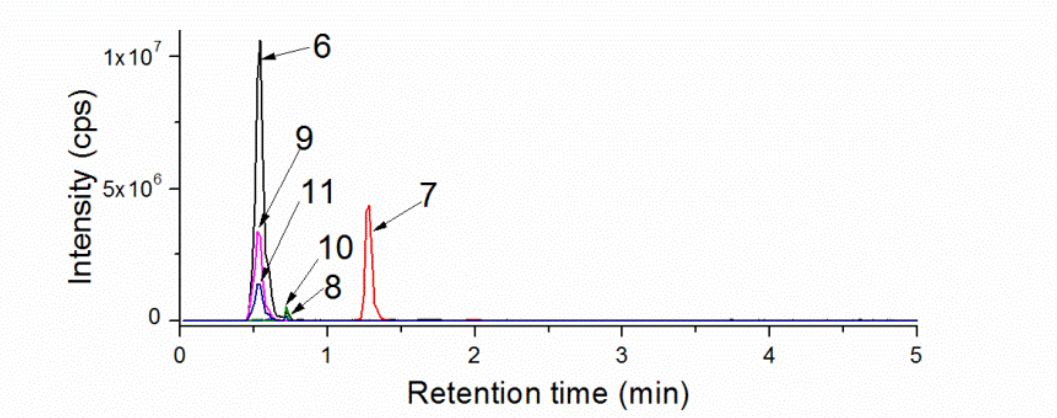

Figure 3. LC-MS analysis of gamma-irradiated solutions of 1.1 mM Gly-Met-Gly at pH 6.8 with continuous bubbling of N_2O:O_2 (90:10 v/v) at a dose of 450 Gy (see **Figure 4** for details about the different compounds).

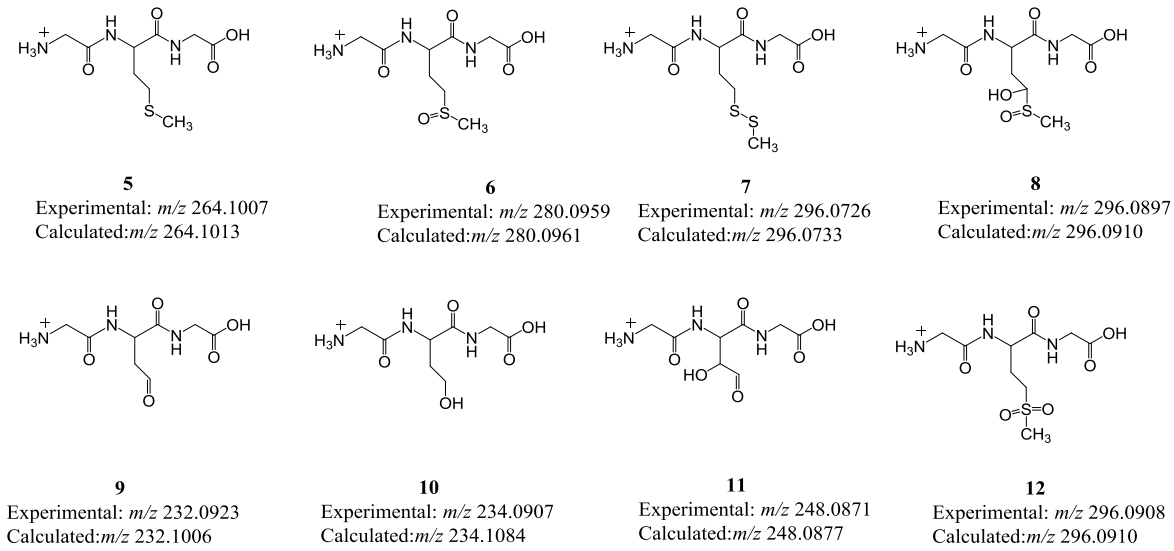

Figure 4. Identification of Gly-Met-Gly (**5**) and its products (**6-11**) obtained by gamma-radiolysis and/or electrochemistry-mediated oxidation, based on high-resolution MS/MS spectra. Compound **12** was obtained by reaction of Gly-Met-Gly (**5**) with H_2O_2 at 90 °C for 2 h. Calculated and experimental *m*/*z* values are shown.

Figure 5 shows the high resolution MS/MS spectrum of the starting material **5** (*m*/*z* 264.1007), as well as the MS/MS spectra of products **6**, **7** and **8**. The accurate mass-to-charge ratios of these products, *m*/*z* 280.0959, 296.0897, 296.0733, correspond to a molecular weight increase of one oxygen atom, two oxygen atoms and one sulfur atom, respectively, compared to the starting material. The assignment of structure of compounds **6** as the sulfoxide was based on high resolution MS/MS and comparison with the sulfoxide and sulfone of the tripeptide obtained by hydrogen peroxide oxidation. The *m*/*z* 296.0733 with the addition of a sulfur atom was assigned to compound **7** based on the characteristic fragmentation pattern of an asymmetric disulfide. It is worth underlining that this is one of the major products of the reaction. The location of the two oxygen atoms of the *m*/*z* 296.0897 product (compound **8**) could

not be derived from the MS/MS spectrum. However, the retention time of the authentic sulfone (**12**, *m/z* 296.0908) was 0.7 min while that of compound **8** was 1.3 min so this product cannot be assigned to the sulfone. The proposed structure of compound **8** is further based on the mechanism proposed by Barata-Vallejo *et al*. [26] Noteworthy is that fragments were assigned based on ion fragmentation rules for peptides in combination with the elemental compositions derived from accurate mass measurements. Since the only differences between compounds **5**, **6**, **7** and **8** are on the side chain of the Met residue, the same high-intensity N-terminal fragment (*m/z* 113.071) and the same neutral loss patterns (loss of C_2NOH_3 from the N-terminus and of $C_2NO_2H_5$ from the C-terminus) were observed, indicating that no other modifications occurred, as might be expected.

Figure 6 shows the high resolution MS/MS spectra of products **9**, **10** and **11** with lower molecular weights compared to the starting material. These products were assigned to compounds where the methionine residue has lost the CH_3S moiety based on the corresponding high-resolution MS/MS fragment ions. The loss of C_2NOH_3 indicates an unmodified N-terminal part in compounds **9** and **11**. The easy loss of water (*m/z* 232.0923 to *m/z* 214.0820 and *m/z* 175.0715 to *m/z* 157.0607) in compound **9**, and in compound **11** (*m/z* 248.0881 to *m/z* 230.0775 and *m/z* 191.0660 to *m/z* 173.0555) is consistent with the presence of a carboxylic acid group. The same water loss was not observed in compound **10** due to low signal intensity. All other fragments were in agreement with the proposed structures for compounds **9**, **10** and **11.**

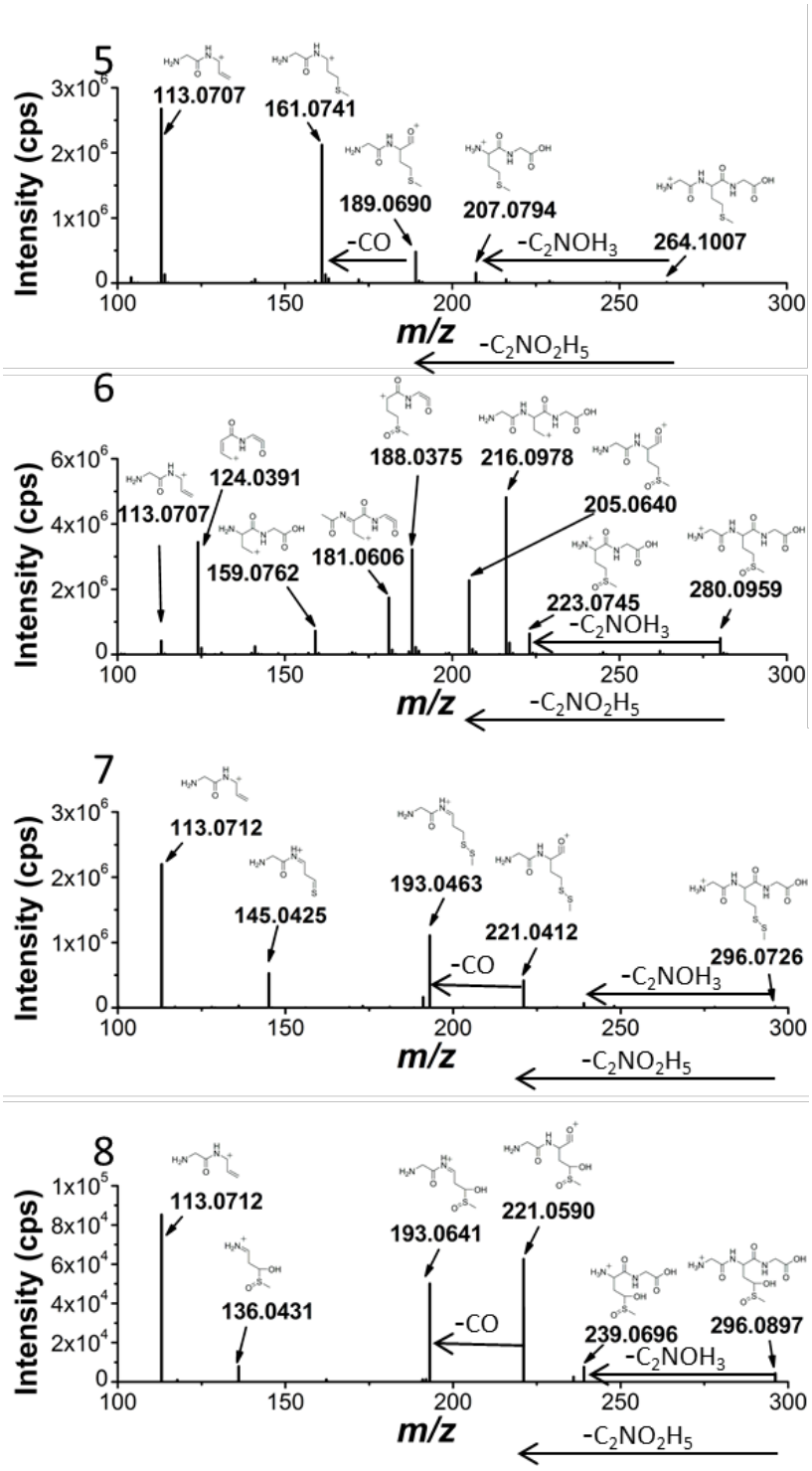

Figure 5. High-resolution MS/MS spectra of starting material **5** (*m/z* 264.1007) and of the products with higher molecular weight **6** (*m/z* 280.0959), **7** (*m/z* 296.0733) and **8** (*m/z* 296.0897) with proposed structures of the fragment ions.

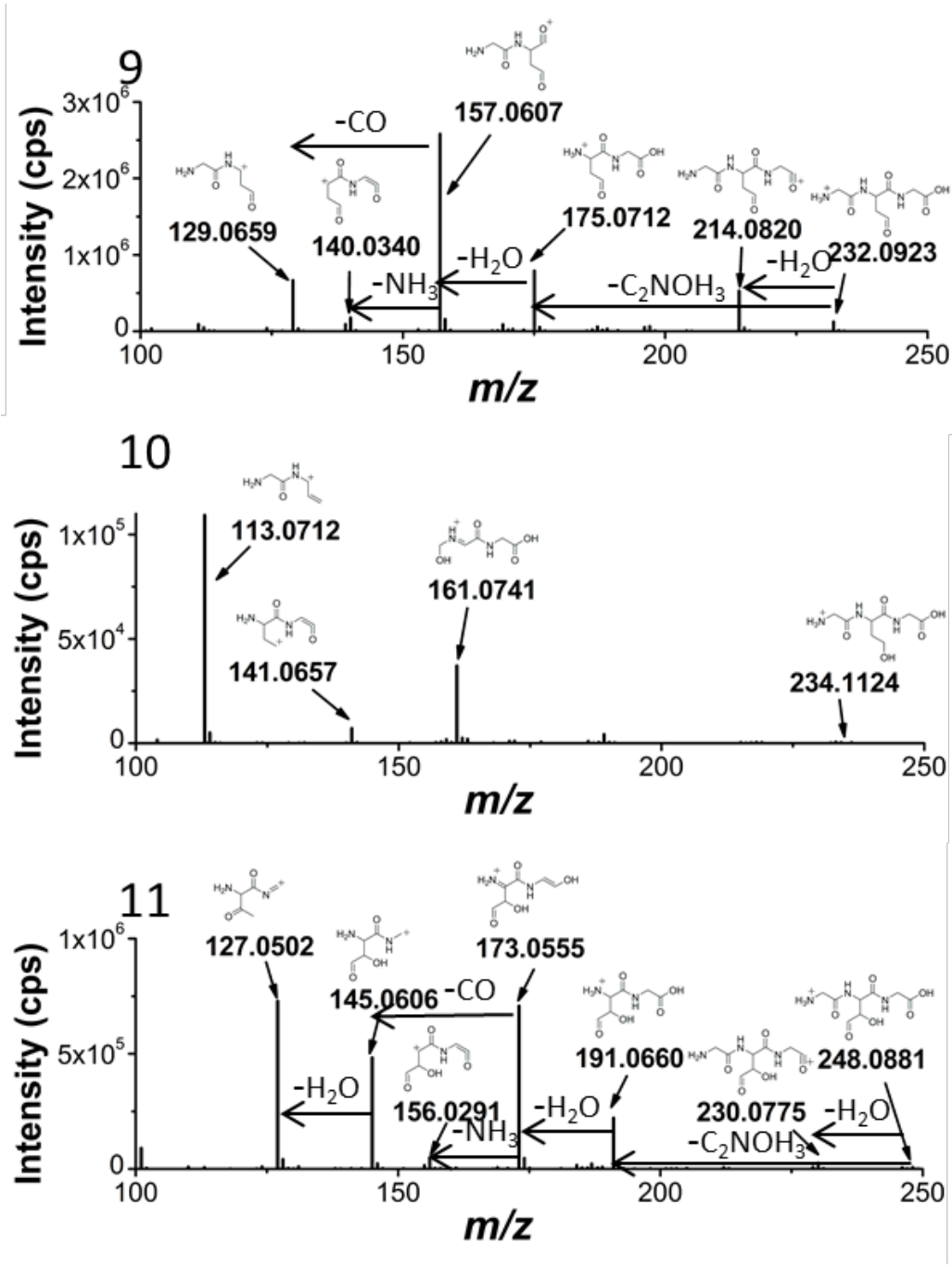

Figure 6. High-resolution MS/MS spectra of the products with lower molecular weight that the starting tripeptide: **9** (*m/z* 232.0923), **10** (*m/z* 234.0907), and **11** (*m/z* 248.0871) with proposed structures of the fragment ions.

5.3.4 Electrochemical oxidation of Gly-Met-Gly.

Electrochemical oxidation of peptides readily occurs at tyrosine (Tyr), tryptophan (Trp) and methionine (Met), [32] while hydroxyl-radical-mediated oxidations, which have been used in protein and peptide chemistry. [33-35], occur also at phenylalanine (Phe). [8-9] We have recently reported that both direct oxidation and hydroxyl-radical-mediated oxidation of peptides can be achieved in thin-layer (amperometric) flow cells with boron doped diamond (BDD) electrodes.[8-9] The specific property of a BDD working electrode to generate hydroxyl radicals by oxidation of water at sufficiently high potential, allows to study reactions with Gly-Met-Gly via electrochemistry and compare products with those obtained by radiolysis.

Direct electrochemical and hydroxyl-radical-mediated oxidations of Gly-Met-Gly were studied using a linear potential sweep in an on-line EC-MS experiment. The measured mass-voltammograms allowed monitoring of specific oxidations and the corresponding products at different potentials. A decrease of the signal for the starting material in **Figure 7** indicated the onset of electrochemical oxidation at about 800 mV. The oxidation efficiency increased further with increasing working electrode potential, reaching an oxidation yield of >75% at potentials higher than 1200 mV, as determined from a decrease in Gly-Met-Gly signal intensity. Signal intensity for the sulfoxide **6** reached a maximum at 1200 mV, followed by a decrease at higher potentials (**Figure 7B**) likely due to the formation of sulfone **12** (Gly-Met(O_2)-Gly). It is clearly shown that formation of **12** starts from ~1200 mV and increases until 2500 mV, after which signal intensity stabilizes up to the upper end of the potential range of 3000 mV (**Figure 7C**). Products **6** and **12** were identified by their high-resolution MS/MS fragment ions (data not shown). We do not see the same oxidation products as upon radiolysis. Only the sulfur oxidation products are obtained electrochemically. This indicates that oxidation conditions during electrochemistry and radiolysis are only partially comparable.

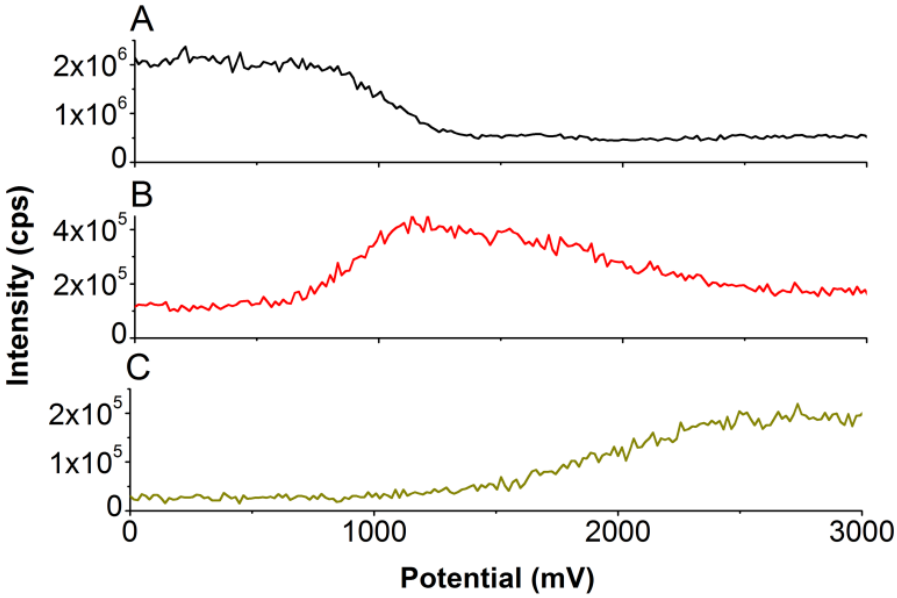

Figure 7. On-line mass-voltammograms of the electrochemical oxidation of Gly-Met-Gly. On-line mass-voltammograms of Gly-Met-Gly (20 µM in 89/10/1 (v/v/v) water/acetonitrile/formic acid) were recorded by ramping the potential from 0 to 3000 mV with a scan rate of 20 mV/s. Traces were extracted and plotted versus cell potential for Gly-Met-Gly (A);, Gly-Met(O)-Gly (B) and Gly-Met(O_2)-Gly (C).

5.4 Discussion

The goal of this study was to compare the oxidation of Gly-Met-Gly under gamma-ray radiolysis conditions as compared to electrochemical conditions. While both methods generate $HO^{\bullet}$ radicals, reaction products during radiolysis are more diverse including not only the expected sulfur oxidation products but also a mixed disulfide, an aldehyde and an alpha-hydroxy aldehyde. These differences may be explained by the more efficient hydroxyl radical formation during radiolysis, notably in the presence of N_2O following the **reaction 2**. Moreover, radiolysis of water leads to the several reactive species including e_{aq}^-, $HO^{\bullet}$, and $H^{\bullet}$ together with H^+ and H_2O_2, yielding a complex mixture of products. We identified seven products in the case of Gly-Met-Gly by high-resolution LC-MS/MS, allowing us to propose mechanisms of Gly-Met-Gly transformation. [26] It is worth mentioning that one of the main products is an

asymmetrical disulfide **7** obtained by the dimerization of an intermediate sulfur radical cation. However, the structure of compounds **7** and **8**, especially with respect to location of the two oxygen atoms, remains to be confirmed.

5.5 Conclusions

The present study offers a multidisciplinary approach to contribute to identification of products from radiolytical and electrochemical oxidation of Gly-Met-Gly, which paves the way for a mechanistic study of product formation. Generation of radical species through different methodologies, such as radiolysis and electrochemistry, provided strong evidence that oxidation of the sulfur atom in Met results from *in situ* formed hydrogen peroxide, while other products like the mixed disulfide, the aldehyde and the alpha-hydroxy aldehyde are due to radical reactions that occur only during radiolysis. This study also demonstrates the value of high-resolution tandem mass spectrometry to characterize the reaction products, notably after radiolysis. Gly-Met-Gly provides a model of how free radicals may react with peptides and proteins *in vivo* and may inspire experiments to study oxidative protein damage under conditions of radiotherapy or during chronic inflammatory disease conditions.

5.6 References

(1) Stadtman, E.R.; Berlett, B. S. *Drug Metab. Rev.* **1998**, 30, 225-243.

(2) Berlett, B. S.; Stadtman, E.R. *J. Bio. Chem.* **1997**, 272, 20313-20316.

(3) Finkel, T.; Holbrook, N. J. *Nature* **2000**, 408, 239-247.

(4) Beckman, J. S.; Koppenol, W. H. *Am. J. Physiol.* **1996**, 271, C1424-C1437.

(5) Barelli, S.; Canellini, G.; Thadikkaran, L.; Crettaz, D.; Quadroni, M.; Rossier, J. S.; Tissot, J. D.; Lion. N. *Proteomics Clin. Appl.* **2008**, 2, 142-157.

(6) Stadtman, E. R. *Free Radic. Res.* **2006**, 40, 1250-1258.

(7) Headlam, H. A.; Davies, M. J. *Free Radic. Biol. Med.* **2004**, 36, 1175-1184.

(8) Roeser, J,; Alting, N. F. A.; Permentier, H. P.; Bruins, A. P.; Bischoff, R. *Anal. Chem.* **2013**, 85, 6626-6632.

(9) van den Brink, F. T. G.; Zhang, T.; Ma, L.; Bomer, J.; Odijk, M.; Olthuis, W.; Permentier, H. P.; Bischoff, R.; Berg, A. van den. *Anal. Chem.* **2016**, 88, 9190-9198.

(10) Poole, L. B.; Karplus, P. A.; Claiborne, A. *Annu. Rev. Pharmacol. Toxicol.* **2004**, 44, 325-347.

(11) Weissbach, H.; Resnick, L.; Brot, N. *Biochim. Biophys. Acta.* **2005**, 1703, 203-212.

(12) Lu. S.; Levine, R. L. *FASEB J.* **2009**, 23, 464-472.

(13) Stadtman, E. R.; Van Remmen, H.; Richardson, A.; Wehr, N. B.; Levine, R. L. *Biochim. Biophys. Acta.* **2005**, 1703, 135-140.

(14) Davies, M. J. *Biochim. Biophys. Acta.* **2005**, 1703, 93-109.

(15) Davies, M. J.; Fu, S.; Wang, H.; Dean, R. T. *Free Radical Biol. Med.* **1999**, 27, 1151-1163.

(16) Jensen, J. L.; Miller, B. L.; Zhang, X.; Hug, G. L.; Schoneich, C. *J. Am. Chem. Soc.* **1997**, 119,4749-4757.

(17) Schoneich, C. *Biochim. Biophys. Acta.* **2005**,1703,111-119.

(18) Barata-Vallejo, S.; Ferreri, C.; Postigo, A.; Chatgilialoglu, C. *Chem. Res. Toxicol.* **2010**, 23, 258-263.

(19) Hiller, K. O.; Masloch, B.; Göbl, M.; Asmus, K. D. *J. Am. Chem. Soc.* **1981**, 103, 2734–2743.

(20) Hiller, K. O.; Asmus, K. D. *J. Phys. Chem.* **1983**, 87, 3682-3688.

(21) Glass, R. S.; Hug, G. L.; Schöneich, C.; Wilson, G. S.; Kuznetsova, L.; Lee, T.; Ammam, M.; Lorance, E.; Nauser, T.; Nichol, G. S.; Yamamoto, T. *J*. *Am*. *Chem*. *Soc*. **2009**, 131, 13791-13805.

(22) Ohara, A. *J*. *Radiat*. *Res*. **1966**, 7, 18-27.

(23) Xu, G.; Chance, M. R. *Anal*. *Chem*. **2005**, 77, 2437-2449.

(24) Ignasiak, M.; Scuderi, D.; de Oliveira, P.; Pedzinski, T.; Rayah, Y.; Houée, Levin, C. *Chem*. *Phys*. *Lett*. **2011**, 502, 29-36.

(25) Ignasiak, M.; de Oliveira, P.; Houée, Levin, C.; Scuderi, D. *Chem*. *Phys*. *Lett*. **201**3, 590, 35-40.

(26) Barata-Vallejo, S.; Ferreri, C.; Zhang, T.; Permentier, H. P.; Bischoff, R.; Bobrowski, K.; Chatgilialoglu, C. *Free Radic*. *Res*. **2016**, 50, S24-S39.

(27) Spinks, J. W. T.; Woods, R. J. An Introduction to Radiation Chemistry, 3rd ed. New York: Wiley; **1990**. p100.

(28) Greene. J.; Henderson, J. W. Jr; Wikswo, J. P. Rapid and precise determination of cellular amino acid flux rates using HPLC with automated deivatization with absorbance detection. *Agilent Technologies* **2009**. https://www.chem.agilent.com/Library/applications/5990-3283EN.pdf.

(29) Bartolomeo, M. P.; Maisano, F. *J*. *Biomol*. *Tech*. **2006**, 17, 131-137.

(30) Buxton, G. V.; Greenstock, C. L.; Helman, W. P.; Ross, A. B. *J*. *Phys*. *Chem*. *Ref*. *Data* **1988**, 17, 513-886.

(31) Ross, A. B.; Mallard, W. G.; Helman, W. P.; Buxton, G. V.; Huie, R. E.; Neta, P. NDRLNIST Solution Kinetic Database Ver. 3, Notre Dame Radiation Laboratory and NIST Standard Reference Data, Notre Dame, IN, and Gaithersburg, MD. **1998**.

(32) Roeser, J.; Permentier, H. P.; Bruins, A. P.; Bischoff, R. *Anal*. *Chem*. **2010**, 82, 7556-7565.

(33) Permentier, H. P.; Jurva, U.; Barroso, B.; Bruins, A. P. *Rapid*. *Commun*. *Mass*. *Spectrom*. **2003**, 17, 1585-1592.

(34) Permentier, H. P.; Bruins, A. P. *J*. *Am*. *Soc*. *Mass*. *Spectrom*. **2004**, 15, 1707-1716.

(35) Herzog, G.; Arrigan, D. W. M. *Analyst* **2007**, 132, 615-632.

Chapter 6

Cleavage of peptide bonds under oxidizing conditions: mechanisms, analytical strategies and future perspectives

Abstract: Oxidation of peptides and proteins under oxidative stress in a wide variety of diseases and during aging leads to multiple chemical modifications that may result in protein damage and degradation. Mimicking oxidative stress via oxidation reactions of peptides and proteins *in vitro* is the first step to establish the highly sensitive and selective analytical methods that are required to study oxidative modifications *in vivo* and to investigating their biological relevance. Oxidative cleavage of peptide bonds was first described as a result of internal free-radical transfer reactions upon exposure of proteins to high-energy radiation. Bond cleavage proceeded primarily via the diamide and α-amidation pathways as well as via oxidation of glutamyl and prolyl residues by radiolytically generated reactive oxygen species (ROS). Specific cleavage of peptide bonds upon oxidation of tyrosine (Tyr) and tryptophan (Trp) was observed when mimicking oxidative stress conditions chemically or electrochemically. Oxidative/radical-induced cleavage of chemical bonds including the peptide bond introduces reactive groups including carbonyl and spirolactone moieties, which may serve as handles for labelling or affinity enrichment as part of highly selective and sensitive analytical approaches. In this chapter, I will give an overview of current analytical approaches for protein carbonyl detection with several carbonyl-derivatization reagents and enrichment protocols prior to mass spectrometric analysis for applications in biological samples. Specific attention will be paid to the formation of spirolactone-containing peptide fragments upon electrochemical cleavage and related derivatization and enrichment strategies. I will finally provide a perspective on the possible role of oxidative/radical-induced peptide bond cleavage in biological systems and in view of current and future methodological developments and potential applications in proteomics and protein analysis.

6.1 Introduction

Important biological processes related to a wide variety of diseases and aging, result in the oxidation of proteins leading to excessive chemical modifications and ultimately loss of biological function. [1-5] Oxidation of proteins is due to exposure to an oxidizing environment containing different types of highly reactive molecules collectively called reactive oxygen species (ROS) and reactive nitrogen species (RNS). Proteins may also be directly attacked by reactive species generated from radiolysis of water, such as solvated free electrons. [6-10] ROS, including hydrogen peroxide (H_2O_2), the superoxide radical anion ($O_2^{-\bullet}$) and the hydroxyl radical ($HO^{\bullet}$), can also be produced naturally in biological systems during metal-catalyzed oxidations (MCO), electron-transport processes, due to the reactivity of environmental pollutants and by enzyme-catalyzed redox reactions. [10-12]

From decades of molecular studies on protein oxidation, it is known that protein oxidation results in a wide range of chemical modifications, including side chain modifications, formation of crosslinked protein complexes and oxidative cleavage of chemical bonds, including the peptide bond. [13, 14]

While all amino acid side chains may be attacked by radicals, some are particularly vulnerable to oxidation. Some reactions are limited to certain residues, whereas others give rise to widespread and nonspecific modifications. With highly reactive ROS or RNS, chemical modification occurs at multiple side chains and along the backbone. Less reactive species exhibit greater selectivity with respect to the targeted amino acid residues and their spatial location. For example, amino acids containing sulfur are easily oxidized with cysteine (Cys) forming a range of derivatives while methionine (Met) forming primarily sulfoxides. [1-2, 15] **Table 1** lists some of the products that are formed during the oxidation of amino acid residues upon attack by different types of ROS or RNS and due to exposure to high-energy radiation as reviewed by Berlett & Stadtman and Stadtman, respectively. [2, 16]

Table 1. Oxidation products of amino acid side chains.

Amino acid	Oxidation products
Arginine	Glutamic-5-semialdehyde
Cysteine	Cystine; cysteine sulfenic acid; cysteine sulfinic acid; cysteine sulfonic acid
Glutamic acid	Oxalic acid; pyruvic acid
Histidine	2-Oxohistidine; 4-hydroxyglutamate
Leucine	3-, 4-, and 5-Hydroxyleucine
Lysine	α-Aminoadipicsemialdehyde; N_{ε}-(carboxymethyl)lysine
Methionine	Methionine sulfoxide; methionine sulfone
Phenylalanine	2-, 3-, and 4-Hydroxyphenylalanine; 2,3-dihydroxyphenylalanine
Proline	Glutamic-5-semialdehyde; 2-pyrrolidone, 4-, and 5-hydroxyproline; pyroglutamic acid
Threonine	2-Amino-3-keto-butyric acid
Tryptophan	2-, 4-, 5-, 6-, and 7-Hydroxytryptophan; formylkynurenine; 3-hydroxykynurenine; 5-nitrotryptophan
Tyrosine	3,4-Dihydroxyphenylalanine; Tyr–Tyr crosslinks; 3-nitrotyrosine

As illustrated in the example in **Figure 1**, oxidative attack of the polypeptide backbone may be initiated by the $HO^{\bullet}$-dependent abstraction of the α-hydrogen atom of an amino acid residue to form a stabilized (via electron delocalization by neighbouring carbonyl and nitrogen functions) carbon-centered radical (**Reaction a**), followed by formation of an alkylperoxyl radical intermediate after reaction with molecular oxygen (**Reaction b**), which reacts further to an alkylperoxide (**Reaction c**) and an alkoxyl radical (**Reaction d**), which may be converted to an α-hydroxyamino acid (**Reaction e**) or proceed to peptide backbone cleavage (**Figure 2**). The alkyl, alkylperoxyl, and alkoxyl radical intermediates in this pathway may react with other amino acid residues in the same or a different protein molecule to generate a new carbon-centered radical capable of undergoing reactions similar to those illustrated in **Figure 1**. It should be noted that each of these processes results in the formation of further reactive species and hence that protein oxidation can propagate via chain reactions (*i.e*. oxidation of multiple sites per single initiating event). In the presence of oxygen, the ROS-generated carbon-

centered radical may further react with another carbon-centered radical, leading to an intra- or inter-protein crosslink. Moreover, the formation of protein-protein crosslinks may, for example, form by reaction between a carbonyl group and an amino group in lysine (Lys), by disulfide bond formation via oxidation of Cys residues, and through crosslinking between tyrosine (Tyr) radicals. Covalent crosslinking is likely one of the main reasons for aggregation of proteins under oxidative stress conditions. For more details on how ROS-mediated oxidation of proteins and nucleic acids leads to formation of protein-protein and protein-DNA cross-linked derivatives, please see the reviews by Berlett & Stadtman, Stadtman and Vaz *et al*.. [2, 16-17]

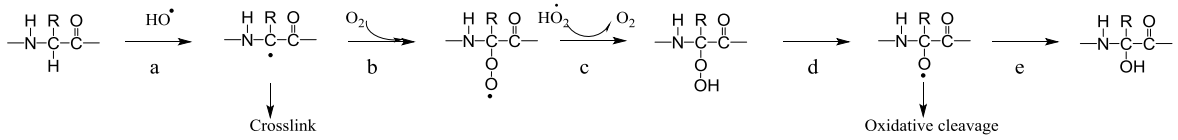

Figure 1. Carbon-centered radical formation by attack of OH-radicals (see **Figure 2** for the cleavage reaction).

Peptide bond cleavage may also occur upon chemical and electrochemical oxidation. [18-22] Electrochemistry (EC) was found to be a useful approach to complement existing oxidation sources such as chemical oxidants and high-energy radiation (γ- and x-rays), and to characterize direct and indirect effects of oxidation reactions on peptides and proteins, specifically resulting in peptide bond cleavage after oxidation of tryptophan (Trp) and tyrosine (Tyr) residues. [23-30] Electrochemistry can also be used to generate ROS, which could be a potential alternative for radiolytic ROS production. [29-30] While many protein modifications observed under electrochemically-induced oxidative stress *in vitro* have been observed *in vivo*, Tyr- and Trp-specific oxidative peptide bond cleavage has not been described. This chapter focuses on the radiolytically- and electrochemically-induced oxidative cleavage of peptides and protein by giving an overview of the reaction mechanisms and current analytical strategies for investigating oxidative cleavage *in vitro* and *in vivo*.

6.2 Cleavage of protein backbone via radiolysis-induced ROS

Oxidation of peptides and proteins via radiolytic oxidation has been extensively studied *in vitro* and *in vivo*. [18-19, 31-34] After decades of research on the mechanism of oxidative cleavage via irradiation-induced ROS, it is widely accepted that the majority of protein backbone cleavage occurs via formation of backbone α-carbon radicals and their subsequent reaction with O_2 to give peroxyl species (**Figure 1**). [35-39] The key role of peroxyl radicals is underscored by the observation that no backbone cleavage is observed in the absence of O_2. [19] In addition, specific oxidative cleavage after proline (Pro) and glutamic acid (Glu) as well as the β-scission of several other amino acid residues were observed and investigated under oxidative stress conditions. These reactions are initiated by ROS attack on the amino acid side chains, instead of the α-carbon.

6.2.1 Peptide bond cleavage via the diamide and α-amidation pathways

Protein and peptide backbones can be attacked by hydroxyl radicals and by the transfer of internal, carbon-centered radicals to the α-carbon of amino acids, yielding an alkoxyl radical upon reaction with molecular oxygen (**Figure 1**). The alkoxyl radical on the α-carbon (**1**) can then induce peptide bond cleavage by either the α-amidation or diamide pathways. As shown in **Figure 2a,** the α-amidation pathway leads to peptide backbone cleavage at the N-C bond, generating an N-terminal fragment with an amide group at the C-terminus (**2**) and a C-terminal fragment with an α-keto amide at the N-terminus (**3**). [16, 20-22, 40-41] In the diamide pathway, the same alkoxyl radical initially induces homolytic cleavage of the peptide backbone at the C-C bond, as shown in **Figure 2b.** Cleavage via the diamide pathway leads to a diamide derivative at the C-terminus of the N-terminal fragment (**4**). The fragment derived from the C-terminal portion of the protein (**5**) has an isocyanate group at the N-terminus, which hydrolyzes to a peptide with an α-amino group at the N-terminus (**6**) and releases CO_2. [16, 20-22] Hellwig *et al*., [42] have shown that there is a strong preference for the α-amidation

pathway in the presence of a thioether group of an adjacent Met residue in peptides, indicating a directing effect of certain amino acid residues.

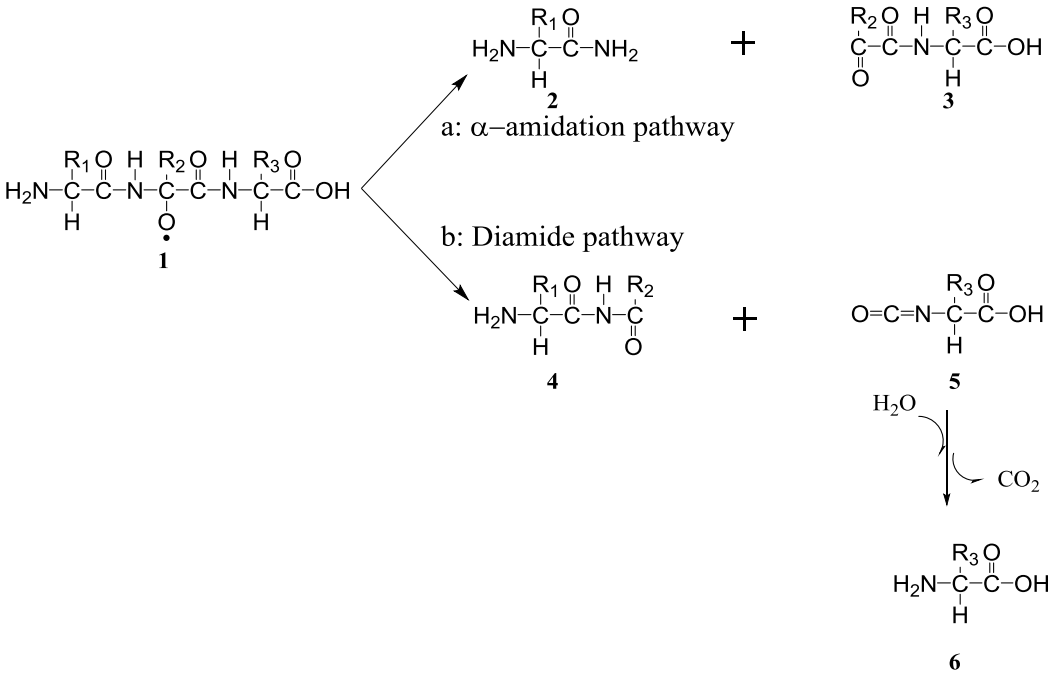

Figure 2. Oxidative peptide bond cleavage via the α-amidation pathway (a) and the diamide pathway (b).

6.2.2 Peptide bond cleavage via oxidation of glutamyl and prolyl residues

Peptide bond cleavage can also occur as a result of ROS attack at glutamyl and prolyl side chains. As described by Garrison, [2, 19] HO•-dependent abstraction of a hydrogen atom from the γ-carbon atom of a glutamyl residue (**7**) generated a series of alkyl, alkylperoxyl, and alkoxyl radical intermediates, analogous to reactions in **Figure 1**. The alkoxyl radical intermediate (**8**) can undergo peptide bond cleavage at the N-C bond via α-amidation pathway (**Figure 3A**). The C-terminal fragment (**10**) contains an N-pyruvyl group at the N-terminus and the N-terminal fragment (**9**) contains an amide at the C-terminus, and oxalic acid (**11**) and water (**12**) are released. [16, 18-19]

The oxidative cleavage of peptide bonds upon oxidation of prolyl residues was first proposed after Schuessler and Schilling observed that the number of fragments was equal to the number of prolyl residues in proteins upon radiolysis. [333] Uchida *et al*. [43] showed that oxidation of Pro residues (**13**) leads to the formation of N-terminal peptide fragments with a 2-pyrrolidone at the C-terminus (**15**), which hydrolyzes to a carboxylic acid, thus forming a normal C-terminus, without the Pro residue (**18**) and α-aminobutyric acid (**19**) (**Figure 3B**). The presence of α-aminobutyric acid (**19**) in protein hydrolysates is an indication of oxidative peptide bond cleavage at Pro residues by the proline oxidation pathway. [16, 18-19] The C-terminal fragment contains a regular α-amino group at the N-terminus (**16**).

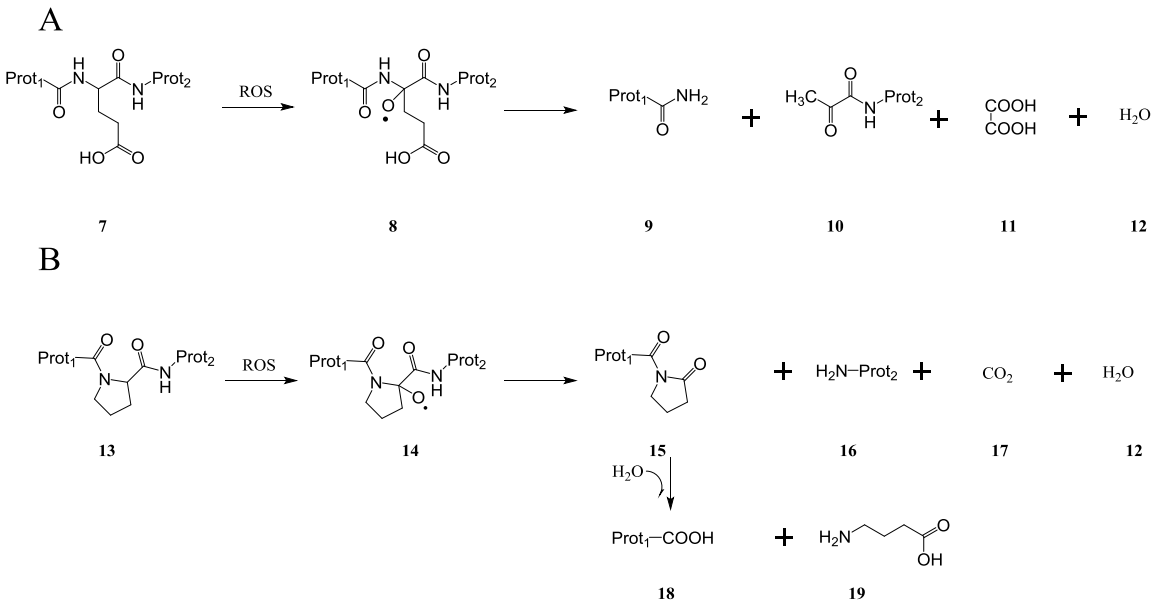

Figure 3. Protein cleavage following oxidation of glutamyl (A) and prolyl residues (B) by ROS. Oxalic acid (**11**) and water (**12**) are produced during oxidative cleavage of the glutamyl side chain while carbon dioxide (**17**) and water (**12**) are generated via oxidative cleavage of the prolyl side chain. $Prot_1$ is the N-terminal side of the protein, and $Prot_2$ the C-terminal side.

6.2.3 Backbone cleavage following β-scission

The alkoxyl radicals formed at the β-carbons of an amino acid side chain (**21**) through radical attack on a range of aliphatic amino acids (**20**) induce a two-step oxidative cleavage reaction, as shown in **Figure 4**. [16, 20-21,] The alkoxyl radical (**21**) leads to a β-scission on the amino acid side chain, yielding an α-carbon-centered radical of the polypeptide chain (**22**) and a carbonyl compound (**23**). β-scission in a range of aliphatic amino acids (alanine (Ala), valine (Val), leucine (Leu) or aspartic acid (Asp)) via ROS oxidation has been described, leading to the generation of formaldehyde, acetone, isobutyraldehyde, and glyoxylic acid, from the respective side chains (**23**). [44-47] The yield of the released carbonyls has been shown to increase in an $HO^{\bullet}$-dependent manner, confirming the role of these radicals in the reaction. Subsequently, the formed α-carbon-centered radical undergoes a second cleavage step of the peptide backbonevia the diamide or α-amidation pathways as described in **Figures 1** and **2**. β-scission is an example of the transfer of oxidative damage from a side chain to the backbone of peptides and proteins.

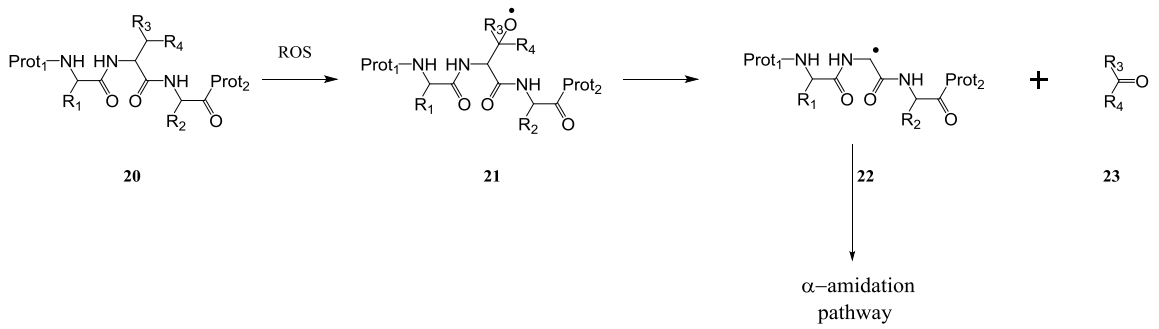

Figure 4. β-scission of side chains of Ala, Val, Leu, or Asp leaving a radical at the α-carbon which is prone to backbone cleavage as shown in **Figures 1** and **2**.

6.3 Cleavage of peptide bonds via electrochemical oxidation

Electrochemical systems have attracted increasing interest because of their ability to

mimic biological oxidation reactions by direct electron transfer oxidations and the generation of hydroxyl radicals under certain conditions. Electrochemical oxidation has the ability to abstract electrons directly from functional groups of amino acids in peptides and proteins to the electrode. Notably, Cys, Met, His, Tyr and Trp are susceptible to direct oxidation. [5] The electrochemical cleavage of peptide bonds at the C-terminal side of Tyr was reported over 50 years ago by Iwasaki *et al*. [24] and specific cleavage of peptide bonds at the C-terminal side of Trp was reported in 1997. [25] The specific electrochemical cleavage of peptide bonds next to Tyr and Trp residues in peptides and proteins was later studied in detail by mass spectrometry. [26-27] Electrochemistry can also be used to generate ROS, leading to specific cleavage next to phenylalanine (Phe) after its oxidation to Tyr by $HO^{\bullet}$ radicals. [29-30] The proposed electrochemical oxidation and cleavage mechanisms of Tyr, Trp and Phe-containing peptides and proteins will be summarized in the following sections.

6.3.1 Peptide bond cleavage via oxidation of Tyr

Electrochemical cleavage of peptide bonds next to Tyr residue is initialized by the abstraction of electrons from the aromatic ring systems to the electrode and concomitant deprotonation (**Figure 5**). Direct electron transfer in Tyr-containing peptides and proteins (**22**) during electrochemical oxidation results in formation of a phenoxonium intermediate (**23**), which can undergo a number of reactions, one of which leading to an intermediate (**30**) containing an (E)-N-(dihydrofuran-2(3H)-ylidene)methanaminium group, which undergoes hydrolysis of the former peptide bond to yield an N-terminal fragment with a spirolactone moiety at the C-terminus (**31**) and a C-terminal fragment with a regular amino terminus (**32**). Intermediate (**23**) can undergo a number of reactions leading to non-cleavage oxidation products (**24**, **25**, **26** and **29**).

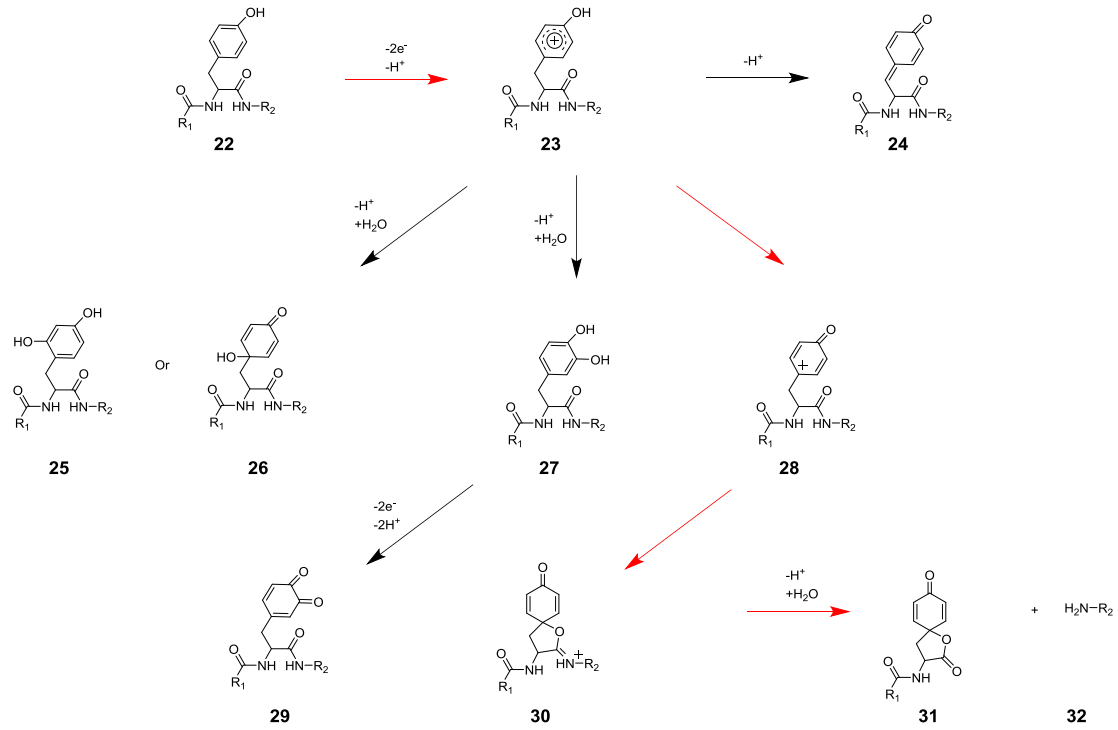

Figure 5. Proposed electrochemical oxidation and cleavage mechanism of Tyr-containing peptides and proteins. The pathway leading to peptide bond cleavage is highlighted with red arrows. R_1 and R_2 are the N- and C-terminal parts of the continuing peptide chain, respectively [26-27]

A specific peptide bond cleavage of Phe via hydroxyl-radical-mediated oxidation has been described, [29-30] where electrochemical oxidation of water on a BDD electrode was employed for hydroxyl radical production. Hydroxyl-radical-mediated oxidation of Phe results in aromatic hydroxylation at the meta- (**34**), ortho- (**35**) and para-positions (**22**) of the aromatic ring of Phe (**Figure 6**). Hydroxylation of Phe in the para-position leads to the formation of Tyr (**22**), which can undergo electrochemical cleavage via Tyr-cleavage pathway as shown in **Figure 5**. [29]

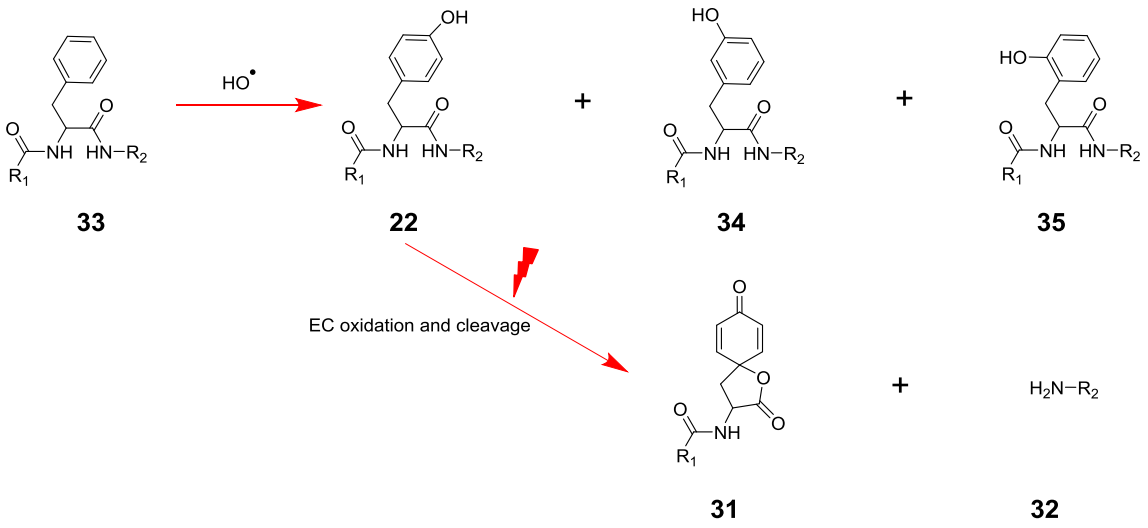

Figure 6. Proposed hydroxyl-radical-mediated oxidation of a Phe-containing peptide or protein in electrochemical oxidation. Hydroxylation in the para-, meta-, and ortho-positions of the aromatic ring by electrochemically-generated HO•-radicals yields products (**22**), (**34**) and (**35**), respectively. Product (**22**) containing a Tyr residue, can undergo further direct electron transfer reactions following the Tyr-cleavage pathway shown in **Figure 5** leading to the formation of cleavage products (**31**) and (**32**). [29-30]

6.3.2 Peptide bond cleavage via oxidation of Trp

Cleavage of peptide bonds adjacent to Trp (**36**) (**Figure 7**) is initiated by the abstraction of two electrons followed by deprotonation and reaction with water to give the hydroxylated indole moiety (**37**). An intermediate with an oxoindole group (**38**) is formed after secondary abstraction of electrons and deprotonation followed by an intramolecular rearrangement yielding an (E)-N-(dihydrofuran-2(3H)-ylidene)methanaminium containing intermediate (**42**). Hydrolysis of this intermediate leads to cleavage of the former peptide bond resulting in an N-terminal fragment (**43**) with a spirolactone moiety at the C-terminus and a C-terminal fragment with a regular amino terminus (**44**). Intermediate (**38**) can undergo a number of reactions leading to non-cleavage oxidation products (**39**, **40** and **41**).

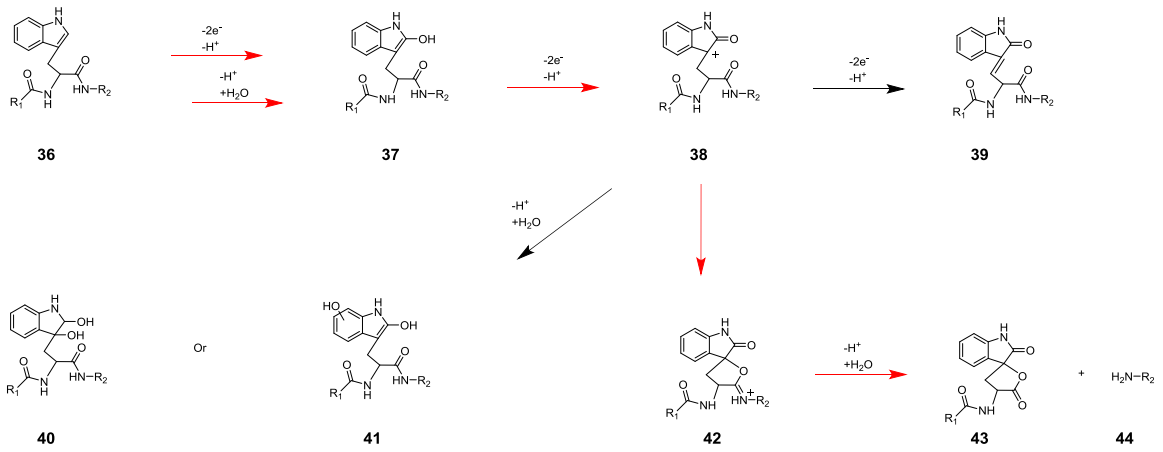

Figure 7. Proposed electrochemical oxidation and cleavage mechanism of Trp-containing peptides and proteins. The pathway leading to peptide bond cleavage is highlighted with red arrows. R_1 and R_2 are the N- and C-terminal parts of the continuing peptide chain, respectively. [26-28]

6.4 Analytical strategies to investigate oxidative cleavage of proteins *in vitro* and *in vivo*

Despite the progress in methodologies to study oxidative protein modifications, the investigation of oxidative peptide bond cleavage in biological and clinical samples remains challenging due to the low abundance of the modifications, sample complexity, the occurrence of other, non-cleavage oxidation products and the potential for further chemical reactions. [49-51] The low abundance of modifications often encountered *in vivo* means that highly sensitive and selective analytical methods are required for investigating oxidative peptide bond cleavage. Developing such methods requires mimicking *in vivo* oxidative stress under controlled conditions and with defined mixtures of biomolecules that will be encountered *in vivo*. External sources of ROS, radiolysis and oxidizing agents, including H_2O_2 and ozone, have been most often used in mimicking the oxidation of peptides and proteins. [16, 40, 44] To study whether the same modifications occur *in vivo* and, if so, what the biological relevance is, necessitates targeted analytical strategies.

Specific chemical labeling and enrichment, combined with MS-based, highly sensitive analytical strategies are central to investigating the oxidative cleavage of peptides and proteins both *in vitro* and *in vivo*. The introduction of carbonyl derivatives via ROS-induced oxidative cleavage supplies a handle for specific chemical labeling and enrichment, which serves as a marker of ROS-mediated protein damage and a number of assays have been developed for the quantitation of these species both *in vitro* and *in vivo*. Similarly, the generation of a unique spirolactone after oxidative cleavage of peptides and proteins next to Tyr and Trp residues may also be employed in the development of targeted analytical strategies to follow this type of peptide bond cleavage *in vitro*, as well as *in vivo*. In this section, the major strategies for the analysis of protein carbonylation generated through radical-mediated, oxidative cleavage and current progress for the analysis of spirolactone-containing peptides will be summarized.

6.4.1 Analytical strategy for carbonyl derivatives

Protein carbonylation is generally regarded as an irreversible post-translational modification (PTM) that yields a new reactive carbonyl moiety in a protein, such as an aldehyde or ketone at the N- and C-termini of the cleavage products. It has been shown that oxidative cleavage of proteins by either the α-amidation pathway, the oxidation of glutamyl side chains or by β-scission leads to peptide fragments with α-ketoacyl groups at the N-terminus. [41, 52-54]

Carbonyls in proteins have been employed extensively as markers of protein oxidation both *in vitro* and *in vivo*. [55-58] Based on the reactivity of carbonyl groups, a number of assays have been developed for their quantitation *in vitro* and *in vivo*. [59-64] On the basis of the carbonyl marker, it was established that oxidative damage of proteins is associated with aging, neurological diseases and some of the major life-style related disorders. Reviews investigating methods for the separation, identification and quantitation of protein carbonyls have been recently published paying particular attention to the advantages and disadvantages of each technique; [65-66] the most relevant techniques are described below.

6.4.1.1 DNPH derivatives

Keto and aldehyde groups react easily and quantitatively with hydrazine derivatives, resulting in the formation of hydrazones. A number of methods have been developed for the detection of protein carbonyls based on this reaction. Derivatization of carbonyl compounds (**45**) with 2,4-dinitrophenylhydrazine (DNPH, **46**) forming the corresponding 2,4-DNP-hydrazones (**47**) is the most widely used analytical method (**Figure 8**). This method has been developed for direct colorimetric detection and quantification by spectrophotometry using diode-array detectors [67-69] or by fluorescence detection after separation by high-performance liquid chromatography, [70-71] or capillary electrophoresis [72]. Anti-DNPH antibodies are available for enzyme-linked immunosorbent assays (ELISA), [73-77] and immunodetection (Western Blotting) after one- or two-dimensional electrophoresis [78-80]. Detailed protocols and techniques can be found in references 81 and 82. The combination of DNPH derivatization with mass spectrometry has become a widely used strategy over the last decades because of the ability to identify and quantify carbonylated proteins in biological samples with high sensitivity (see following sections).

45 **46** **47**

Figure 8. 2,4-dinitrophenylhydrazine (DNPH) reacts with protein carbonyl groups producing a protein-DNP hydrazone moiety that can be detected spectrophotometrically, by immunochemical techniques, mass spectrometry and other detection techniques.

6.4.1.2 Affinity detection and enrichment

The hydrazide chemistry can be used to introduce affinity tags on protein carbonyls and to perform subsequent affinity detection and enrichment. [83] Yoo and Regnier established a sensitive detection method for carbonylated proteins after 2D-gel

separation using biotin-hydrazide followed by avidin-FITC affinity staining, which achieved carbonyl specificity and a five times higher detection sensitivity compared with silver staining. [84] Following this work, affinity tags including biotin-hydrazide and N'-amino-oxymethylcarbonyl hydrazino-D-biotin (ARP) were employed for specific enrichment of carbonylated peptides and proteins via affinity chromatography on avidin columns. [85-90] Similarly, hydrazine-modified glass beads were developed for isolation of carbonylated proteins using simple spin down procedures. Subsequently, Girard's P reagent bearing a hydrazine group and a permanent positive charge was employed to enrich peptides with strong cation exchange chromatography, [91] and quantification by mass spectrometry was done through isotopically labelled Girard's P reagents [92]. Oxidation-dependent element coded affinity tags (O-ECAT) bearing an aminooxy group and a metal-chelator moiety were introduced by Lee *et al*. [93] In this work, the aminooxy group was used for coupling to aldehydes or ketones, while the metal-chelator moiety served for the affinity enrichment of derivatised peptides and proteins. [93]

Another strategy is to use DNPH derivatisation in combination with anti-DNPH antibodies to immunoprecipitate and enrich carbonylated proteins, which has been demonstrated by England and Cotter in the study of endoplasmic reticulum proteins under oxidative stress by 2D-gel and matrix-assisted laser desorption ionization time-of-flight (MALDI-TOF)-MS, [94] and by Kristensen *et al*. [95] in the study of mitochondrial proteins under oxidative stress by 2D LC-MS/MS.

6.4.1.3 MS-based analytical strategies

MS-based proteomics has been shown to be a powerful technique in the analysis of protein carbonylation, especially in the identification of modified proteins and their relative quantification. Nevertheless, most MS-based methods still involve derivatization of the carbonyl group, often combined with enrichment protocols to achieve high specificity, and sensitivity, especially for the analysis of biological samples.

MALDI-MS was employed for fast screening and mapping of carbonylated sites by comparing peptide mass fingerprints (PMF) of samples after various levels of oxidative stress. DNPH can be used as a matrix for MALDI-MS to analyze carbonylated peptides and proteins, since UV absorption of the hydrazones at 337 nm is sufficiently high to allow direct analysis without addition of typical matrices. [96] Isotope-labeled $^{13}C_6$-DNPH was synthesized to detect and quantify carbonylated peptides, with an isotope dilution approach. The doublet peaks with a mass difference of 6 Da in oxidized angiotensin I and lysozyme (after digestion) can be easily identified by MALDI-MS. [97] Wang *et al*. described an approach combining 2-D gel, DNPH derivatization, Western blotting and PMF. Elevated levels of protein carbonyls in the temporal cortex of 24-month-old rats compared to 1-month-old rats were found. [98] Chemical labeling with a hydrazide-functionalized isotope-coded affinity tag (ICAT), which contains a biotin and a hydrazide linker in light (^{12}C) and heavy (^{13}C) form, has been performed and analyzed by MALDI-TOF-MS by Han *et al*. [99] Thirty derivatized peptides from 18 mitochondrial proteins were identified and quantified.

LC-MS/MS analysis using untargeted analysis or targeted approaches has recently been used in a proteome-wide study of protein carbonylation. [100] For example, Madian and Regnier reported the detection of 15 carbonylation sites in low-abundance proteins in human plasma. [101] The whole approach includes biotinylation of carbonyl groups with biotin hydrazide, affinity isolation with avidin chromatography, trypsin digestion of carbonylated proteins and identification by LC-MS/MS.

6.4.1.4 Analysis in biological samples

Since highly sensitive methods are now available for the detection and quantification of protein carbonyl groups in biological samples, many reports have focused on the analysis of the level, location and biological relevance of protein carbonyls in animals or in cell cultures exposed to various oxidative stress conditions related to aging or various diseases. [102-106] For example, 643 carbonylation sites were identified in the HeLa cell proteome treated by H_2O_2, utilizing enrichment of carbonylated peptides after

DNPH derivatization. [107] Increased levels of protein carbonyls have also been detected in tissues from patients with Alzheimer's disease, [108-110] and in aged rat skeletal muscle by iTRAQ-based relative quantification methods. [111] Chavez *et al*. determined carbonylation sites in rat cardiac mitochondrial proteins using ARP and avidin-based affinity enrichment, [112] and Oikawa *et al*. reported increased levels of carbonyls in monkey hippocampus under ischaemia/reperfusion and described their locations [113]. Bollineni *et al*. used the carbonyl-reactive probe O-(biotinylcarbazoylmethyl) hydroxylamine followed by avidin affinity chromatography to demonstrate differences in the profiles of carbonyl-containing proteins in plasma of obese subjects and patients with type-2 diabetes. [114-115] This group also investigated carbonyl-containing proteins in plasma of breast cancer patients, and 460 proteins were identified and quantified, 95 of which changed 1.5 fold or more in concentration than in plasma of healthy controls. [116]

6.4.2 Current strategies for the analysis of spirolactone derivatives

While carbonyl groups on proteins have been widely detected *in vivo* as a result of oxidation-, or radical-mediated bond cleavage, spirolactones generated as a result of oxidative peptide bond cleavage next to Tyr and Trp residues have so far not been reported *in vivo*. This may be due to the reactivity of spirolactones with nucleophiles such as primary amines and their susceptibility to hydrolysis. It is thus currently unclear whether cleavage reactions next to Tyr and Trp play a role *in vivo*. Addressing this point depends on the development of sensitive and selective analytical methods. The basis for such methods is that spirolactones may be captured by nucleophilic tagging reagents for detection and/or enrichment and that reactions between spirolactones and molecules occurring *in vivo* may be mimicked *in vitro*. Progress in the development of sensitive and selective analytical strategies for the detection of spirolactone-containing peptides will be described in this section.

The development of analytical strategies for the detection of spirolactone-containing peptides has thus far relied on the combination of electrochemistry and mass spectrometry (EC-MS). Electrochemical cleavage at the C-terminal side of Trp and Tyr

residues followed by spirolactone formation was first investigated in detail in model tripeptides [24-25] and later extended to larger peptides and proteins with multiple cleavage sites. [26-27] The yield of the cleavage products is affected by the electrode material, its pretreatment, the oxidation potential and the pH. [26-30]

The complexity of reaction mixtures, due to the generation of non-cleavage oxidation products in addition to cleaved peptides, poses a problem for the accurate analysis of spirolactone-containing peptides (**Figures 5, 6** and **7**). It is thus desirable to enrich spirolactone-containing peptides (**45**) by targeted chemical labeling with nucleophilic primary amines (**Figure 9, red**). [117] This labeling is not straightforward as the DNPH derivatization of carbonyls. The main challenges related to this reaction are preventing hydrolysis of spirolactones (**49**) during the coupling reaction, preventing intramolecular rearrangements to unreactive, isomeric diketopiperazines (**50**) and decreasing the large molar excess of reagents. To address these challenges, we developed a strategy to prevent intramolecular rearrangement by acetylating the N-terminal amino group prior to electrochemical oxidation and cleavage allowing the complete and selective chemical labeling of cleaved peptides with amine-containing reagents under non-aqueous conditions (**Figure 9, blue arrows**). As examples, we show the successful introduction of a fluorescent label for detection and biotin for affinity enrichment. [118] More recently we developed a specific affinity enrichment method combining electrochemical digestion, copper (II)-mediated spirolactone biotinylation and selective affinity chromatography to label and enrich cleaved peptides after electrochemical oxidation of peptides and proteins (**Figure 10**). [119] Copper (II) was effective in preventing intramolecular rearrangement in the presence of a non-protected N-terminal amino group allowing biotinylation of spirolactone-containing peptides and their subsequent affinity enrichment by avidin chromatography followed by mass spectrometric analysis. As this reaction does not require prior acetylation of cleaved peptides, it is more compatible with enrichment of spirolactone-containing peptides from biological samples.

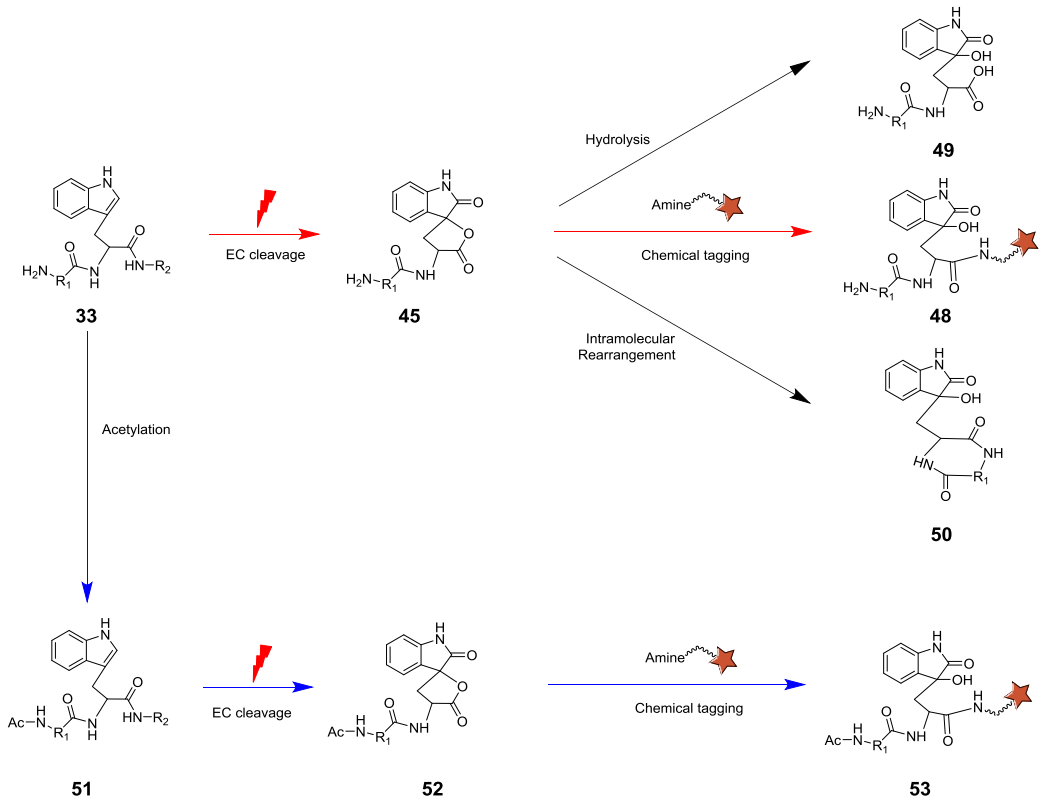

Figure 9. Scheme showing the chemical conversion of a Trp-containing peptide from electrochemical cleavage to a biotinylated residue using amine-PEG_2-biotin. R_1 and R_2 represent the peptide chains N-terminal and C-terminal to the Trp residue, respectively.

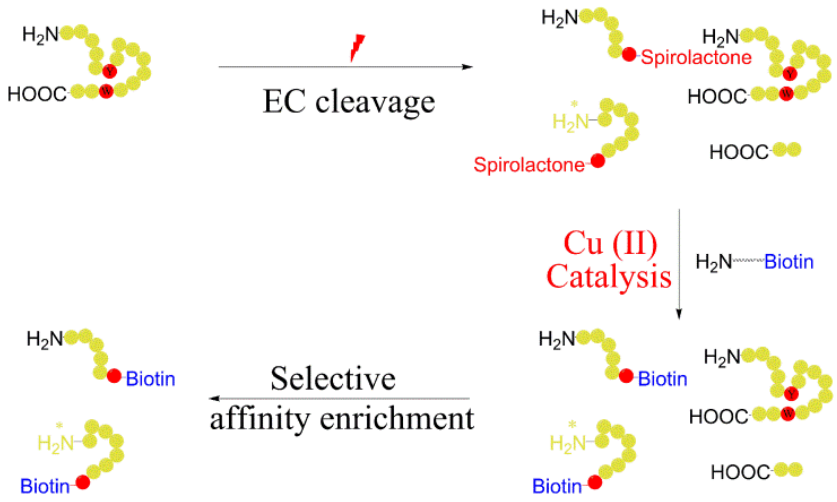

Figure 10. Scheme for enriching fragments after electrochemical cleavage of peptides and proteins via Cu (II)-mediated biotinylation and selective affinity enrichment with avidin chromatography.

6.5 Conclusion and perspective

The study of the cleavage of chemical bonds and notably peptide bonds due to oxidative stress *in vivo* has been of great importance to further our understanding of the mechanisms of a broad spectrum of diseases and biological processes related to ageing. However, we are still far from understanding oxidation mechanisms and their effects *in vivo*. Mimicking *in vivo* reactions by studying them under *in vitro* conditions has helped in deciphering the underlying mechanisms and can be used to produce reaction products for further research. Radiolytic oxidation and electrochemical oxidation are two of the most important approaches to study oxidation reactions and reaction mechanisms *in vitro*.

Radiolytic oxidation of peptides and proteins produces carbonyl derivatives due to ROS-induced oxidative cleavage of chemical bonds supplying a handle for chemical labeling and enrichment, and constituting an important marker of oxidative stress. A variety of targeted analytical methods for the separation, identification and quantitative analysis of protein carbonyls have been established and applied in the study of biological samples. MS-based analytical strategies have greatly increased our knowledge in this area, and are expected to continue to do so. Chemical labelling and enrichment approaches, together with advanced MS/MS routines, provide very powerful, though time-consuming tools for investigating the relationship between specific oxidative protein modifications and disease mechanisms. Despite this progress, we are just at the beginning of understanding the relevance of oxidative cleavage of chemical bonds, and notably peptide bonds, in biological processes. A variety of aspects, including optimization of existing protocols, development of mimicking conditions and analytical techniques, and software for processing large LC-MS/MS data sets, followed by biological studies providing functional insights are needed to advance the field. In this view, optimized and standardized, highly sensitive and specific techniques that can be automated to analyze the protein carbonyls in complex biological samples are needed

in conjunction with synthetic, stable-isotope-labelled, carbonylated peptides for accurate and precise quantification.

Electrochemical oxidation of peptides and proteins is emerging as a new method to mimic oxidative stress conditions *in vitro*. Specific oxidative cleavage after Try and Trp raised interest to investigate whether this sequence-specific, non-enzymatic peptide bond cleavage occurs *in vivo* under conditions of oxidative stress and if so what the biological relevance may be. EC-MS was developed to study the electrochemical oxidation and cleavage mechanism in detail with the identification of spirolactone-containing peptide fragments. Considerable progress has been made in the development of an electrochemical reactor for higher cleavage efficiency combined with tagging of the electrochemically-generated reactive spirolactone. [26-30] To tackle the increased complexity of sample mixtures, specific enrichment based on efficient chemical labeling of electrochemically-cleaved peptides was developed. [117-119] However, compared to the analytical strategies developed for the analysis of protein carbonyls, method development for the analysis of spirolactone-containing peptides is in its infancy.

6.6 References

(1) Stadtman, E. R.; Berlett, B. S. *Drug Metab. Rev.* **1998**, 30, 225-243.

(2) Berlett, B. S.; Stadtman, E. R. *J. Biol. Chem.* **1997**, 272, 20313-20316.

(3) Finkel, T.; Holbrook, N. J. *Nature* **2000**, 408, 239-247.

(4) Davies, M. J. *Biochem. J.* **2016**, 473, 805-825.

(5) Xu, G.; Chance, M. R. *Chem. Rev.* **2007**, 107, 3514-3543.

(6) Halliwell, B.; Gutteridge, J. M. C. *Free Radicals in Biology and Medicine* **2015**, Oxford University Press, Oxford.

(7) Sayre, L. M.; Moreira, P. I.; Smith, M. A.; Perry, G. *Ann. Ist. Super. Sanita* **2005**, 41, 143-164.

(8) Cabiscol, E.; Tamarit, J.; Ros, J. *Int. Microbiol.* **2000**, 3, 3-8.

(9) Beckman, J. S.; Koppenol, W. H. *Am. J. Physiol.* **1996**, 271, C1424-C1437.

(10) Barelli, S.; Canellini, G.; Thadikkaran, L.; Crettaz, D.; Quadroni, M.; Rossier, J. S.; Tissot, J. D.; Lion. N. *Proteomics Clin. Appl.* **2008**, 2, 142-157.

(11) Nathan, C.; Ding, A. *Cell* **2010**, 140, 951-951, e2.

(12) Dalle-Donne, I.; Scaloni, A.; Butterfield, D. A. *Redox Proteomics: From Protein Modifications to Cellular Dysfunction and Diseases* **2006**, *Wiley & Sons*, New York.

(13) Stringfellow, H. M.; Jones, M. R.; Green, M. C.; Wilson, A. K.; Francisco, J. S. *J. Phys. Chem. A* **2014**, 118, 11399-11404.

(14) Ekkati, A. R.; Kodanko, J. J. *J. Am. Chem. Soc.* **2007**, 129, 12390-12391.

(15) Bischoff, R.; Schlüter, H. *J. Proteomics* **2012**, 75, 2275-2296.

(16) Stadtman, E. R. *Free Radic. Res.* **2006**, 40, 1250-1258.

(17) Vaz, B.; Popovic, M.; Ramadan, K. *Trends Biochem. Sci.* **2017**, 42, 483-495.

(18) Garrison, W. M.; Jayko, M. E.; Bennett, W. *Radiat. Res.* **1962**, 16, 487-502.

(19) Garrison, W. M. *Chem. Rev.* **1987**, 87, 381-398.

(20) Stadtman, E. R. *Ann. Rev. Biochem.* **1993**, 62, 797-821.

(21) Hawkins, C. L.; Davies, M. J. *Biochim. Biophys. Acta* **2001**, 1504, 196-219.

(22) Faraggi, M.; Tal, Y. *Radiat. Res.* **1975**, 62, 347.

(23) Permentier, H. P.; Bruins, A. P.; Bischoff, R. *Mini*. *Rev*. *Med*. *Chem*. **2008**, 8, 46-56.

(24) Iwasaki, H.; Cohen, L. A.; Witkop, B. *J*. *Am*. *Chem*. *Soc*. **1963**, 85, 3701–3702.

(25) Walton, D. J.; Richards, P. G.; Heptinstall, J.; Coles, B. *Electrochim*. *Acta* **1997**, 42, 2285-2294.

(26) Permentier, H. P.; Jurva, U.; Barroso, B.; Bruins, A. P. *Rapid*. *Commun*. *Mass*. *Spectrom*. **2003**, 17, 1585-1592.

(27) Permentier, H. P.; Bruins, A. P. *J*. *Am*. *Soc*. *Mass*. *Spectrom*. **2004**, 15, 1707-1716.

(28) Roeser, J.; Permentier, H. P.; Bruins, A. P.; Bischoff, R. *Anal*. *Chem*. **2010**, 82, 7556-7565.

(29) Roeser, J.; Alting, N. F. A.; Permentier, H. P.; Bruins, A. P.; Bischoff, R. *Anal*. *Chem*. **2013**, 85, 6626-6632.

(30) van den Brink, F. T. G.; Zhang, T.; Ma, L.; Bomer, J.; Odijk, M.; Olthuis, W.; Permentier, H. P.; Bischoff, R.; van den Berg, A. *Anal*. *Chem*. **2016**, 88, 9190-9198.

(31) Swallow, A. J. In: Swallow, A. J. editor. *Radiation chemistry of organic compounds*, **1960**, New York: Pergamon Press, p 211-224.

(32) Garrison, W. M.; Weeds, B. M. *Radiat*. *Res*. **1962**, 17, 341-352.

(33) Schuessler, H.; Schilling, K. *Int*. *J*. *Radiat*. *Biol*. **1984**, 45, 267-281.

(34) Kopoldova. J.; Liebsier, J. *Int*. *J*. *Appl*. *Radiat*. *Isot*. **1963**, 14, 493-498.

(35) Garrison, W. M.; Kland-English, M.; Sokol, H. A.; Jayko, M. E. *J*. *Physiol*. *Chem*. **1970**, 74, 4506-4509.

(36) Borg, D. C.; Schaich, K. M. Iron-derived radicals. In: Halliwell, B. editor. *Proceedings of an UpJohn symposium*, Federation of American Societies for Experimental Biology. Bethesda, MD: **1988**, p 20-26.

(37) Stadtman, E. R.; Berlett, B. S. Free radical-mediated modification of proteins. In: Wallace, D. B. editor. *Free radical toxicology*, Washington: Taylor and Francis, **1997**, p 71-78.

(38) Stadtman, E. R. Free radical-mediated oxidation of proteins. In: Ozben, T. editor. *Free radicals, oxidative stress, and antioxidants: Pathological and physiological significance*, NATO ASI series, Series A: Life sciences. Vol. 296. New York: Plenum Press, **1998**, p 51-143.

(39) Butterfield, D. A.; Stadtman, E. R. Protein oxidation processes in aging brain. In: Timiras, P. S.; Bittar, E. E. editors. *Advances in cell aging and gerontology*, Vol. 2. Greenwich, CT: JAI Press, **1997**, p 161-191.

(40) Davies, M. J. *Biochim*. *Biophys*. *Acta* **2005**, 1703, 93-109.

(41) Stadtman, E. R.; Oliver, C. N. *J*. *Biol*. *Chem*. **1991**, 266, 2005-2008.

(42) Hellwig, M.; Löbmann, K.; Orywol, T. *J*. *Pept*. *Sci*. **2015**, 21, 17-23.

(43) Uchida, K.; Kato, Y.; Kawakishi, S. *Biochem*. *Biophys*. *Res*. *Commun*. **1990**, 169, 265-271.

(44) Headlam, H. A.; Davies, M. J. *Free Radic*. *Biol*. *Med*. **2004**, 36, 1175-1184.

(45) Dean, R. T.; Fu, S.; Stocker, R.; Davies, M. J. *Biochem*. *J*. **1997**, 324,1-18.

(46) Headlam, H. A.; Mortimer, A.; Easton, C. J.; Davies, M. J. *Chem*. *Res*. *Toxicol*. **2000**, 13, 1087-1095.

(47) Headlam, H. A.; Davies, M. J. *Free Radic*. *Biol*. *Med*. **2002**, 32, 1171-1184.

(48) Stadtman, E. R.; Levine, R. L. *Amino Acids* **2003**, 25, 207-218.

(49) Thornalley, P.J.; Rabbani, N. *Biochim*. *Biophys*. *Acta* **2014**, 1840, 818-829.

(50) Luo, S.; Wehr, N.B. *Redox Rep*. **2009**, 14, 159-166.

(51) Augustyniak, E.; Adam, A.; Wojdyla, K.; Rogowska-Wrzesinska, A.; Willetts, R.; Korkmaz, A.; Atalay, M.; Weber, D.; Grune, T.; Borsa, C.; Gradinaru, D.; Chand, B. R.; Fedorova, M.; Griffiths, H. R. *Redox Biol*. **2014**, 4, 149-157.

(52) Stadtman, E. R.; Berlett, B. S. *J*. *Biol*. *Chem*. **1991**, 266, 17201-17211.

(53) Stadtman, E. R.; Levine, R. L. *Amino Acid*s **2003**, 25, 207-218.

(54) Moller, I. M.; Rogowska-Wrzesinska, A.; Rao, R. S. *J*. *Proteomics* **2011**, 74, 2228-2242.

(55) Levine, R. L.; Williams, J. A.; Stadtman, E. R.; Shacter, E. *Methods Enzymol*. **1994**, 233, 346-357.

(56) Chevion, M.; Bernenshtein, E.; Stadtman, E. R. *Free Radic*. *Res*. **2000**, 33, 99-108.

(57) Levine, R. L.; Wehr, N.; Williams, J. A.; Stadtman, E. R.; Shacter, E. *Methods Mol*. *Biol*. **2000**, 99, 15-24.

(58) Levine, R. L. *Free Radic*. *Biol*. *Med*. **2002**, 32, 790-796.

(59) Dalle-Donne, I.; Rossi, R.; Colombo, R.; Giustarini, D.; Milzani, A. *Clin*. *Chem*. **2006**, 52, 601-623.

(60) Dalle-Donne, I.; Scaloni, A.; Giustarini, D.; Cavarra, E.; Tell, D.; Lungarella, G.; Colombo, R.; Rossi, R.; Milzan, A. *Mass Spectrom*. *Rev*. **2005**, 24, 55-99.

(61) Winterbourn, C. C.; Buss, H. *Methods Enzymol*. **1999**, 300, 106-111.

(62) Davies, M. J.; Fu, S.; Wang, H.; Dean, R. T. *Free Radic*. *Biol*. *Med*. **1999**, 27, 1151-1163.

(63) Chaudhuri, A. R.; de Waal, E. M.; Pierce, A.; van Remmen, H.; Ward, W. F.; Richardson, A. *Mech*. *Ageing Dev*. **2006**, 127, 849-861.

(64) Reznick, A. Z.; Packer, L. *Methods Enzymol*. **1994**, 233, 357-363.

(65) Purdel, N. C.; Margina, D. Ilie, M. *Annu*. *Res*. *Rev*. *Biol*. **2014**, 4, 2015-2026.

(66) Fedorova, M.; Bollineni, R. C. Hoffmann, R. *Mass Spectrom. Rev.* **2014**, 33, 79-97.

(67) Fagan, J. M.; Sleczka, B. G.; Sohar, I. *Int. J. Biochem. Cell Biol.* **1999**, 31, 751-757.

(68) Calabrese, V.; Sultana, R.; Scapagnini, G.; Guagliano, E.; Sapienza, M.; Bella, R.; Kanski, J.; Pennisi, G.; Mancuso, C.; Stella, A. M.; Butterfield, D. A. *Antioxid. Redox Signal.* **2006**, 11-12, 1975-1986.

(69) Smith, C.; Carney, J.; Starke-Reed, P.; Oliver, C.; Stadtman, E. R.; Floyd, R. A.; Markesbery, W. R. *Proc Natl Acad Sci. USA.* **1991**, 88, 10540-10543.

(70) Agarwal, S.; Sohal, R. S. *Mech. Ageing Dev.* **1995**, 85, 55-63.

(71) Akagawa, M.; Sasaki, D.; Ishii, Y.; Kurota, Y.; Yotsu-Yamashita, M.; Uchida, K.; Suyama, K. *Chem. Res. Toxicol.* **2006**, 19, 1059-1065.

(72) Mantle, D.; Falkous, G.; Walker, D. *Clin. Chim. Acta.* **1999**, 284, 45-58.

(73) Buss, H.; Chan, T. P.; Sluis, K. B.; Domigan, N. M.; Winterbourn, C. C. *Free Radic. Biol. Med.* **1997**, 23, 361-366.

(74) Robinson, C. E.; Keshavarzian, A.; Pasco, D. S.; Frommel, T. O.; Winship, D. H.; Holmes, E. W. *Anal. Biochem.* **1999**, 266, 48-57.

(75) Alamdari, D. H.; Kostidou, E.; Paletas, K.; Sarigianni, M.; Konstas, A. G.; Karapiperidou, A.; Koliakos, G. *Free Radic. Biol. Med.* **2005**, 39, 1362-1367.

(76) Shacter, E. *Drug Metab. Rev.* **2000**, 32, 307-326.

(77) Domingues, R. M.; Domingues, P.; Melo, T.; Perez-Sala, D.; Reis, A.; Spickett, C. M. *J. Proteomics* **2013**, 92, 110-131.

(78) Levine, R. L.; Garland, D.; Oliver, C. N.; Amici, A.; Climent, I.; Lenz, A. G.; Ahn, B. W.; Shaltiel, S.; Stadtman, E. R. *Methods Enzymol.* **1990**, 186, 464-78.

(79) Nakamura, A.; Goto, S. *J. Biochem.* **1996**, 119, 768-774.

(80) Yan, L. J.; Orr, W. C.; Sohal, R. S. *Anal. Biochem.* **1998**, 263, 67-71.

(81) Hawkins, C. L.; Morgan, P. E.; Davies, M. J. *Free Radic. Biol. Med.* **2009**, 46, 965-988.

(82) Dalle-Donne, I.; Rossi, R.; Giustarini, D.; Milzani, A.; Colombo, R. *Clin.Chim. Acta* **2003**, 329, 23-38.

(83) Madian, A. G.; Regnier, F. E. *J. Proteome Res.* **2010**, 9, 1330-1343.

(84) Yoo, Y. S.; Regnier, F. E. *Electrophoresis* **2004**, 25, 1334-1341.

(85) Soreghan, B. A.; Yang, F.; Thomas, S. N.; Hsu, J.; Yang, A. J. *Pharm. Res.* **2003**, 20, 1713-1720.

(86) Mirzaei, H.; Regnier, F. *Anal*. *Chem*. **2005**, 77, 2386-2392.

(87) Mirzaei, H.; Regnier, F. *J*. *Proteome Res*. **2006**, 5, 2159-2168.

(88) Temple, A.; Yen, T. Y.; Gronert, S. *J*. *Am*. *Soc*. *Mass Spectrom*. **2006**, 17, 1172-1180.

(89) Mirzaei, H.; Regnier, F. *J*. *Chromatogr*. *A* **2007**, 1141, 22-31.

(90) Meany, D. L.; Xie, H. W.; Thompson, L. V.; Arriaga, E. A.; Griffin, T. J. *Proteomics* **2007**, 7, 1150-1163.

(91) Mirzaei, H.; Regnier, F. *Anal*. *Chem*. **2006**, 78, 770-778.

(92) Mirzaei, H.; Regnier, F. *J*. *Chromatogr*. *A* **2006**, 1134, 122-133.

(93) Lee, S.; Young, N. L.; Whetstone, P. A.; Cheal, S. M.; Benner, W. H.; Lebrilla, C. B.; Meares, C. F. *J*. *Proteome Res*. **2006**, 5, 539-547.

(94) England, K.; Cotter, T. *Biochem*. *Biophys*. *Res*. *Commun*. **2004**, 320, 123-130.

(95) Kristensen, B. K.; Askerlund, P.; Bykova, N. V.; Egsgaard, H.; Miller, I. M. *Phytochemistry* **2004**, 65, 1839-1851.

(96) Teuber, K.; Fedorova, Maria.; Hoffmann, Ralf.; Schiller, J. *Anal*. *Lett*. **2012**, 45, 968-976,.

(97) Tomoya, K.; Issey, O.; Akio, H.; Takaaki, K.; Hiroyuki, M.; Kazuo, T. *J*. *Mass Spectrom*. *Soc*. *Jpn*. **2009**, 57, 371-377.

(98) Wang, Q.; Zhao, X.; He, S.; Liu, Y.; An, M.; Ji, J. *Neurochem*. *Res*. **2010**, 35, 13-21.

(99) Han, B.; Stevens, J. F.; Maier, C. S. *Anal*. *Chem*. **2007**, 79, 3342-3354

(100) Bollineni, R.; Hoffmann, R.; Fedorova, M. *J*. *Proteomics* **2011**, 74, 2338-2350.

(101) Madian, A. G.; Regnier F. E. *J*. *Proteome*. *Res*. **2010**, 9, 3766-3780.

(102) Dalle-Donne, I.; Aldini, G.; Carini, M.; Colombo, R.; Rossi, R.; Milzani, A. *J*. *Cell*. *Mol*. *Med*. **2006**, 10, 389-406.

(103) Verrastro, I.; Pasha, S.; Jensen, K.; T.; Pitt, A. R. Spickett, C. M. *Biomolecul*es **2015**, 5, 378-411.

(104) Telci, A.; Cakatay, U.; Kayali, R.; Erdoğan, C.; Orhan, Y.; Sivas. A.; Akcay, T. *Horm Metab Res*. **2000**, 32, 40-43.

(105) Winterbourn, C. C.; Bonham, M. J.; Buss, H.; Abu-Zidan, F. M.; Windsor, J. A. *Pancreatology* **2003**, 3, 375-82.

(106) Lenz, A.; Costabel, U.; Shaltiel, S.; Levine, L. *Anal*. *Biochem*. **1989**, 177, 419-425.

(107) Bollineni, R. C.; Hoffmann, R.; Fedorova, M. *Free Radic*. *Biol*. *Med*. **201**4, 68, 186-195.

(108) Choi, J.; Malakowsky, C. A.; Talent, J. M.; Conrad, C. C.; Gracy, R.W. *Biochem*. *Biophys*. *Res*. *Commun*. **2002**, 293, 1566-1570.

(109) Sultana, R.; Perluigi, M.; Newman, S. F.; Pierce, W. M.; Cini, C.; Coccia, R.; Butterfield, D. A. *Antioxid*. *Redox Signal*. **2010**, 12, 327-336.

(110) Choi, J.; Rees, H. D.; Weintraub, S. T.; Levey, A. I.; Chin, L. S.; Li, L. *J*. *Biol*. *Chem*. **2005**, 280, 11648-11655.

(111) Feng, J.; Xie, H.; Meany, D.L.; Thompson, L.V.; Arriaga, E.A.; Griffin, T.J. *J*. *Gerontol*. *A Biol*. *Sci*. *Med*. *Sci*. **200**8, 63, 1137-1152.

(112) Chavez, J. D.; Wu, J.; Bisson, W.; Maier, C. S. *J*. *Proteomics* **2011**, 74, 2417–2429.

(113) Oikawa, S.; Yamada, T.; Minohata, T.; Kobayashi, H.; Furukawa, A.; Tada-Oikawa, S.; Hiraku, Y.; Murata, M.; Kikuchi, M.; Yamashima, T. *Free Radic*. *Biol*. *Med*. **2009**, 46, 1472-1477.

(114) Bollineni, R. C.; Fedorova, M.; Bluher, M.; Hoffmann, R. *J*. *Proteome Res*. **201**4, 13, 5081-5093.

(115) Madian, A. G.; Myracle, A. D.; Diaz-Maldonado, N.; Rochelle, N. S.; Janle, E. M.; Regnier, F. E. *J*. *Proteome Res*. **2011**, 10, 3959-3972.

(116) Madian, A. G.; Diaz-Maldonado, N.; Gao, Q.; Regnier, F. E. *J*. *Proteomics* **2011**, 74, 2395-2416.

(117) Roeser, J.; Alting, N. F. A.; Permentier, H. P.; Bruins, A. P.; Bischoff, R. *Rapid*. *Commun*. *Mass*. *Spectrom*. **2013**, *27*, 546-552.

(118) Zhang, T.; Niu, X.; Yuan, T,; Tessari, M,; de Vries, M. P.; Permentier, H. P.; Bischoff, R. *Anal*. *Chem*. **2016**, 88, 6465-6471.

(119) Zhang, T.; de Vries, M. P.; Permentier, H. P.; Bischoff, R. *Anal*. *Chem*. **2017**, 89, 7123-7129.

Chapter 7

Summary and future research

Electrochemical protein oxidation is emerging as an instrumental alternative to chemical and enzymatic cleavage in MS-based proteomics and as a powerful tool to study oxidation of peptides and proteins *in vitro*. The main drawbacks of electrochemical peptide cleavage compared to traditional enzymatic and chemical cleavage is the comparatively low cleavage yield and the increased complexity of reaction mixtures due to the generation of non-cleavage oxidation products in addition to cleaved peptides. An efficient and selective labeling and capturing strategy for the cleaved peptides of interest based on reactions of the spirolactone moieties with affinity labels would decrease sample complexity and boost proteomics analysis efficiency after electrochemical protein digestion.

The theme of this thesis is to develop new methods on the basis of electrochemistry combined with mass spectrometry (EC-MS) to improve electrochemical protein cleavage and its application in MS-based proteomics combined with the tagging of electrochemically-generated reactive intermediates. We have developed improved methods for peptide and protein cleavage, including miniaturization and improved cell configuration with boron doped diamond (BDD) electrodes in collaboration with colleagues from Twente University (**Chapter 2**). An efficient and selective labeling and capturing strategy for the cleaved peptides of interest based on specific reactions with the spirolactone moieties has been established to decrease sample complexity and boost proteomics analysis efficiency after electrochemical protein digestion (**Chapters 3 and 4**). The second aim of this thesis is to check the feasibility of using electrochemical oxidation *in vitro* to mimic *in vivo* oxidative reactions of peptides and proteins and to study oxidation mechanisms. Product studies of Gly-Met-Gly generated by radiolytic and electro-

chemical oxidation were performed in collaboration with colleagues from the University of Bologna (ISOF), Italy (**Chapter 5**).

In **chapter 2**, a microfluidic electrochemical cell that combining an optimized cell geometry for efficient electrochemical conversion with an integrated BDD working electrode has been developed for electrochemical cleavage of peptides and proteins. Efficient cleavage of bovine insulin and chicken egg white lysozyme was observed at 4 out of 4 and 7 out of 9 of the predicted cleavage sites, respectively. Chicken egg white lysozyme was identified based on 5 electrochemically generated peptides using a proteomics database search algorithm. These results show that electrochemical peptide bond cleavage in a microfluidic cell is a novel, fully instrumental approach towards protein analysis and eventually proteomics studies in conjunction with mass spectrometry.

Chapter 3 describes a highly efficient and selective chemical labeling approach based on spirolactone chemistry. A strategy was established to prevent intramolecular rearrangement by acetylating the N-terminal amino group prior to electrochemical oxidation and cleavage allowing the complete and selective chemical labeling of the tripeptide LWL and the decapeptide ACTH 1-10 with amine-containing reagents. As examples, we show the successful introduction of a fluorescent label and biotin for detection or affinity enrichment. However, this approach has limitations when it comes to the electrochemical cleavage of larger peptides or proteins, because of the unavoidable generation of neo-N-termini and the increasing difficulty to achieve complete acetylation of all amino groups.

In **chapter 4**, copper (II) was employed to achieve efficient chemical tagging of spirolactones and to prevent intramolecular rearrangement in the presence of an N-terminal amino group. Newly generated spirolactone-containing peptides were labeled with a biotin derivative containing an amino group allowing their affinity enrichment by avidin affinity chromatography and protein analysis followed by mass spectrometry. This method allows specific enrichment of electrochemically cleaved spirolactone-containing peptides from a complex mixture.

In **chapter 5,** gamma-ray radiolysis and electrochemistry were employed for generation of $HO^{\bullet}$, and their reactivity with Gly-Met-Gly was compared to study the feasibility of mimicking oxidation reactions. Detailed product analysis by LC-MS and high resolution MS/MS provided detailed insight into the reactivity of the Met-containing peptides under hydroxyl-radical-mediated oxidation conditions. This study demonstrates that reaction products after gamma-ray radiolysis and electrochemical oxidation overlap to some extent but that some radiolysis products are not observed upon electrochemical oxidation.

Further development of the analytical strategy and translation to complex biological systems requires several steps as outlined below:

(i) To investigate electrochemical oxidation of biological samples (*e.g.* plasma, cell extracts) in (microfluidic) electrochemical systems.
(ii) To study peptide bond cleavage and related reaction products by LC-MS and prepare standards for *in vivo* studies.
(iii) To spike such standards into biological samples of increasing complexity and to develop targeted LC-MS/MS methods.
(iv) To expose cells in culture to conditions of oxidative stress (*e.g.* H_2O_2, cigarette smoke, ageing) and to study peptide bond cleavage with the targeted analytical methods.
(v) To analyze samples from animal models of oxidative stress (*e.g.* related to cigarette smoke exposure, an unbalanced energy metabolism or to ageing).
(vi) To analyze samples from human subjects (*e.g.* epithelial lining fluid prior to and after an episode of controlled exposure to cigarette smoke).

This work may not only provide a specific analytical strategy to study whether this sequence-specific peptide cleavage occurs *in vivo*, but may also lead to establish its biological relevance based on a thorough understanding of the cleavage mechanism and dedicated, targeted analytical methods.

Chapter 8

Samenvatting en toekomstig onderzoek

Electrochemische eiwitoxidatie ontwikkelt zich als een instrumenteel alternatief voor chemische en enzymatische splitsing in massaspectrometrie-gebaseerde proteomics, en als een krachtig gereedschap om oxidatie van peptides en eiwitten *in vivo* te bestuderen. De voornaamste nadelen van electrochemische peptidesplitsing vergeleken met de traditionele enzymatische en chemische splitsing zijn de verhoudingsgewijs lage splitsingsopbrengst en de hogere complexiteit van de reactiemengsels door de vorming van niet-splitsingsproducten na oxidatie, naast gesplitste peptides. Een efficiënte en selectieve strategie voor het labelen en afvangen van de gesplitste peptides van interesse, gebaseerd op reacties van de spirolacton-groepen met affiniteitslabels, zou de monstercomplexiteit verminderen en de efficiëntie van proteomics-analyses na electrochemische eiwitdigestie sterk verbeteren.

Het thema van dit proefschrift is het ontwikkelen van nieuwe methodes op basis van electrochemie gecombineerd met massaspectrometrie (EC-MS) om electrochemische eiwitsplitsing alsmede de toepassing in MS-gebaseerde proteomics, gecombineerd met het labelen van electrochemisch gevormde reactieve intermediairen, te verbeteren. We hebben betere methodes ontwikkeld voor peptide- en eiwitsplitsing, waaronder het miniaturiseren en het verbeteren van de celconfiguratie met boron doped diamond (BDD) electrodes, in samenwerking met collega's van de Universiteit Twente (**hoofdstuk 2**). Een efficiënte en selectieve strategie voor het labelen en afvangen van de gesplitste peptides van interesse, gebaseerd op specifieke reacties van de spirolacton-groepen, is ontwikkeld om de monstercomplexiteit te verminderen en de efficiëntie van proteomics-analyses na electrochemische eiwitdigestie sterk te verbeteren (**hoofdstukken 3 en 4**). Het tweede doel van dit proefschrift is het bepalen van de haalbaarheid van het gebruik van electrochemische oxidatie *in vitro* om oxidatieve reacties van peptides en eiwitten

in vivo na te bootsen en oxidatiemechanismes te bestuderen. Studies van producten van Gly-Met-Gly, gevormd door radiolytische en electrochemische oxidatie, zijn uitgevoerd in samenwerking met collega's van de Universiteit van Bologna (ISOF), Italië (**hoofdstuk 5**).

In **hoofdstuk 2** is een microfluïdische electrochemische cel ontwikkeld, die een geoptimaliseerde celgeometrie voor efficiënte electrochemische conversie combineert met een geïntegreerde BBD werkelectrode, voor electrochemische splitsing van peptides en eiwitten. Efficiënte splitsing van runderinsuline en lysozym van kippeneiwit is gevonden op respectievelijk 4 van de 4 en 7 van de 9 voorspelde splitsingsplekken. Lysozym van kippeneiwit is geïdentificeerd op basis van 5 electrochemisch gevormde peptides met behulp van een proteomics database-zoekalgoritme. Deze resultaten tonen aan dat electrochemische splitsing van de peptidebinding in een microfluïdische cel een nieuwe, volledig instrumentele aanpak is voor eiwitanalyse en uiteindelijk voor proteomics studies in combinatie met massaspectrometrie.

Hoofdstuk 3 beschrijft een zeer efficiënte en selectieve chemische labelingsaanpak gebaseerd op spirolacton-chemie. Er is een strategie ontwikkeld voor het voorkomen van intramoleculaire herschikking door het acetyleren van de N-terminale aminogroep voorafgaand aan electrochemische oxidatie en splitsing, die complete en selectieve chemische labeling mogelijk maakt van het tripeptide LWL en het decapeptide ACTH 1-10 met amine-bevattende reagentia. We tonen als voorbeelden de succesvolle introductie van een fluorescent label en biotine voor detectie of affiniteitszuivering. Deze aanpak heeft echter beperkingen voor de electrochemische splitsing van grotere peptides of eiwitten, vanwege de onvermijdelijke vorming van neo-N-termini en de toenemende uitdaging om volledige acetylering van alle aminogroepen te bewerkstelligen.

In **hoofdstuk 4** is koper (II) gebruikt voor efficiënte chemische labeling van spirolactonen en om intermoleculaire herschikking in de aanwezigheid van een N-terminale aminogroep te voorkomen. Nieuwgevormde spirolacton-bevattende peptides zijn gelabeld met een afgeleide van biotine met een aminogroep, zodat affiniteitszuivering met

avidine-affiniteitschromatografie en eiwitanalyse gevolgd door massaspectrometrie mogelijk zijn. Deze methode maakt specifieke verrijking mogelijk van electrochemisch gesplitste spirolacton-bevattende peptides uit een complex mengsel.

In **hoofdstuk** 5 zijn radiolyse met gammastraling en electrochemie gebruikt voor de vorming van $HO^{\bullet}$ en de reactiviteit hiervan met Gly-Met-Gly is vergeleken om de haalbaarheid van het nabootsen van oxidatiereacties te bepalen. Gedetailleerde productanalyse met LC-MS en hoge resolutie MS/MS leverde gedetailleerd inzicht op in de reactiviteit van Met-bevattende peptides onder hydroxylradicaal-afhankelijke oxidatieomstandigheden. Deze studie toont aan dat reactieproducten na radiolyse met gammastraling en electrochemische oxidatie tot op zekere hoogte overlappen maar dat een aantal radiolyseproducten niet gevonden kunnen worden met electrochemische oxidatie.

Verdere ontwikkeling van de analytische strategie en het vertalen naar complexe biologische systemen vereist een aantal stappen:

(i) Het onderzoeken van electrochemische oxidatie van biologische monsters (b.v. plasma, celextracten) in (microfluïdische) electrochemische systemen

(ii) Het bestuderen van de splitsing van de peptidebinding en verwante reactieproducten met LC-MS en het maken van standaarden voor *in vivo* studies

(iii) Het spiken van deze standaarden in biologische monsters met toenemende complexiteit en het ontwikkelen van specifieke LC-MS/MS methodes

(iv) Het blootstellen van cellen in cultuur aan oxidatieve stress-condities (b.v. H_2O_2, sigarettenrook, veroudering) en het bestuderen van splitsing van peptidebindingen met specifieke analytische methodes.

(v) Het analyseren van monsters van diermodellen voor oxidatieve stress (b.v. gerelateerd aan blootstelling aan sigarettenrook, een energiemetabolisme dat uit balans is, of veroudering)

(vi) Het analyseren van monsters van proefpersonen (b.v. de vloeistoflaag van het luchtwegepitheel voor of na een periode van gecontroleerde blootstelling aan sigarettenrook)

Dit onderzoek zou niet alleen een specifieke analytische strategie voor het bestuderen van deze sequentie-specifieke peptidesplitsing kunnen opleveren, maar ook kunnen leiden tot het vaststellen van de biologische relevantie, gebaseerd op een grondig begrip van het splitsingsmechanisme.

List of Publications and Patent

1. **Tao Zhang**, Marcel P. de Vries, Hjalmar P. Permentier and Rainer Bischoff. Specific affinity enrichment of electrochemically cleaved peptides based on Cu (II)-mediated spirolactone tagging. *Analytical Chemistry*, **2017**, 89, 7123-7129.

2. **Tao Zhang**, Xiaoyu Niu, Tao Yuan, Marco Tessari, Marcel P. de Vries, Hjalmar P. Permentier and Rainer Bischoff. Efficient and selective chemical labeling of electrochemically-generated peptides based on spirolactone chemistry. *Analytical Chemistry*, **2016**, 88, 6465-6471.

3. Floris T.G. van den Brink*, **Tao Zhang***, Liwei Ma, Johan Bomer, Mathieu Odijk, Wouter Olthuis, Hjalmar P. Permentier, Rainer Bischoff and Albert van den Berg. Electrochemical protein cleavage in a microfluidic cell with integrated boron doped diamond electrodes. *Analytical Chemistry*, **2016**, 88, 9190-9198. (**Equal first author**).

4. Floris T.G. van den Brink, **Tao Zhang**, Liwei Ma, Mathieu Odijk, Wouter Olthuis, Hjalmar P. Permentier, Rainer Bischoff and Albert van den Berg. Electrochemical protein cleavage in a microfluidic cell for proteomics studies. *Procedia Technology*, **2017**, 27, 62-64.

5. Sebastian Barata-Vallejo, Carla Ferreri, **Tao Zhang**, Hjalmar P. Permentier, Rainer Bischoff, Krzysztof Bobrowski and Chryssostomos Chatgilialoglu. Radiation chemical studies of Gly-Met-Gly in aqueous solution. *Free Radical Research*, **2016**, 50, S24-S39.

6. Tao Yuan, Jiquan Wu, **Tao Zhang**, Petra Rudolf, Rainer Bischoff and Hjalmar P. Permentier. Catalytic N-dealkylation of drug molecules on a nanoporous gold surface. *Submitted*.

7. Jiaying Han, Andrea Schmidt, **Tao Zhang**, Hjalmar P. Permentier, Geny. M. M. Groothuis, Rainer Bischoff, Fritz E. Kühn, Peter L. Horvatovich and Angela Casini. Bioconjugation strategies to couple supramolecular exo-functionalized palladium cages to peptides for biomedical applications. *Chemical Communications*, **2017**, 53, 1405-1408.

8. **Tao Zhang**, Rainer Bischoff, Hjalmar Permentier. Means and methods for site-specific labeling of proteins, European patent application EP16169957.4 (application date: May 19, 2016).

Acknowledgement

I have much enjoyed my PhD journey, both in science and in life.

I would like to gratefully acknowledge to the many people who supported me along the way.

First and foremost, I would like to express my deepest gratitude to my supervisors, Prof. Rainer Bischoff and Dr. Hjalmar Permentier. Dear Rainer, thank you very much for giving me the opportunity to be part of the Analytical Biochemistry group. I am grateful for your inspiring guidance, continuous encouragement and invaluable constructive criticism. I really appreciate your passion and support during my PhD. I would always get detailed feedback within a few days after sending you the manuscript, often at odd hours of the night, even in the weekend and during your vacation. I wish I could have learnt more from you. Dear Hjalmar, I would like to say you are such a super excellent supervisor to encourage me to be more confident in science and your insightful advice always gave me the inspiration to find the way out. Many thanks Hjalmar for your valuable contribution and support both on my scientific research and private life. From my view, you are such a kind person, kind to everyone and kind to the whole world. I can't forget the moment when I found the gift to my daughter on my desk. Yifei likes it very much. I really learned a lot from you inside and outside of academia. I wish you and your family all the best with special wishes to dear Thalia.

I also would like to thank the members of the assessment committee: Prof. F. J. Dekker, Prof. U. Karst and Prof. E. M. J. Verpoorte for the time and the evaluation on my thesis. I want to express my special thanks to you for your valuable comments and helping me improve the manuscript.

Next, I am deeply grateful to colleagues from Twente University in The Netherlands, University of Bologna (ISOF) in Italy, and some industry partners contributed in this thesis. Very special thanks are given to Dr. Floris T. G. van den Brink in Twente Uni-

versity. It was a great experience and fruitful collaboration with you. I am looking forward to see you again and hope you all the best in your future. Many thanks to some of our industry partners, notably Antec Leyden and ESA/Dionex (now Thermo Scientific), who provided electrochemical cells and support with the specific construction, modification and treatment of cells and electrode surfaces. Dr. Mathieu Odijk and Dr. Jean-pierre Chervet, many thanks to you for your valuable discussions and suggestions during STW project meeting. Prof. Chryssostomos Chatgilialoglu, your great passion and agile thinking are very impressive.

I sincerely express my appreciations to all the colleagues in the Analytical Biochemistry group. Through my PhD you all made me feel like a family. Dear Marcel, my chicken partner, it was my pleasure to work with you in the past few years. I will miss you and your nice joke a lot. Dear Andries, thanks a lot for your guidance when I joined the group. I enjoyed the super BBQ in your garden and hope you enjoy your life after retirement. Dear David, Sara and Alex, all of the parties and moment with you were amazing! David, I am super happy to have you at my side during my defense. I wish you have a great and happy life with Tiffany. Sara, I wish you all best with Lucas and your little Mario in Germany. Dear Alex, I still remember how happy I was when I got your email and phone call in Leiden. I feel very happy to hear you are enjoying your life with your wife and beautiful daughter. I am looking forward to see you all soon. Turan and Tao, it was so great to work with you as one of the TTT-boys in the AB group. I will remember all of nice time we spent together. Turan, my dear friend, it is so nice that both of us are living in Leiden and we can meet each other more often after leaving Groningen. Tao, don't forget to start a Chinese restaurant in the near future. I will be there no matter where and when. I also thank Nicolas Abello for fruitful discussion and suggestions in this thesis and my personal career. Best wishes to you and your family, and I am looking forward to meet you again. Jiaying, my dear little sister, I am proud of you, Jing and Milan. Best wishes to all of you. Dear Peter H. and Nico, I appreciate your help and discussion in my PhD training and project. Peter Bults, I am so happy to have you as my colleague and friend. I hope you enjoy the fancy floating system, and I

am looking forward to go fishing with you in the near future. Wenxuan, I am glad to hear that Wei is coming to Groningen with you. Then, have fun in the Netherlands. Jos, thank you very much for helping me in the lab, and saving Tao and me in the lab outing day. Frank, you are definitely a talent in scientific research and a happy motor in life. Dear Natalia, I enjoy all of the moment with you and will miss you a lot. Dear Karin, I appreciate your help very much in both scientific training and personnel support. Andres, I hope you can drink more CH_3CH_2OH when I meet you next time. Daniel, I hope you have a happy life with your pretty girlfriend and beautiful dog. Kees, hope you always enjoy the time with your parents-in-law. I like the tasty hot chili very much. Dear Annie, I enjoyed the party at your place and liked the chickens in your garden. Dear Margot, thank you very much for coming to my daughter's one-month celebration. I would like to have a same fancy bicycle. Marcel K., thank you for trusting me on my age, but I was 18 five years ago. Jan Willem, thanks for explaining me the cool motorcycle. I also would like to thank our secretary Jolanda for continuous helps. I would like to thank also my other colleagues Yang, Daan, Victor, Annalisa and Anastasia for their friendship.

Of course many thanks to all of nice person that I met in Groningen, Floris, Mattieu, Sarah, Gert, Maciej, Peter, Jonas, Allessio, Elina, Jan Willem and Agnieszka. I enjoyed the life with you together and would like to keep contact with you for the rest of my life.

Importantly, my very special thanks to my paranymphs David and Jing. Dear David, I was so lucky to meet you immediately after I arrived Groningen. You are definitely one of my best who made my PhD life great. It is also my honor to have you beside me during my defense. I would like to take any chance to get together with you. I wish you and Tiffany have great and happy life after marriage. Dear Jing, many thanks for organizing my defense ceremony. We shared a lot together, and you are indeed more than a friend to me. Your home is always the first destination for my family and me in Groningen. Take care of Jiaying and Milan, they are the whole of your life. Further, I would like to thank Jiaying and Katarina, my dear ceremony secretaries. Jiaying is definitely

the most frequently name in my acknowledgement. I have already asked Jing to take care of you and your Milan. Dear Katarina, my most important friend and PGC partner in CPM, LUMC, I am very happy to work with you together in the past and in the future. You are such a kind girl. I wish you everything goes well in the future. I believe we will do great job.

I would like to take this chance to express my sincere gratitude to my new colleagues in CPM, LUMC. My special thanks to Prof. Manfred Wuhrer for offering me the opportunity to join the glyco family. I believe this was one of the best decisions I ever made in my life. I am really glad to meet those great colleagues in Leiden. Within such a short time period you mad me to feel as a part of glyco family. My family and I enjoy the life in Leiden very much.

And the last but not least I would like to show my great appreciation to my wife, my family and my special friends who were as close as a family member in Groningen for me. I prefer to thank them in Chinese since I have better words to express my love to them.

感谢我的硕士研究生导师屈锋教授，在北京理工大学学习期间，由衷的感谢您对我科研上的悉心指导，生活中的点滴关怀，以及在我读博期间的鼓励和关心，让我不断地进步。学生在此祝您身体安康，心想事成！也要特别感谢青青师姐和新颖师姐在读书期间对我的帮助。

感谢我在荷兰认识的的朋友们。凯哥和娟娟一家，感谢我能在荷兰认识你们以及及时珍惜在一起嗨皮的生活。太多的美好回忆，以及我电脑里你酒后的 AVI，我都会好好保存。作为我在西半球最好的兄弟，很荣幸又一次被你忽悠了。虽然你不能来做我滴答辩伴郎，我仍然要祝福你，娟娟，Esther 和 Grace，生活幸福美满，事业前程似锦。涛哥和蕾姐，好想念和你们在一起的日子，好好照顾好我们的干女儿小 Annie，我们有空会去看你们的哈。佳颖和静静，你们的名字又一次出现了，已经够你们骄傲的了吧，祝福你们和小 Milan 生活快乐，科研顺利，我会时常去看你们的。飞哥，飞嫂和小鲁，很想念在格村在一起聚会的时间，我们

也会珍惜之后能继续在荷兰见面的机会。搬来莱顿后的孤单感觉因为你的拜访而一扫而空，期待着下次与你见面。我亲爱的国伟，我跟我老婆一直在比较究竟谁更喜欢你多一点，衷心的祝福你，幸福的生活与你终生相伴。小孟，庆哥以及梦安一家，好怀念咱们一起麻将的时光，以及飞哥逗比的赌神 PGM，期待咱们嗨皮的麻将可以继续搞起，也要谢谢你熬夜帮我设计封面，祝你们接下来的生活顺利安康。袁涛和周丽一家，很高兴在博士期间和你一起工作，聚会，打牌，烧烤以及钓鱼，祝你在瑞士工作顺利，早日实现梦想，搞一个大大的池塘，我好去钓鱼。小全，忠洪以及禾禾，可惜颜值担当的禾禾没能继承你的奥斯卡影帝基因，却天生习得一身撩妹神功，可不要太羡慕自己的儿子哈。很高兴认识美女许瑾以及谢谢你的诸多帮助，祝福你生活爱情事业顺心顺利。老石和盼盼，相信你们是最棒的，你做的烤鸭，火锅以及扯面都是最棒的，加油，坐等你们的好消息哈。军哥和军嫂，每次都跟你们吃到好爽，喝到好嗨，祝你们在米国工作生活双丰收，早日把军哥养的白白胖胖的。我亲爱的的中国好室友，吕铭吕少爷，还想继续蹭你做的饭，还想跟你一起打坦克，还想跟你一起去钓鱼。对不起失约没能做你的答辩伴郎，我会想办法给你介绍女朋友补偿你的。其宏，谢谢你给格村带回了 MVP，也谢谢你给准备了那么丰盛的送行晚餐，还有神奇的独家秘制陈氏火锅蘸料，我受益终生。博群，你做的火锅，铁板烧都那么好吃，哄住了老曹的胃果然就管住了他的心。还有我们的美女金凤，晓琳，张杨和卓然，祝你们幸福安康。

还要继续感谢缘分下认识的好多朋友。边哥一家，谢谢你们的信任，在你家住的这段时间好高兴，也谢谢你们对我们生活和工作上的支持和帮助，以后常联系。小宇姐，Hein 和珠儿，缘分是妙不可言的，我很珍惜和你一起工作的时间，正如文君也一样珍惜和 Hein 一起工作的时光。怀念当年的深夜 Pub 三人组，转眼之间都已为人父，很高兴看到小赵和田财的从良和成长，祝福你们，别忘了咱们的约定。金涛和林林一家，佳伟和鹤鹤一家，好幸运能在格村及时认识你们，也好怀念咱们一起在法国潜水以及旅行的时光，谢谢你们骑行那么久去帮我买退烧药，还想再和你们一起旅行。艳萍，祝你和王飞在上海幸福快乐，下次回国要去上海看你们了。娜娜和大哥，每次去北京都要受到你们的热情招待，过去五年里去你家的次数都比去我弟弟家次数多，祝你们幸福开心，期待你们的好消息。家文和

蓓蓓一家，再努力一下下，早日整出来个足球队吧，我来给家文队赞助飞机和足球。庆凯和萌萌，很高兴能在格村各种机缘下认识你们，谢谢庆凯每次精心准备的饭菜，下次回格村一定去看你们，咱再搞次大闸蟹来嗨皮，祝你们在格村生活幸福美满。培亮和丽娟，谢谢你们那么多次的热情招待，很可惜没能参加培亮的答辩，祝你们接下来事业顺利，生活幸福。杨朔和婧祎一家，朔哥的羊腿和羊腰子永远是烧烤桌上的重头戏。非常高兴能在格村认识张峥以及阿 Jan 一家，王丽&建军&糖果一家，步大夫以及琅嬛琳一家，蒋义和赵婷一家，小面团，李明，孟祥峰，柏玉香，赵德鹏，祝你们所有人一切顺风顺水，心想事成。

非常感激还能在欧洲和我的发小&兄弟宫然相见，好怀念咱们一起在荷兰，德国，比利时，冰岛和意大利旅行的时光。从高二开始就把你当成弟弟一样看，太多美好的记忆伴随着我们一起成长，高中的刷夜和迟到，大学的书信，硕士的聚会，比利时的宿醉，意大利的美食，冰岛的极光环岛，德国的啤酒以及荷兰的小蘑菇。祝福你和弟妹小溪在韩国开心快乐，工作顺利。期待着下一次和你再次相遇。也因为你们结识了好多新的朋友，祝福优秀的小山越来越美丽，在西门子生活幸福，期待着你的婚礼和好消息。还有美丽温柔的文夭夭，好喜欢和你聊天以及开玩笑，期待再次吃到你的美食以及祝福你在新加坡工作顺利。

感谢在格联一起踢球的朋友们。怀念在小韵韵家烧烤，吃螃蟹，包水饺，打牌，打麻将，做游戏的时光，祝司韵和雪哥找工作顺利，生活幸福美满。石头在马城嗨皮无限，没事多回格村看看。其宏，MVP 的光芒照耀着你，千万不要过度风骚，我一直记得你的终身大事呢，等我的好消息吧。家文的凌空抽射已经成为球场的一大亮点，期待着你和蓓蓓再努力一点，带领你的陈家军创造格村辉煌。朔哥这个容易受伤的男人，天冷加衣，加强锻炼，在埃因霍芬生活快乐。很高兴这么快就见证了国伟的幸福生活，你说过我答辩你要来的，不要象刘院士那样不靠谱就好哈，我很期待。老陈，很高兴和你因足球认识，你踢过球的地方我也都去过了，格罗宁根，代尔夫特和乌特勒支，很高兴和你一起继续踢球。超哥生意兴隆，财源广进。同时祝福振辰，庆凯，晨玺，范大将军，李攀，伟立，张亮，子旭，敏铭，老姜，覃伟，林柯，启珉，语真在格村踢球快乐，期待在球场上再次相见。

还有我亲爱的格罗宁根欢乐足球队的兄弟们。这是从建队开始我一直倾注心血的大家庭，感谢大家过去四年里的支持和陪伴，希望这只球队在老曹的带领下走向辉煌。虽然在最后的一年里暂时离开了球队，但是我永远关心和关注着你们，谢谢你们精心准备的送行和礼物，被你们扒成那样我这老脸也是没地方搁了。再次祝福老曹和胖子相爱一生，在球场继续摩擦。希望凯哥，飞哥和军哥还能再次踢球，希望凯哥不要再迟到，期待飞哥潇洒的盘带过人，怀念军哥飘逸飞奔的身影。还有祝福妖娆的凌儿不要再抽筋，风骚的振辰继续骚气外漏，期待再次见到小全漂亮的黄油脚，静静风中的飞奔，李军性感的紧身裤，袁涛球场的冷笑话，小明的大长腿，卓华的边路突破，田财舞蹈般的带球，小赵微驼猥琐的背影，铮哥坚实肉体的冲撞，虎哥漂亮的脚后跟传球，大牌性感的飞奔，培亮的坚固防守，李牧的突破过人，还有黄刚，冯琮，刘庆，杨埔，老刘等等。感谢足球让大家凝聚在一起，期待再次与你们相见，祝福你们！

离得远了，会更珍惜相见的时光，期待和你们再次相会。

最后，诚挚的感谢我的家人，你们的支持永远是我不竭的动力源泉。感谢父母的养育之恩，以及多年来对我的默默付出。妈妈来荷兰照顾我们的时间，爸爸在家里辛苦了。感谢岳父岳母把您的女儿嫁给我，让我有机会照顾她和我们的暖儿。谢谢各位父母多次来荷兰照顾我们和暖儿，祝福你们心想事成，幸福安康。感谢弟弟和弟妹一直以来对我们无私的帮助和支持，我们在国外的时间家里都辛苦你们了。好高兴看到你结婚长大了，祝福你和文卓永远幸福快乐。还有振国和莹莹，谢谢你们的支持，爸妈才能安心来荷兰照顾我们，也谢谢你们时刻惦记着想着暖儿，期待你们早生贵子。特别感谢我的老婆，这么多年我们一路相随，为了我们的家和暖儿，你牺牲和辛苦太多，我会加油努力，一定让你和暖儿幸福快乐。最后，感谢上苍把你带给我们，我最亲爱的暖儿，依霏，爸爸妈妈希望你永远健康快乐，永远爱你和支持你！

Tao Zhang

2017-10-26

Leiden